ASSESSING MOTION STRESS LEVELS ON BOARD FISHING VESSELS OF THE NEWFOUNDLAND FLEET

JAVIER A. VERA

ASSESSING MOTION STRESS LEVELS ON BOARD FISHING VESSELS OF THE NEWFOUNDLAND FLEET

BY

JAVIER A. VERA

A Thesis submitted to the School of Graduate Studies
in partial fulfillment of the requirements for the degree of
Master of Engineering

Faculty of Engineering and Applied Science

Memorial University of Newfoundland

December 2004

Your file Votre référence
ISBN: 978-0-494-30528-7
Our file Notre référence
ISBN: 978-0-494-30528-7

Abstract

The aim of this study is to develop a numerical tool that could be used to assess the physical stress levels associated with the vessel motions on board fishing vessels of the Newfoundland fleet. A number of full-scale sea trials of typical fishing vessels of the fleet are underway to validate the numerical tool. Model experiments are expected to follow in the next year. If desirable correlations between the trials and the numerical results are obtained, simulations will be performed to obtain typical 'motion stress' profiles of various fishing boats over a typical fishing season. 'Motion Stress' will be quantified in terms of a parameter known as 'Motion Induced Interrupt' frequency (MII). Other parameters that can quantify the motion stress levels can also be incorporated into the numerical tool. Among them would be seasickness criteria and another postural stability index, which relates the motion levels on board to the 'motion stress'.

For full-scale trials, two vessels will be used initially. In terms of their sizes, these represent one of the smallest vessels and one of the larger vessels of the fleet. During the trials a directional wave buoy was used to measure the wave characteristics.

The Thesis will include the results from the full-scale sea trials and the numerical tool. Additionally, some sample results for motion stress levels will be presented.

Acknowledgements.

I would like to thank my supervisor Dr. Don Bass for the support that I received. He introduced me to the field of ship dynamics and the research in that area. The guidance and help he provided while pursuing my Masters program was greatly appreciated.

I also wish to express my thanks to Dr. Ayhan Akinturk and Mr. David Cumming for their assistance with experimental work, and for their time in answering my questions.

The assistance and constant support of my dear friend Fr. David Shulist S.J. is gratefully acknowledged.

Without my wife Ingrid, I would not have been able to complete this project. She was always there when I needed her support. My other family members are an important part of my life and their support is always invaluable.

Table of Contents

Abstract ii

Acknowledgements iii

Table of Contents iv

List of Figures vii

List of Tables x

Nomenclature xii

List of Symbols xiii

Chapter 1: Introduction 1

Chapter 2: Fishing Vessels Safety and MII 11

2.1 Fishing vessels safety. 11

2.2 Motion Induced Interrupt MII Criteria. 14

Chapter 3: Recent Work on MII and Background in Seakeeping 17

3.1 Fundaments of MII Theory. 18

3.1.1 The Frequency Domain Method. 19

3.1.2 Prediction of MII. 19

3.2 Recent work on MII. 30

3.2.1 Description of MII experimental tasks. 32

3.2.1.1 General and Task Performance Synchronization. 32

3.2.2 Ship motion drive time history definition. 37

3.2.3 Analysis of the model for Tipping and Sliding MIIs. 40

3.2.4 Sources of variability in basic parameters. 41

3.2.5 Results and conclusions of the ABCD experiments. 42

3.3 Background in Wave Theory. 50

3.4 Background in Ship Motions. 52

3.5 Background in Seakeeping. 54

Chapter 4: The Numerical Model **61**

4.1 The numerical model. 62

4.2 The MII numerical calculation. 65

4.3 The Numerical simulation. 67

Chapter 5: Full Scale Experiment: Sea Trials **71**

5.1 Fishing Vessels in Sea Trials. 71

5.1.1 Instrumentation. 71

5.1.2 Sea Trials. 79

5.1.3 Sea trial data evaluation. 84

5.2 Comparison between Sea Trials and Numerical Results. 86

5.3 Analysis. 94

Chapter 6: Numerical Results **95**

6.1 Motions Results. 95

6.2 Analysis of Motions. 99

6.3 The MII Results. 100

6.3.1 Averaged MII for Bow Headings. 101

6.3.2 Expected values of MIIs. 103

Chapter 7: Analysis of Wave Conditions **126**

7.1 Wave Conditions. 126

7.2 Motion Stress Profile. 128

Chapter 8: Conclusions **133**

List of References **137**

Appendix A: Numerical results of amplitudes of motion for each length class **139**

Appendix B: MII for five points and five headings **151**

List of Figures

1 Proportion of vessels lost from 1992 to 1999. 2

2 Accidents to fishing vessels by accident type. 3

3 Accidents to crew. 3

4 Vessels lost from 1992 to 1999. 4

5 SAR incidents by vessel length class between 1993 and 1999. 5

6 Total SAR incidents between 1993 and 1999. 6

7 The ratio of incidents per registered vessels. 7

8 Registered fishing vessels from 1987 to 1999. 7

9 Coordinate System for MII calculations. 20

10 Subject Model. 22

11 Subject Body *C.G.*, x, y and z Accelerations and Turn Rates about x, y and z. . . 34

12 NBDL Ship Motion Simulator – Schematic View Forward Toward Bow. 35

13 Description of SMS Cab Floor Plan, Cab Walls and Camera Locations. 36

14 Severe Discomfort boundaries for z-axis acceleration (ISO 2631). 38

15 Sample Tipping Coefficients for Global and Local Analysis (ABCD Group). . . 46

16 Energy expenditure (ABCD Group) 47

17 Computer generated geometry of a 65 foot fishing vessel. 67

18 Data Acquisition System. 72

19 Rudder Angle Measurements. 73

20 MotionPak Installation. 74

21 Wave Sentry Buoy and Radar Reflector. 77

22 Datawell Wave Buoy Deployed. 79

23 The 35 feet "Atlantic Swell" 83

24 The 75 feet "The Shamook" 83

25 ITTC Recommended Run Pattern. 84

26-29 Amplitudes of Motions for 35 feet "Atlantic Swell" at 4 kt 88-89

30-33 Amplitudes of Motions for 65 feet "Shamook" at 4 kt 90-91

34-37 Amplitudes of Motions for 65 feet "Shamook" at 8 kt. 92-93

38-40 Averaged Amplitudes of Motion at Fn=0.2. 96-97

41-43 Averaged Amplitudes of Motion at Fn=0.4. 97-98

44 Selected Locations on Board. 101

45 Averaged MII in Bow Headings at Fn=0.2. 102

46 Averaged MII in Bow Headings at Fn=0.4. 102

47 AMI comparisons at Fn=0.2. 112

48 AMI comparisons at Fn=04. 113

49 AMI comparisons at Fn=02. 114

50 AMI comparisons at Fn=04. 115

51 AMIp at Fn=0.2. 116

52 AMIp at Fn=0.4. 117

53 Maximum MII at Fn=0.2. 118

54 Maximum MII at Fn=0.4. 118

55 MII in all Headings at Fn=0.2. 121

56 MII in all Headings at Fn=0.4. 121

57 MII in Wave fields at Fn=0.2. 123

58 MII in Wave fields at Fn=0.4. 123

59 AMIp versus Vessel Speed. 125

60 Comparison of SWH off the Coast of Newfoundland. 127

61 Number of 5 day trip off the East Coast of Newfoundland. 127

62 Uni-directional JONSWAP Spectrum at Fn=0.2. 129

63 Uni-directional Bretschneider Spectrum at Fn=0.2. 130

64 Uni-directional JONSWAP Spectrum at Fn=0.4. 130

65 Uni-directional Bretschneider Spectrum at Fn=0.4. 131

66-71 Motions of Heave, Roll and Pitch in 35' Length Class. 139-141

72-77 Motions of Heave, Roll and Pitch in 45' Length Class. 142-144

78-83 Motions of Heave, Roll and Pitch in 65' Length Class. 145-147

84-89 Motions of Heave, Roll and Pitch in 75' Length Class. 148-150

90-97 MII of 35'. 151-155

98-105 MII of 45'. 155-159

106-114 MII of 65'. 159-163

115-122 MII of 75'. 164-167

List of Tables

1 Number of vessels registered in 1988 compared with 1999 and rate of change. . . 7

2 Fatalities occurred in vessels less than 25 feet of length. 8

3 Lateral Force Estimator (*LFE*) limits in terms of Acceleration of Gravity (G). . . 18

4 Computed Coefficient of Friction (μ). 24

5 Comparison of LFE_{RMS} values computed in the Time-Domain with Equation 19. . 28

6 Definition of MII Test Cycle. 32

7 Format of an Identification ASCII file on subject information details. 33

8 Particulars of Final MII Drive Time Histories (ABCD Group 1992). 39

9 Total Number of MIIs observed. 43

10 Classification of MII types. 44

11 Classification of the other types of MII. 45

12 Empirical Tipping Coefficients. 45

13 Criteria versus ship subsystems. 58

14 General operability limiting criteria for Fishing Vessels. 58

15 Points of view considered in the criteria. 59

16 Twelve types of seakeeping performance criteria. 59

17 Selected Points on board Fishing Vessels. 67

18 Characteristics of the Wave Field. 68

19 Characteristics of the 35' Fishing Vessel "Atlantic Swell." 69

20 Characteristics of the 45' Fishing Vessel "Bold Wind". 69

21 Characteristics of the 65' Fishing Vessel "Ocean Billow" 69

22 Characteristics of the 75' Fishing Vessel "Shamook" 70

23 Period of Roll and Pitch 86

24 MII for 35' Length Class at Fn=0.2 104

25 MII for 45' Length Class at Fn=0.2 105

26 MII for 65' Length Class at Fn=0.2 106

27 MII for 75' Length Class at Fn=0.2 107

28 MII for 35' Length Class at Fn=0.4 108

29 MII for 45' Length Class at Fn=0.4 109

30 MII for 65' Length Class at Fn=0.4 110

31 MII for 75' Length Class at Fn=0.4. 111

32 AMIp at Fn=0.2. 113

33 AMIp at Fn=0.4. 113

34 Maximum Individual Values at Fn=0.2. 115

35 Maximum Individual Values at Fn=0.2. 115

36 AMI and Maximum MII at Fn=0.2 117

37 AMI and Maximum MII at Fn=0.4 117

38 Location at Fn=0.2. 119

39 Location at Fn=0.4. 119

40 MII at Fn=0.2. 120

41 MII at Fn=0.4. 120

42 MII of each length class at four wave fields. 122

43 AMIp at two speeds. 124

Nomenclature

Abbreviations

MAIB	Marine Accident and Investigation Branch of the United Kingdom
SAR	Search and Rescue
MRSC	Maritime Rescue Sub-Centre
CGA	Coast guard Auxiliary
DFO	Department of Fisheries and Oceans
WHSCC	Workplace, Health, Safety, and Compensation Commission
TC-Marine Safety	Transport Canada - Marine Safety
CIHR	Canadian Institutes of Health Research
SFVS	Safer Fishing Vessel Seakeeping
CCG	Canadian Coast Guard
DREA	Defence Research Establishment Atlantic
ISO	International Organization for Standardization
NATO	North Atlantic Treaty Organization
ABCD	American-British-Canadian-Dutch Working Group on Human Performance at Sea
SNAME	The Society of Naval Architects and Marine Engineers
IOT	Institute of Ocean Technology
ITTC	International Towing Tank Conference
ABS	American Bureau of Shipping
NBDL	U.S. Naval Biodynamic Laboratory
TNO	The Human Factors Research Institute
SMS	Ship Motion Simulator Platform
MII	Motion Induced Interrupt
MSI	Motion Sickness Interrupt
MIF	Motion Induced Fatigue
AMIp	Average Motion Interrupt over points
LFE	Lateral Force Estimator
g	Acceleration of Gravity Force
C.G.	Centre of Gravity
e	Earth Coordinate System
s	Ship Coordinate System
RMS	Root Mean Square
GMT	Transversal Metacentric Height
DAS	Data Acquisition System
GPS, DGPS	Global Positioning System and Differential Global Positioning System

List of Symbols

$\vec{D} = (D_1, D_2, D_3)$	Vector of Displacement
$\vec{P} = (X, Y, Z)$	Vector of an Arbitrary Point
$\vec{\eta} = (\eta_1, \eta_2, \eta_3)$	Vector of Translation
$\vec{\xi} = (\eta_4, \eta_5, \eta_6)$	Vector of Rotation
$\vec{F}_e$	Inertial Force in the Earth Coordinate System
$\vec{F}_s$	Force in the Ship Coordinate System
F_{Long} , F_{Lat} , F_{Vert}	Longitudinal, Lateral and Vertical Force per Unit Mass
l/h	Tipping Coefficient of Friction
μ_s	Static Coefficient of Friction
μ	Computed Coefficient of Friction
T_L	Zero-Crossing Period
T_T	Period of an Arbitrary Task
GLFE, GL1, GL2	General Lateral Estimators, Starboard and Port
$\vec{x} = (x, y, z)$	Displacement Vector along Fixed Axes
$\vec{\omega} = (\omega_1, \omega_2, \omega_3)$	Angular Velocity Vector around Instantaneous Axes
(θ, ϕ, ψ)	Rotation Angles of Roll, Pitch and Yaw
I	Moment of Inertia Matrix
ω_Z	Natural Frequency of Heave
ω_Φ	Natural Frequency of Pitch
ω_θ	Natural Frequency of Roll

Chapter 1

Introduction

Fishing is a high risk occupation. The safety records of the fishing industry in contrast to other industries, shows that this occupation is still one of the most dangerous by a considerable margin [1]. Thousands of men have died performing this occupation, and many others have been seriously injured. Despite technological advances, no drop in mortality rates has been observed. Technical improvements cannot control the natural forces of the wind and the oceans, eliminate human error or ensure accident proof machinery [2].

Analyzing the safety records from the Marine Accident and Investigation Branch of the United Kingdom (MAIB) [1], the fishing industry, compared to other industries, is clearly the most dangerous of all by a significant margin. MAIB states that between the year 1995 and 1996 there were 77 fatal injuries per 100,000 fishermen compared to 23.2 per 100,000 employees of the mining and quarrying industry, the second most dangerous. This institution received 1,418 accident and incident reports in 1999, and 641 were related to vessels. Moreover, this number is probably higher because many accidents are not reported to the authorities. The statistics from the United Kingdom presented in Figure 1, show the dramatic increase in the percentage of vessels lost since 1998. This percentage is between 0.27% and 0.45% of the total registered vessels in the UK, (7,460 vessels registered in 1999).

The largest contribution to the number of accidents is due to machinery damage, and is present in more than 50% of the accidents. The other important contributions, indicated in Figure 2, are foundering and flooding, grounding, collision, and contact. The percentage rate of accidents due to flooding and foundering is estimated at 15% to 20%. An estimation of severity of these accidents is evaluated in Figure 3.

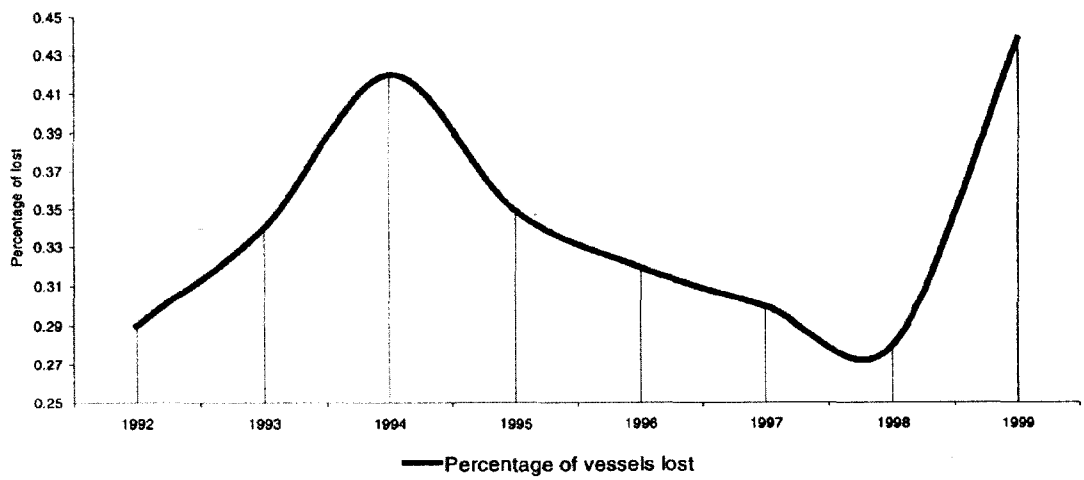

Figure 1. Proportion of vessels lost from 1992 to 1999.

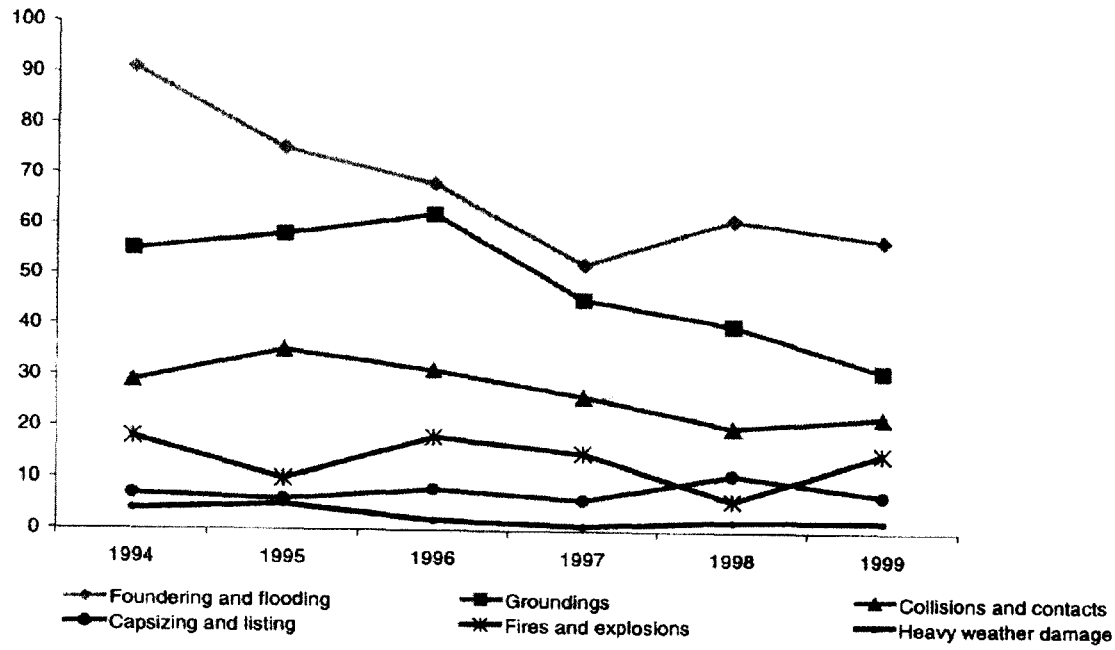

Figure 2. Accidents to fishing vessels by accident type.

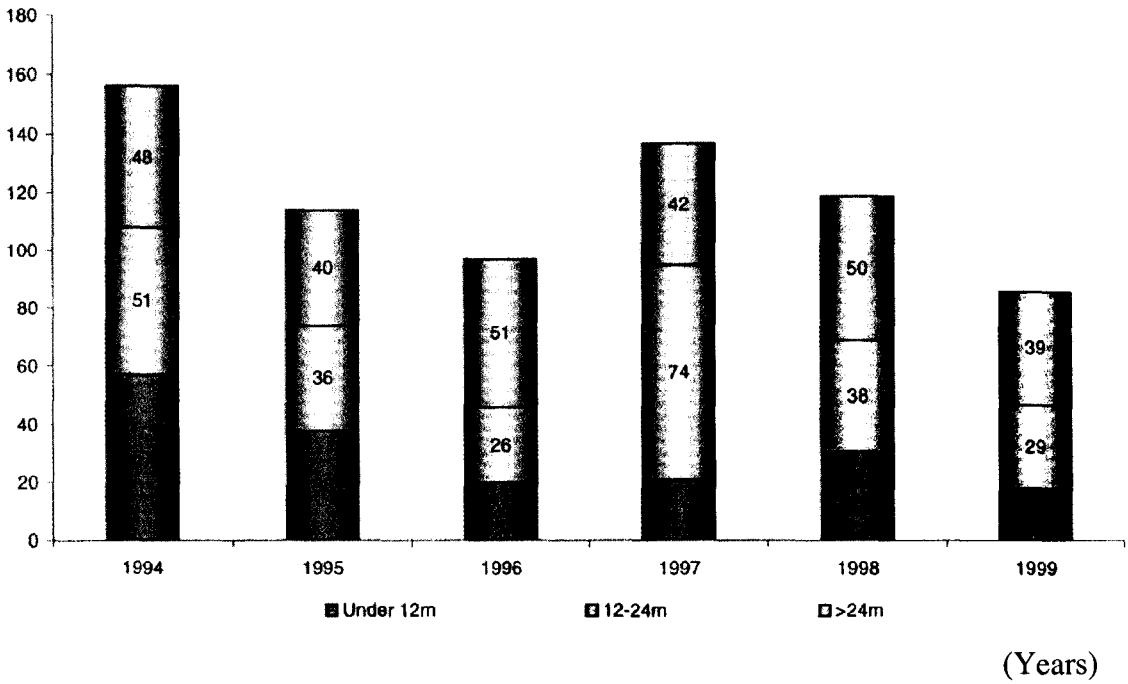

Figure 3. Accidents to crew.

The statistics gives an important source of information about how the size vessel influences the occurrence of accidents. Almost 30% of crew related accidents on board vessels less than 12 meters (39 feet) in length results in fatalities. In this length class, the crew also suffer the most severe injuries when non fatal accidents occur [1]. In general, vessels less than 12 meters (39 feet) in length are prone to accidents, see Figure 4. From statistical estimations it can be concluded that small vessels in the UK have the highest rate of accidents. Moreover, the number of registered vessels for this length class has been decreasing since 1997.

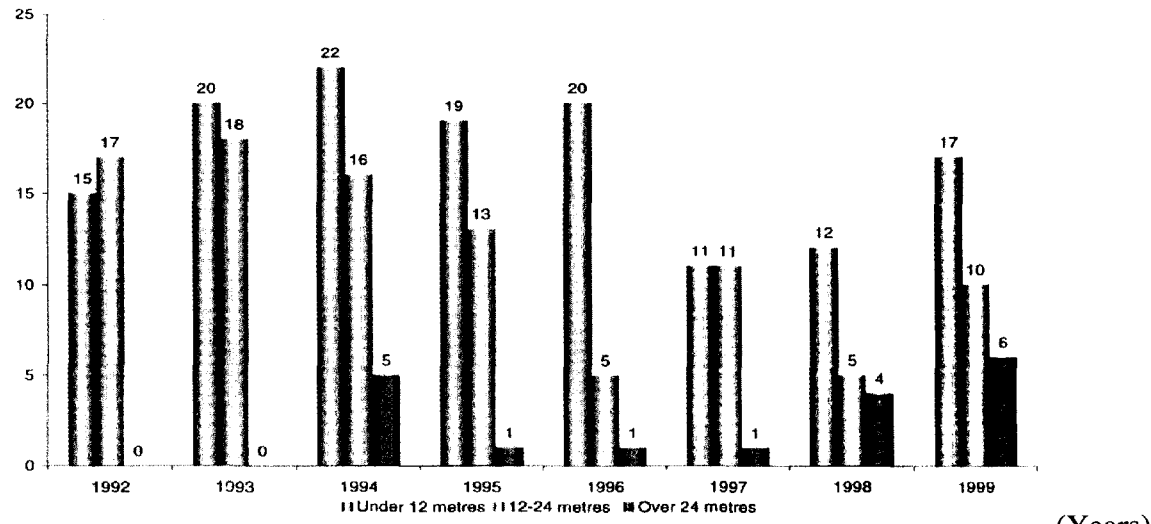

Figure 4. Vessels lost from 1992 to 1999.

The Canadian fishing industry faces almost the same problem. Although Canadian fishing vessels are some of the most highly regulated in the world [4], the problems with registration and accidents in small vessels are very similar to Europe.

Based on the records of Canadians organizations – SAR, MRSC, CGA, DFO, WHSCC and TC-Marine Safety – involved in fishing safety, they establish that fishing is the most dangerous occupation in northern Canadian waters [3]. More specifically, the Newfoundland fishing industry is faced with this same challenge. Newfoundland, an island off the east coast of Canada, has the Maritime Rescue Sub-Centre (MRSC) in St. John's. In its 1999 report [3], it is stated that the Centre mainly assisted ships of 45 to 65 feet in length, representing 38% of the total registered fleet for that year.

The information given by the Maritime Search and Rescue (SAR) of Newfoundland and Labrador, presented in Figure 5, indicates a serious increase in the number of accidents for small boats. The records from SAR reveal that most accidents, for vessels less than 65 feet, involved mechanical failures and steering problems. The report indicates that other relevant causes are sinking, taking on water, fire, and medical emergencies. The number of incidents due to these other causes was 193 during 1993, and 382 in 1999, an increase of 98 % in six years, see Figure 6.

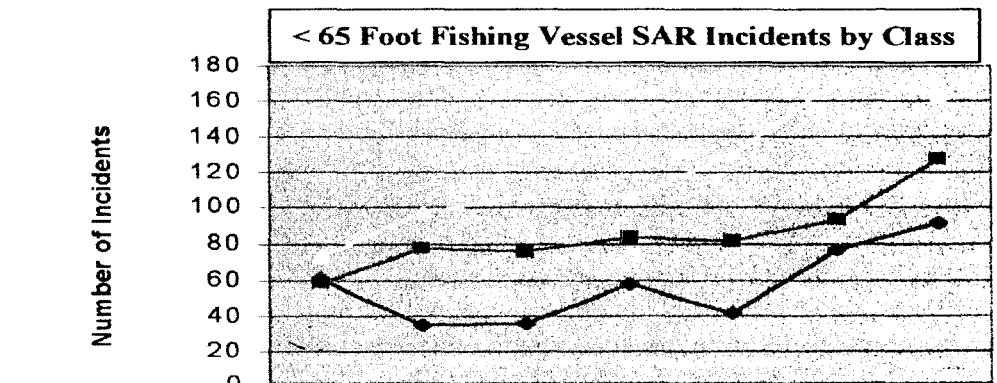

	93	94	95	96	97	98	99
< 35 FT	61	35	36	58	42	77	91
35 < 45 FT	59	78	76	84	82	93	128
45 < 65 FT	73	97	106	105	130	171	163

Figure 5. SAR incidents by vessel length class between 1993 and 1999.

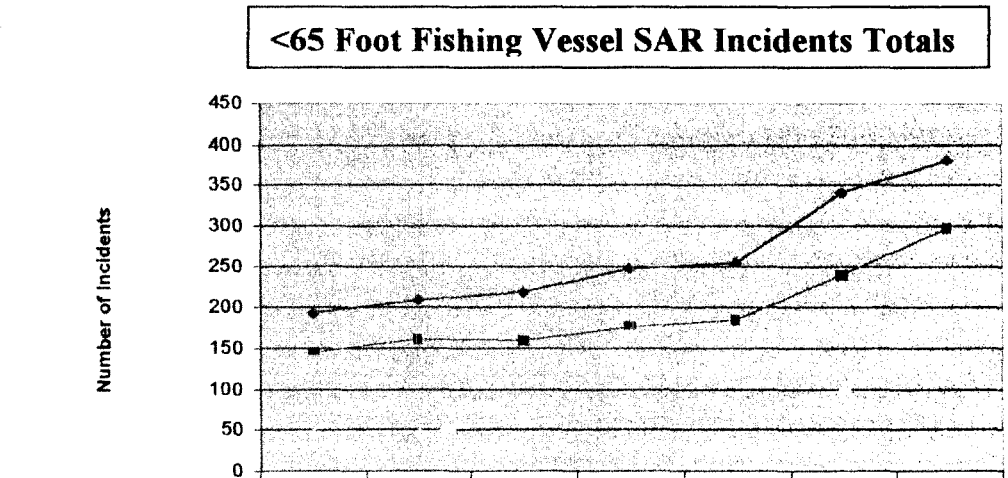

	93	94	95	96	97	98	99
Total SAR Incidents	193	210	218	247	254	341	382
Disabled Incidents	147	163	161	178	187	241	299
All Other Incidents	46	47	57	69	67	100	83

Figure 6. Total SAR incidents between 1993 and 1999.

But the report also shows that the number of registered vessels decreased from 13,915 to 9,573 in that period of time. As in the UK, Newfoundland SAR reported a dramatic increase in the incidents ratio for vessels less than 65 feet in length since 1993, and a decrease in the registration since 1988, see Figure 7 and 8.

The incident ratio is the relationship between two years, 1999 and 1993, expressed as a proportion, which in the present case is related to the increase in the amount of incidents. A comparison of vessel registration between years 1988 and 1999 is presented in Table 1. Likewise, from Table 2 it is possible to conclude that most of the fatalities occurred in fishing vessels less than 25 feet in length, the length class with the smallest registration.

Fishing Vessel Registration Comparison			
Vessel Size	1988	1999	% Change
< 35'	15843	8589	-46%
35' - 39'11"	561	209	-63%
40' - 44'11"	157	325	107%
45' - 54'11"	350	212	-39%
55' - 64'11"	142	231	63%
TOTAL	17053	9566	-44%

Table 1. Number of vessels registered in 1988 compared with 1999 and rate of change.

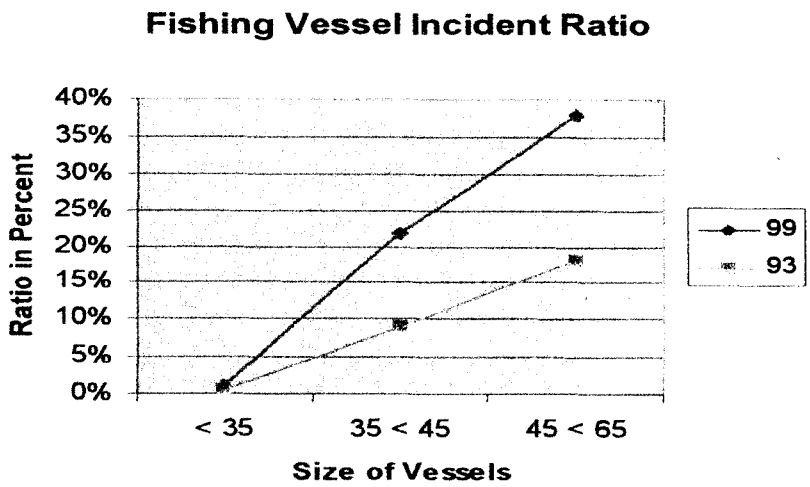

Figure 7. The ratio of incidents per registered vessels.

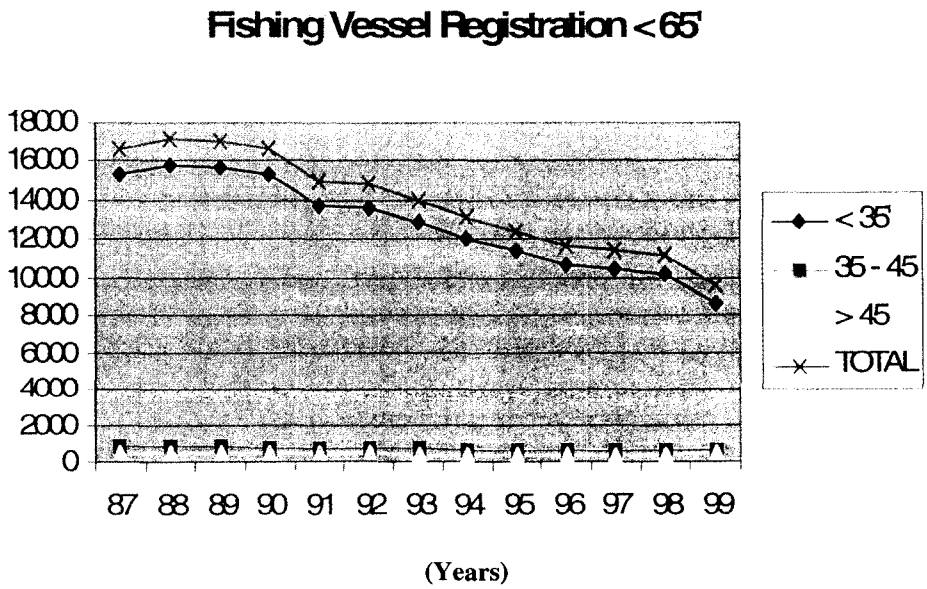

Figure 8. Registered fishing vessels from 1987 to 1999.

Fatalities < 65 Foot Fishing Fleet						
Year	< 25	25 - 35	35 - 45	45 - 65	Fatalities by Fishery	Total fatalities
93	9	0	1	0	4 seal, 3 lobster, 1 shrimp, 1 crab, 1 groundfish	10
94	2	0	6	1	1 lobster, 7 groundfish, 1 crab	9
95	0	3	0	0	3 scallop	3
96	3	0	0	0	1 seal, 2 groundfish	3
97	5	1	0	1	1 seal, lobster, 4 groundfish	7
98	4	0	0	0	4 ground fish	4
99	0	0	0	0	0	0
00	6	2	0	2	2 shrimps, 3 lobster, 5 ground fish	10
TOTAL	29	6	7	4		46
6 Seal, 9 Lobster, 3 Shrimps, 2 Crab, 23 Ground fish, 3 Scallop						

Note: only includes fatalities while vessels were active in the fishery.

Table 2. Fatalities occurred in vessels less than 65 feet of length.

Because of this dramatic increase in the number of accidents on board small boats, fishing vessel safety has been an important concern of international and local fishing industries for a long time. One of the problems today for commercial fishers in Newfoundland is that the inshore supply has been depleted forcing the fishers to go out into the offshore waters. Particularly for vessels less than 65 feet of length, this requirement to fish in the open sea, forces the crews to work in a more hostile environment under the same safety measures implemented for coastal zones.

Furthermore, new and larger fishing quota allocations are given to the small fishing vessel fleet, for species that live usually in the offshore areas. Some of these species include Crab, Shrimp, Seal, Turbot and Tuna fish. Therefore, small vessels must navigate further out into the Economic Zone Limit to find adequate supply of those species. This inevitably increases the length of fishing periods on the open sea. Often those vessels neither have been properly converted to fish a particular species nor have been able to accommodate the more adverse physical conditions of the offshore region.

The marine environment of Newfoundland and Labrador brings an additional high risk level for the fishing operations. The rough weather has the most effect on the small vessels and often affects their capacity to safely navigate and to return to their home port. The rough weather condition, coupled with fishing far from base port, highlights another risk element: inadequate stability of the vessel. Many of the smaller vessels are not designed to catch these offshore species. This lack of proper outfitting decreases the stability and reduces the safety margins of the vessels. However, there is a need to maximize the catches and to save time by returning quickly to harbour before weather conditions worsen.

As a result of the weather conditions and the poor motions, the vessels and the personnel begin to suffer the consequences of longer periods of fishing in the open sea and the inadequate matching of the catch species to the vessel. In the first case, due to short periods of inactivity, the vessels spend less time at dock. The resulting low level of maintenance produces dangerous strains and stress levels in the hull structures, engines and equipment.

In the second case, the crew are stressed and their safety is jeopardized. Having motion fatigue, working many hours in small quarters or on the open decks, along with the pressure to reach the minimum quota, become factors which often contribute to accidents and economic loss.

Under these conditions the crew must work longer periods, during the day and throughout the night, carrying heavy loads on wet decks, operating several types of equipment in unpredictable sea states, and constantly having to resist the irregular motion of the vessel. As a result, the crew starts to lose their ability to effectively perform assigned tasks. This crew operational performance degradation can be measured in terms of

Seakeeping Performance criteria and in terms of Motion Induced Interrupt (MII) criteria as well.

Having noted the above circumstances, this research attempts to assess the motions of the Newfoundland fleet's fishing vessels and to establish MIIs on the crew of these vessels using an existing numerical code called Motion Simulation Program (MOTSIM). In order to achieve this objective, the validation of the MOTSIM numerical code by means of the Sea Trials is conducted.

With the aim of accomplishing this, Chapter 1 presents an introduction to the fishing occupation. Then, Chapter 2 introduces a general description of the project, fishing vessels safety and the MII definition. In Chapter 3, the recent work on MII, the background of wave theory and ship motions, and Seakeeping criteria is reviewed. The numerical model is explained in detail in Chapter 4. In Chapter 5 a description of the Sea Trials and the comparison between the Full Scale experiment and the Numerical Simulations is evaluated. The numerical calculations for different wave field representations and the MII values are presented in Chapter 6. Furthermore, this chapter analyses the effect of the vessel length, position on deck, and speed. Likewise, Chapter 7 detemined the wave field conditions in two locations of the Newfoundland coast and the vessel's profile due to change in wave parameters. Finally, Chapter 8 presents the conclusions.

Chapter 2

Fishing Vessels Safety and MII

In order to investigate occupational health and safety of marine and coastal work, a government program called *SafetyNet* was created. "This program is a Community Alliance for Health Research with major funding from the Canadian Institutes of Health Research (CIHR). *SafetyNet* includes researchers in medicine, nursing, social sciences, natural sciences, engineering and marine sciences, and involves partners in the public sector, private sector and in the very coastal communities in which the research is taking place."

One of the components of this program is the *SafeCatch* program. The latter is a "multi-disciplinary and inter-sectoral research program that incorporates a substantial knowledge translation component". The program establishes a complete methodology to study the factors that influence fishing safety via six different related aspects. One of these aspects is the Safer Fishing Vessel Seakeeping (SFVS). In this particular research, selected data from sea trials are collected. These are used to validate an existing numerical code for the prediction of motions on board of the fishing vessels. This prediction evaluates the influence of vessel design and fishing operations on seakeeping performance and fish harvester occupational safety.

2.1 Fishing vessels safety.

Since the discovery of the wheel and even before this time, human beings have forever tried to overcome their limitations by creating their own tools. For these ancient

persons, the designer was often the same person as the producer and the user of the technology. After several ages, the human drive to have greater control of the environment influenced greatly the imagination to create even more complex tools.

"With this evolutionary increase in complexity and differentiation, there arose further specialization with the designing of technology that separated the designer from the producer and the user. More recently, with the development of the electronic dimension of technology, there has come an increased demand for accuracy, performance, efficiency, and replication. While admirably this has been achieved on several levels, there is an essential side to any development in technology. This side considers the effects of invention on the human population and the natural environment" [7].

One dimension of this is the working environments in which the technology is created. The other is the conditions in which it is used and the intent behind its use. The propensity to overlook the importance of the human factor usually prevails revealing how easily this can occur and be carried out by all those involved: designer, producer and user at their respective levels of engagement with the technology [7].

In the particular case of the fishing industry, the design of the vessel plays an important role in the safety of the crew. For the past 300 years, in the building of ships, designers have formulated rules and regulations to consider personal safety, for example, in the very early design stage of the design spiral. Those regulations have evolved out of many years of experience of vessel construction and they depended on the type of vessel being created.

Applying these regulations gave rise to certain specifications for vessel design. From the experience of using these designs, modifications were made, giving rise to new

regulations. Likewise, the same process of evolutionary design has occurred in the catch methods of the vessels and further influenced by the country in which the methods are used.

Regulations define the principal functions of a fishing vessel. There are four basic functions of a fishing vessel [7]:

- Floating and sailing.
- Tracing and catching fish.
- Fish processing, storing and quality control.
- Transporting and landing.

From these functions the shipbuilding and shipping rules established safety aspects regarding the construction, stability and watertight compartmentation, materials, layout and outfitting linked with the general design. The major problem that exists is that shipyards do not include, within the above aspects, sufficient safety considerations, which involve the human well-being and the improvement of the working conditions.

For the past 25 years designers and shipowners have become aware of the relevance of this issue and have begun to include it in their deliberations with the intention of improving the safety regulations and hence the standard of vessel design and the quality of work place for the crew. Moreover, academic research and the computational tool has contributed to optimize the vessels safety-design and to decrease the risk level for the workers on board.

Today, despite these scientific developments it is not possible yet to predict accurately the occurrence of accidents on board small fishing vessels or simulate the motions and the effects of them on human stability and balance. This approach requires the

implementation of a recent concept into a numerical model. This concept is called "Motion Induced Interrupt" MII.

2.2 Motion Induced Interrupt MII Criteria.

The maritime industry is unique in many aspects; one of the most representative aspects is that workers must live at their workplaces. This condition affects workers on offshore platforms as well as vessels. They must not only consider living away from home for long periods of time, but also confront motions of roll, pitch and heave in adverse weather conditions. These motions produce vibrations and noise harmful to their health. As a consequence the mental fatigue increases, affecting the performance of the crew on board. Certainly these aspects contribute to augment the risk of human error.

In order to reduce this potential danger the habitability aspect in the design of the vessel is accounted for. This factor involves facility design and the ambient environmental conditions. The American Bureau of Shipping (ABS) in [8], define habitability as: "the acceptability of conditions on-board a ship in terms of vibration, noise, indoor climate and lighting as well as physical and spatial characteristics, according to prevailing research and standards for human efficiency and comfort."

The human efficiency and comfort is reflected in the individual performance of operations on board. The type, quality and quantity of the accommodations can be a positive factor for the crew, but the variety of environmental conditions could be a negative factor for their performance.

For this reason, the prediction of the operational performance of vessels with respect to the environmental conditions in the very early stage of the design is extremely important. Based on this idea, Graham [9] presents three basic considerations:

1. A statistical description of the wave and wind environment.
2. Computer programs for determining the ship response.
3. Numerical seakeeping criteria to quantify the effects of motions on systems of interest.

Currently, the wave and wind environment is very well represented by means of the wave and wind theory combined with the computational tool. Likewise, there are many computer programs based on the strip theory, potential theory, and panel methods that can predict with a high level of accuracy the behaviour of large vessels in a seaway. However, there is a need to develop the actual seakeeping criteria in order to predict with an acceptable level of accuracy the operability of the crew on board and complement the other two aspects. A review of the common seakeeping criteria currently in use by the designers and the measure of performance is covered in Chapter 3.

In terms of personnel operational performance, the seakeeping criteria consider only individual effects on the crew due to the motions of roll, pitch, lateral and vertical acceleration on board. But from the point of view of the operability, the criteria do not cover the effect due to a combination of motions together with accelerations in small floating platforms. This combination could be a more realistic and significant contribution to the physical degradation of personnel on board these type of vessels.

Another shortcoming of the current seakeeping criteria is that most of the limiting values within the criteria are the result of operational experiments in frigates and destroyers. Consequently, the predicted operational limits for personnel on board any other vessel unlike navy vessels are not well represented.

Furthermore, as Graham states, roll, pitch, and vertical and lateral accelerations are not the proper physical parameters for "expressing personnel criteria" [9]. The limiting values measured for each one of these parameters "found through operational experience are representative of the motion levels at which certain degrading effects start to become important" [9]. But, in case of crew working on deck, the level for quantifying degradation is different and should be represented in terms of loss of balance produced by a number of occurrences of tipping and sliding during a period of time. These criteria are Motion Induced Interrupts (MII) defined as the number of loss of balance events in a period of time which occur during an arbitrary operation due to forces transmitted to the body by the ship motion.

Chapter 3

Background in Seakeeping and Recent Work on MII

With the aim of establishing the effects of ship motions on operational performance in individuals, different experiments were carried out in the US Navy by Baitis [10] and by Graham [11], [12] during the eighties and the nineties. These studies involve only naval platforms and the ship-helicopter mission. This operation considers the launch and recovery of the helicopter, the transit, and the performance of the crew members responsible for the helicopter once it is on deck.

Baitis's research [10] was an outline for future expansion of the "operator guidance manual", which focuses on consideration of human factors in the deployment of helicopters for navy frigates. Thus, he applies the concept of the MII in the fifteen minutes touch-down helicopter task. Hence, computational ship motion time history was developed to measure the likelihood and severity of MIIs. Within this time history, parameters such as ship speed, heading angles, and modal periods were included. A computer simulation model established the crew performance during the task, incorporating the change of position, stance and center of gravity for each person. Then, from the computer model and the ship time history analysis, the effect of the ship-induced forces on the flight-deck crew was established. As a result, the MII and Root Mean Square RMS acceleration criteria were proposed.

Because the ship motion data used by Baitis and Graham [9] were evaluated in the frequency domain and the limit of acceleration for MII was measured in the time domain, a

direct application of MII criteria to the ship motion was not possible. Hence, the limits values were expressed in terms of a Lateral Force Estimator (*LFE*). This estimator represents a combination of earth- and ship -referenced lateral acceleration due to ship roll and expresses the lateral force with respect to the gravitational force (g). The *LFE* limit values in terms of g represent the incidence of MIIs in the form of tipping, sliding, or lifting off the deck on the hook-up crew. These limits are presented in Table 3.

Risk Level	*LFE*
Occasional or possible occurrence of MII	0.08g
Probable occurrence of at least one MII for every two recovery operations	0.10g
Serious, 1.44 occurrences of MII per operation	0.12g
Severe limitations, 2.61 occurrences per operation	0.14g
Extremely hazardous conditions, 4 occurrences per recovery manoeuvre	0.16g and above

Table 3. Lateral Force Estimator (*LFE*) limits in terms of Acceleration of Gravity Force (g).

3.1 Fundamentals of MII Theory.

In order to implement the above approach to improve the current seakeeping criteria, Graham and Baitis [9] recommend two steps:

1. Frequency domain methods must be developed to predict the incidence and severity of degrading events such as sliding of helicopters or MII's personnel on deck.
2. Operational data are required to determine acceptable limits for the incidence of occurrence of the degrading events.

The first step is discussed in this chapter and the second step is applied in Chapter 4 to the fishing vessels of the Newfoundland fleet as a part of the present research.

3.1.1 The Frequency Domain Method.

With the aim of introducing a practical tool for ship design, a frequency-domain method for predicting the occurrence and severity of MIIs on personnel or equipment, including the linearized forces due to roll, pitch, longitudinal, lateral and vertical accelerations, is described.

The prediction of MII is calculated assuming small longitudinal acceleration and zero wind effects.

3.1.2 Prediction of MII.

Consider a coordinate system for the MII calculations located outside the ship, (see Figure 9), representing an earth reference system (e) that translates with the mean velocity of the ship maintaining a fixed position about the free surface. Based on this arrangement, the motions of surge, sway, heave, roll, pitch, and yaw are denoted as $\eta_i, i = 1,.....,6$ [11].

The displacement $\vec{D} = (D_1, D_2, D_3)$ at an arbitrary point $\vec{P} = (X, Y, Z)$ is expressed by the equation:

$$\vec{D} = \vec{\eta} + \vec{\xi} \times \vec{P} \tag{1}$$

where $\vec{\eta}$ is the translatory displacement of the ship's *C.G.* and $\vec{\xi}$ is the angular displacement of the ship with respect to earth fixed system.

Using the above notation of $\vec{\eta} = (\eta_1, \eta_2, \eta_3)$ and $\vec{\xi} = (\eta_4, \eta_5, \eta_6)$ from Equation 1 it is possible to establish the equations for the displacements at P. In case of the vertical direction, the equation is:

$$D_3 = \eta_3 + \eta_4 Y - \eta_5 X \tag{2}$$

Equation 2 represents the displacement at P in the vertical direction influenced by the motions of heave, roll and pitch. Then, differentiating with respect to time in Equation 1, the velocities and accelerations are given by:

$$\dot{\vec{D}} = \dot{\vec{\eta}} + \dot{\vec{\xi}} \times \vec{P} \tag{3}$$

$$\ddot{\vec{D}} = \ddot{\vec{\eta}} + \ddot{\vec{\xi}} \times \vec{P} \tag{4}$$

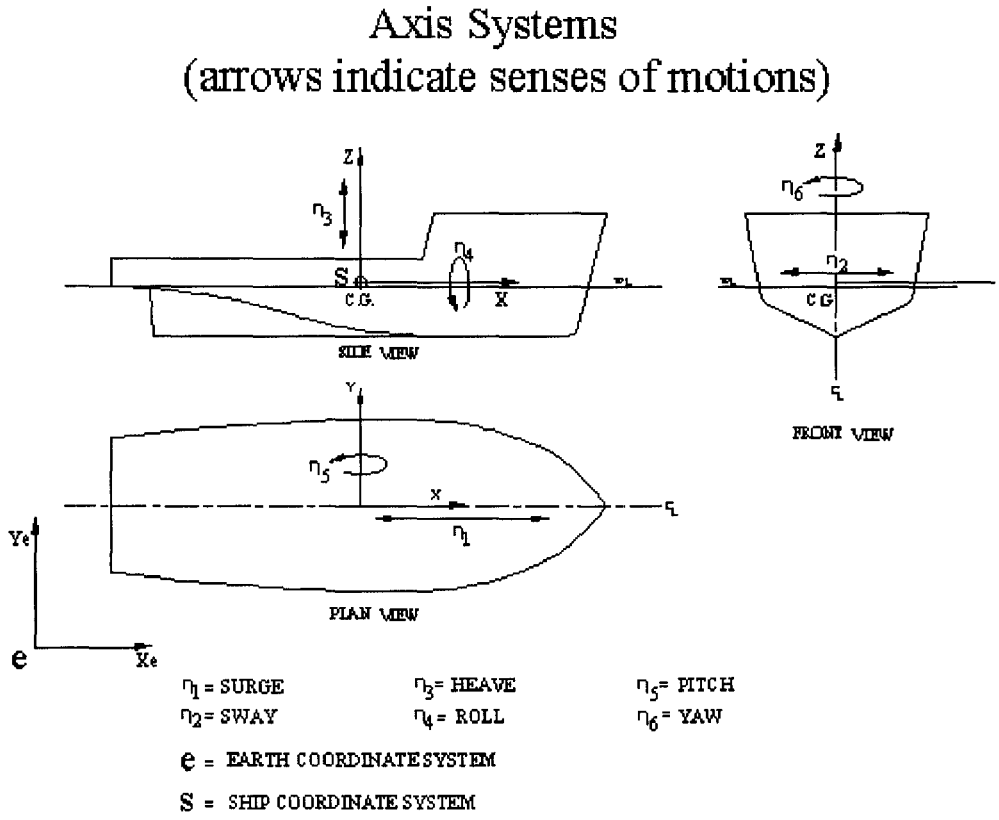

Figure 9. Coordinate System for MII calculations.

Consider an object of mass m placed on the ship with center of gravity *C.G.* at a point $\vec{P}$ subjected to an inertial force. This force is defined with respect to the earth coordinate system (F_e) in the following expression:

$$\vec{F}_e = -m(\ddot{D}_1, \ddot{D}_2, \ddot{D}_3 + g) \tag{5}$$

where g is the acceleration due to gravity and m is the mass of the object, which could represent a helicopter or a person. Subsequently, consider the forces parallel to the deck acting on a person standing or an object placed in an arbitrary location on the ship. In this case, these forces are referred to a ship coordinate system (s) positioned at its center of gravity *C.G.*, see Figure 9. Considering only the linear terms in the mathematical transformation from one coordinate system to the other, the forces in the ship coordinate system ($\vec{F}_s$) at position $\vec{P}$ are given by:

$$\vec{F}_s = m(-\ddot{D}_1 + g\eta_5, -\ddot{D}_2 - g\eta_4, -\ddot{D}_3 - g) \equiv m(F_{Long}, F_{Lat}, F_{Vert}) \tag{6}$$

where F_{Long} is the longitudinal force per unit mass given by:

$$F_{Long} = -\ddot{D}_1 + g\eta_5 \tag{7}$$

the lateral force per unit mass, F_{Lat}, by:

$$F_{Lat} = -\ddot{D}_2 - g\eta_4 \tag{8}$$

and the vertical force per unit mass, F_{Vert},by:

$$F_{Vert} = -\ddot{D}_3 - g \tag{9}$$

Equations (7) and (8) represent the linearized longitudinal and lateral forces per unit mass called Lateral Forces Estimators *LFE* [10]. The limit values of *LFE* in terms of g are presented in Table 3. The experiences with monohulls [13] determine that the longitudinal accelerations are small and do not influence the incidence of MII. On the contrary, the main contributor to MII is the lateral motion. Furthermore, for other type of floating platforms the presence of MII due to longitudinal accelerations is highly possible. Therefore, the

method described below can be adapted to include the MIIs due to longitudinal accelerations.

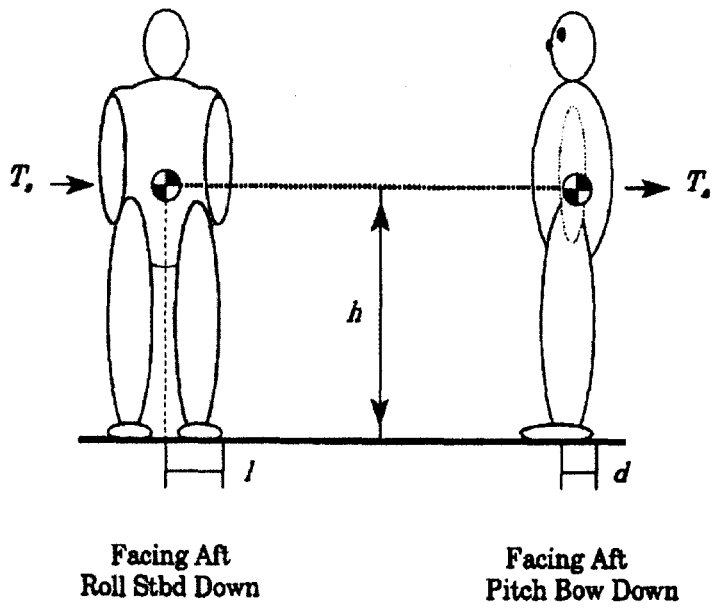

Figure 10. Subject Model.

Suppose that a person is walking or standing on deck, facing forwards or aft. Considering the center of gravity of that person at a height h, measured from the deck floor and the width of his/her stance as $2l$, (see Figure 10). Then, under the assumption of $F_{Long} \approx 0$, which implies that slides can occur in the port or starboard directions, a slide to port at point $\vec{P}$ is expressed by:

$$mF_{Lat} > -m\mu_s F_{Vert} \tag{10}$$

and a slide to starboard at point $\vec{P}$ occurs whenever:

$$mF_{Lat} < m\mu_s F_{Vert} \tag{11}$$

where μ_s is the static coefficient of friction.

It is assumed that the vertical force is always negative. This assumption is based on the fact that the vertical acceleration of the ship is always less than *g*. If not, no evaluation of MII is required, because an acceleration bigger than *g* makes any operation unfeasible.

Continuing with Equations (10) and (11) and taking moments about either foot, the condition for tipping at point $\vec{P}$ is:

$$h\left|F_{Lat}\right| > -lF_{Vert} \tag{12}$$

Graham proposed in reference [11] typical values for *h* and *l*, such as:

$$\left.\begin{array}{l} h = 0.91 \text{ m} \\ l = 0.23 \text{ m} \end{array}\right\} \quad \frac{l}{h} \tag{13}$$

Then, the parameter $\frac{l}{h}$ is called "tipping coefficient of friction" and is equal to 0.25.

The shortcoming of Equation 12 is that the capability of a person to shift his or her center of gravity is not included. This aspect is mentioned by Graham as a "conservative equation". In Table 4 are presented the results of Computed Coefficients of Friction (μ) as a result from experiments carried out by Graham using a sliding-chair on board the USCG *Morganthau* [9]. This table presents 17 of 25 sliding incidents.

Time of event	μ
34.9	0.184
54.6	0.182
75.5	0.205
302.6	0.174
500.1	0.174
559.7	0.166
776.8	0.168
803.8	0.162
827.1	0.161
967.3	0.191
1038.9	0.219
1117.2	0.207
1125.8	0.175
1141.8	0.176
1152.5	0.211
1176.1	0.211
1186.1	0.245

Table 4. Computed Coefficient of Friction (μ).

However, the value of the coefficient of friction varies with respect to the deck conditions. In dry deck conditions, for example, tipping is more significant. In reference [10] the dry conditions has a friction coefficient value of 0.7. In case of wet deck conditions, slipping is significant and perhaps tipping became important as well.

Expanding Equation 12, tipping occurs when:

$$-g\eta_4 - \ddot{D}_2 - \frac{l}{h}\ddot{D}_3 > \frac{l}{h}g \qquad \text{or,} \qquad (14)$$

$$g\eta_4 + \ddot{D}_2 - \frac{l}{h}\ddot{D}_3 > \frac{l}{h}g \qquad (15)$$

It must be noted that in the particular case of zero vertical acceleration Equations 14 and 15 reduce to:

$$\left|g\eta_4 + D_2\right| > \frac{l}{h}g \qquad (16)$$

where the expression in absolute value is called the Lateral Force Estimator (*LFE*).

Determine MIIs in the Frequency Domain considering Vertical Acceleration $\ddot{D}_3 = 0$.

Following the above consideration, Equation 15 is evaluated assuming "a symmetric relationship between tipping events to port and to starboard" [11]. The calculation of MII frequency is established assuming that the distribution of *LFE* amplitudes is described by a Rayleigh distribution.

A Rayleigh distribution is a continuous probability distribution, commonly used in analysis of waves. It represents the probability that MII occurred within an interval of time [a,b], with $a \leq b$.

Based on this assumption, the probability that *LFE* is greater than $\frac{l}{h}g$ is denoted by:

$$P\left\{LFE > \left(\frac{l}{h}\right)g\right\} = e^{-\frac{1}{2}\left(\frac{\left(\frac{l}{h}\right)g}{LFE_{RMS}}\right)^2} \tag{17}$$

where LFE_{RMS} represents the Root Mean Square value of *LFE*. There are two forms of MII, one to port and the other to starboard, represented by $LFE > \left(\frac{l}{h}\right)g$.

An arbitrary operation on board requires a period of T_T seconds to be achieved. In the same way a zero-crossing period of performance *LFE* is denoted by T_L seconds. Subsequently, the total number of MII during the development of one operation is given by:

$$M = \frac{2T_T}{T_L} e^{-\frac{1}{2}\left(\frac{\left(\frac{l}{h}\right)g}{LFE_{RMS}}\right)^2} \tag{18}$$

For the evaluation of LFE_{RMS} in the frequency domain the expression is given by:

$$LFE_{RMS} = \left[\int_0^{\infty} \left(\frac{L_0(\omega_e)}{\zeta_0(\omega_e)} \right)^2 S_\zeta(\omega_e) d\omega_e \right]^{\frac{1}{2}} \tag{19}$$

where L_0 is the LFE amplitude, ζ_0 is the wave amplitude, S_ζ is the wave spectral density, and $\left(\frac{L_0(\omega_e)}{\zeta_0(\omega_e)} \right)$ is the transfer function of *LFE*. All the terms are with respect to ω_e, which is the angular frequency of encounter. Then, expanding the transfer function of *LFE* it is possible to obtain:

$$\left(\frac{L_0(\omega_e)}{\zeta_0(\omega_e)} \right)^2 = g^2 \left(\frac{\eta_{40}(\omega_e)}{\zeta_0(\omega_e)} \right)^2 + \omega_e^4 \left(\frac{D_{20}(\omega_e)}{\zeta_0(\omega_e)} \right)^2$$

$$-2g\omega_e^2 \left(\frac{\eta_{40}(\omega_e)}{\zeta_0(\omega_e)} \right) \left(\frac{D_{20}(\omega_e)}{\zeta_0(\omega_e)} \right) \cos(\delta_{\eta 4}(\omega_e) - \delta_{D2}(\omega_e)) \tag{20}$$

where η_{40} is the roll amplitude, $\left(\frac{\eta_{40}(\omega_e)}{\zeta_0(\omega_e)} \right)$ is the transfer function for the motion of roll, D_{20} is the amplitude of D_2 and $\left(\frac{D_{20}(\omega_e)}{\zeta_0(\omega_e)} \right)$ describes the transfer function for the displacement in the transverse direction D_2. In the same way, $\delta_{\eta 4}$ describes the roll phase angle relative to the wave elevation at the *C.G.*, δ_{D2} represent the sway displacement phase angle relative to the wave elevation at the *C.G.* and $(\delta_{\eta 4}(\omega_e) - \delta_{D2}(\omega_e))$ denotes the phase angles of roll and sway displacement with respect to the wave elevation at the ship's *C.G.* As in the previous equation, all the terms are with respect to ω_e.

On the other hand, the expression for the calculation of the zero-crossing period of the *LFE* is given by:

$$T_L = 2\pi\left(\frac{m_0}{m_2}\right)^{\frac{1}{2}} \tag{21}$$

Under the assumption that *LFE* amplitudes follows a Rayleigh distribution and based on the results provided, Graham considers, *LFE* for port and starboard as "zero-mean Gaussian processes, and not restricted to narrow-band processes" [9]. Then, the spectral moments for the wave spectral density S_ζ in terms of the transfer function of *LFE* and the frequency of encounter, is presented as:

$$m_n = \int_0^\infty \omega_e{}^n \left(\frac{L_0(\omega_e)}{\zeta_0(\omega_e)}\right)^2 S_\zeta(\omega_e) d(\omega_e) \tag{22}$$

Baitis's results in Table 5 are obtained from experiments in the US Navy FFG-8 Frigate class during the task of securing a helicopter message line [10]. This table presents the values for different risk levels of MII in terms of *LFE* calculated using a US Navy Standard Ship Motion Program. In Baitis's experience, significant wave height of 10.2 feet (3.11 m) and 13 feet (3.96 m) were considered. The change in the C.G. of the person during the message line hook up operation was neglected.

Furthermore, the data in this experiment were insufficient for estimating accurate values of T_L in significant MII events. Therefore, the roll natural period $T_\phi = 10$ s instead of the value of T_L was assumed.

This assumption was introduced based on predictable and reliable roll behaviour of the frigate class, which experience its more extreme roll amplitudes in the natural period. However, this assumption is only appropriate in resonant rolling situations, because the frequencies near the roll resonance are often very low.

In Table 5 a comparison between LFE_{RMS} values calculated throughout an analysis of ship motion time domain and LFE_{RMS} obtained from Equation 19 is presented. Both results for LFE_{RMS} were very similar, except for case of high LFE values. This could be a consequence of the previously mentioned assumptions, but in the same way, it demonstrates a high dependence of MII on the T_L in Equation 17. The T_L period depends as well on the ship speed and the angle of heading. This dependence can be inferred from the occurrence of more MII due to high encounter frequency values than due to low encounter frequency values.

Risk Level	MIIs	LFE_{RMS} from Time-Domain (g)	LFE_{RMS} in frequency domain (19)
1	0.06	0.08	0.08
2	0.50	0.10	0.11
3	1.44	0.12	0.13
4	2.61	0.14	0.15
5	4.00	0.16	0.19

Table 5. Comparison of LFE_{RMS} values computed in the Time-Domain with Equation 19.

Baitis' results underestimate the importance of the ship speed and the heading angle. Hence, the high dependence of MII on T_L was completely ignored. He also mentioned the inaccuracy of the current mathematical modelling of human factors and the necessary improvement of it in future validations. The orientation of the crew member relative to the ships axes is also ignored.

Determine MIIs in the Frequency Domain considering Vertical Acceleration $\ddot{D}_3 \neq 0$.

In this case the symmetry between occurrence of tipping incidences to port and to starboard is no longer present. For this reason the conditions of Equation 14 and 15 are now accounted for. Thus, there are two lateral force estimators called "Generalized Lateral Estimators" (*GLFE*) and divided in *GL1* and *GL2* in the following expressions:

$$GL1 = g\eta_4 + \ddot{D}_2 + \frac{l}{h}\ddot{D}_3 \tag{23}$$

$$GL2 = g\eta_4 + \ddot{D}_2 - \frac{l}{h}\ddot{D}_3 \tag{24}$$

Assuming that *GLFE*s follows a Rayleigh distribution, then the probability that $GLi > \left(\frac{l}{h}\right)g$ is given by:

$$P\left\{GLi > \left(\frac{l}{h}\right)g\right\} = e^{-\frac{1}{2}\left(\frac{(l/h)g}{GLi_{RMS}}\right)^2} \qquad i = 1,2 \tag{25}$$

Considering that M_1 describe the number of MIIs events in the performance of one evolution of an arbitrary task of T_T seconds, which resulted from *GL*1 satisfying Equation 14. In the same way, M_2 comes from *GL*2 and satisfy Equation 25 and represents the MII due to Equation 15.

Let T_{GLi} represents the zero-crossing period of GLi. Then, the general expression for MII is the following:

$$M\,i = \frac{T_T}{T_{GLi}} e^{-\frac{1}{2}\left(\frac{(1/h)g}{GLi_{RMS}}\right)^2} \qquad i = 1,2 \tag{26}$$

and the total number of MII in a complete task is given by:

$$M = M_1 + M_2 \tag{27}$$

From Equation 18 it is possible to obtain the values of RMS for GL_1 and GL_2. Likewise, the values of T_{GLi} and m_n can be calculated from Equation 21 and Equation 22 respectively.

3.2 Recent work on MII.

After the work of Baitis [10] and Graham [9], the Defence Research Establishment Atlantic (DREA) during a workshop on operability in 1989, proposed under a NATO umbrella, a multi national task group among Canada, the United States and the United Kingdom. The purpose was the development of experiments on human factors at the U.S. Naval Biodynamic Laboratory (NBDL) in New Orleans. At that time, NBDL owned the only Ship Motion Simulator (SMS) in existence in the world. The facility was able to simulate a limited number of motions and accelerations suitable enough for the experiment scope.

After one year, the group included researchers from the Netherlands within the original team and adopted the name of "American-British-Canadian-Dutch (ABCD) Working Group on Human Performance at Sea." In that year the Netherlands was

constructing their own SMS at The Human Factors Research Institute (TNO) and carried out several experiments in this area.

From that time until today, ABCD is conducting experiments and research in order to establish the effects of ship motion on the performance of the crew aboard NATO naval platforms. The ABCD task group presents to ship dynamics researchers and human sciences researchers an instance for "information exchange, collaborative planning and joint sponsorship of research and development work designated to investigate the effects of ship motions on human performance" [14]. Following this statement, the group contributes with their own experiences in naval platforms to expand the application of the research on different types of ships involving civilian governments and commercial agencies.

The aim of ABCD is to "develop methods and criteria for assessing the effects of ship motions on crews performing real tasks in the naval environment" [14]. In order to quantify the performance of crew in daily tasks on board naval platforms, a series of experiments in SMS were conducted. Different responses, such as incidence of stumbling, combinations of events as a consequence of environmental motions, ergonometric and postural stability, and psychological parameters were measured.

All the series of experiments were carried out with the contribution of 21 male volunteers enlisted in the U.S. Navy. Their age range was between 17 to 24 years. They performed specific physical and cognitive operations using accurate instrumentation under the supervision of the ABCD researchers and a medical staff. The results were analyzed and compared with the corresponding ship motion.

The SMS of NBDL describes motions of vertical displacements, roll angle and pitch angle and is able to save data electronically. Additional instrumentation included three

video cameras positioned in different locations inside the SMS, multi-component transducers mounted in each corner of the platform and communication equipment.

3.2.1 Description of MII experimental tasks:

The primary purpose of the experiments was to establish empirical expressions for the lateral and longitudinal tipping coefficient presented by Graham [12]. These values were established as 0.25 and 0.17 respectively. Thus, two validations were accomplished:

1. A time domain validation with the mathematical model values in the subject's lateral and longitudinal directions.
2. A frequency domain validation of the MII time average prediction.

Task Segment	Task	Task Description	Observation
Minute 1	Routine 1	Standing facing aft (lateral MIIs)	MIIs
Minute 2	Routine 2	Standing facing aft (lateral MIIs)	MIIs
Minute 3	Routine 3	Weight positioning task standing facing forward moving weight laterally through guide	MIIs
Minute 4	Routine 4	Standing facing aft with foam cylinder held overhead	MIIs
Minute 5	Routine 5	Repeated walking and turning port to starboard and back	MIIs
Minute 6	Routine 6	Athwart ships standing facing port (longitudinal MIIs)	MIIs

Table 6. Definition of MII Test Cycle.

3.2.1.1 General and Task Performance Synchronization:

With the cooperation of fifteen volunteers the static training experiments inside the SMS cab were conducted. Sequences of six one-minute tasks were carried out. A definition of the MII Test Cycle is presented in Table 6. There were two characteristic ship motion profiles denoted as Hotel (H) and Lima (L), see Table 7.

HOTEL MOTION PROFILE				
Run	Subj	CG Hght	Stan wdth	Tipng Coeff
638	252	39.04	17	0.218
638	252	40.79	18	0.221
638	252	37.54	12.5	0.166
638	252	39.04	17	0.218
638	252	39.04	18	0.231
638	252	39.04	17	0.218
638	252	40.79	17	0.208
638	252	39.04	12.5	0.16
626	254	41.13	17.5	0.213
626	254	40.63	18.5	0.228
626	254	41.13	11.8	0.143
615	255	39.89	22.5	0.282
615	255	43.14	23	0.267

Table 7. Format of an Identification ASCII file on subject information details.

Based on results from pilot studies conducted by the U.S. Navy [14], two of these tasks differ with respect to the others, which require the person to stand facing aft for two consecutives minutes. The results of the pilot studies relate the presence of MIIs with the transition in to or out of this task. As a consequence, the transition time is longer, maximizing the validation of the encountered lateral MII by the collection of more data during a two minutes task instead of collecting them in one minute task.

Except for the two tasks mentioned in the above paragraph, every task takes 1 minute to accomplish. Hence, with the SMS in motion, every volunteer executed several routines such as standing, walking and weight positioning on or close to three force plates (see Figures 11 and 12). There were 10 repetitions for each task, which means one hour per subject in each motion profile.

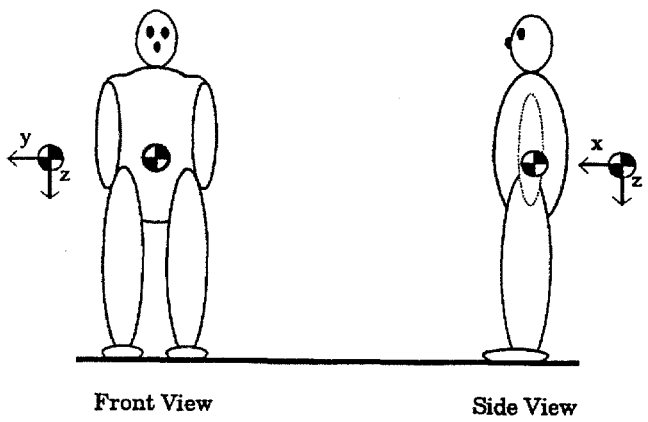

Figure 11. Subject Body *C.G.*, x, y and z Accelerations and Turn Rates about x, y and z.

In the case of task number three, the weight was 20 lbs, and it slid over a track set up on the forward cab wall at a height of 5 feet. Another weight that required lifting was a foam cylinder of 20 ounces, 6 inches in diameter, and 24 inches in length.

All the verbal communication during the experiments was recorded, and two observers located both inside and outside the control stations, marked the MII events.

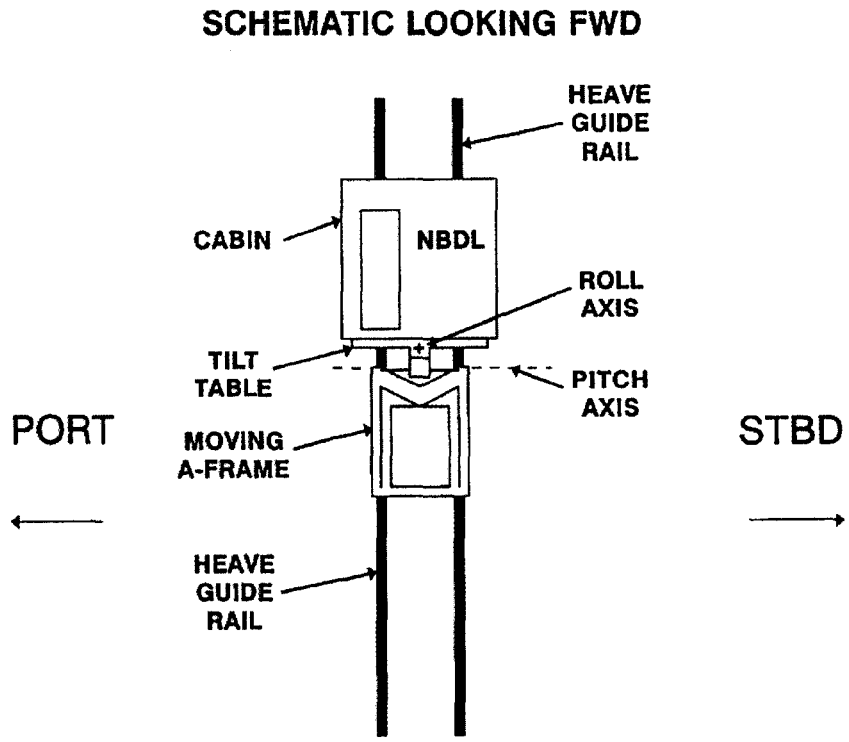

Figure 12. NBDL Ship Motion Simulator – Schematic View Forward Toward Bow.

Every routine was designed to measure a specific parameter related to the occurrences of MII. Based on reference [14], a brief description of the tasks is presented as follows:

1. Task routine 1: Subject stood on the SMS centreline facing aft.

   This is a priority task that established an empirical tipping coefficient for the lateral MII. The completion of this task lasted two consecutives minutes out of the whole six minute routine. Because of the duration, this task provides a large number of experimental MII data. The extension of this task was based on Graham's default values of lateral tipping coefficients [14].

2. Task routine 2: Subject stood on the SMS centreline near the wall facing forward.

This task described a typical mechanical operation, which compromised the shift of the subject C.G. forward by moving a weight towards the feet.

3. Task routine 3: Subject stood on the SMS centreline facing aft.

This task was selected in order to validate the MII tipping model. A foam cylinder weight simulated the position of a load above subject's head, producing an upward shift of subject's C.G.

4. Task routine 4: Subject walked athwart ships.

The subject starts walking from the port and goes to the starboard, continuously turning and returning. This routine described the influence of the ship's motions on walking, in a small quarter of the ship.

5. Task routine 5: Subject positioned on plates 3 and 4 next to SMS centre line.

This performance was established to validate the longitudinal MIIs with a subject located on the force plates of the SMS Cab floor, (see Figure 13).

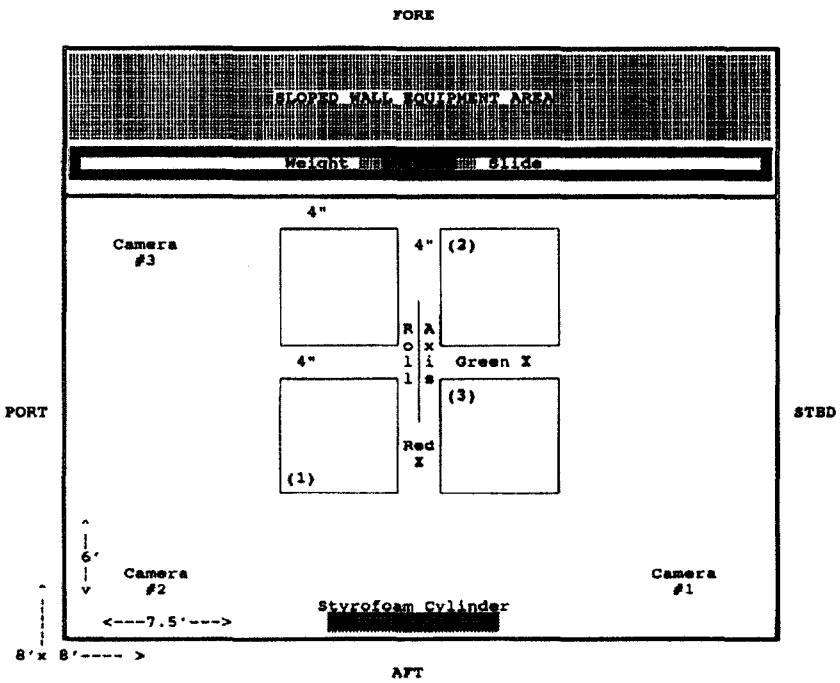

Figure 13. Description of SMS Cab Floor Plan, Cab Walls and Camera Locations.

3.2.2 Ship motion drive time history definition:

Because of the limitation in the motions of the SMS with respect to its vertical displacement, pitch and roll, the value of effective roll and pitch was accounted for. These effective motions simulated the same lateral and longitudinal accelerations on the flight deck as those of the real ship. Therefore, the SMS was driven using the vertical displacement and the effective values of roll and pitch motions.

The problem with the above assumption was that a high rate of Motion Sickness Incidence (MSI) was presented, aborting the experiment runs. This phenomenon occurred as a result of high-resonance frequency at 0.25 Hz in the current motion spectra. Based on regulations of ISO [15] presented in Figure 14, this frequency value is in the region of MSI. Another contributor to this problem was the *LFE*. The SMS was conducted under these estimators, in an effort to reach realistic values of lateral and longitudinal acceleration on the flight deck However, this resulted in unrealistic amplitudes of angular motions for typical frigates class vessels.

Another study was conducted in order to quantify the Motion Induced Fatigue (MIF) based on the energy expenditure in every subject [14]. The results demonstrate that even if subjects expend more physical energy in a moving environment, this amount of extra energy expended is small in a test of real sea conditions. It was discovered that standing, walking and moving a weight on board in Sea State 5 for one hour was comparable to walking at 2 miles per hour (mph) on land. A normal value for an average adult male is 3.5 mph.

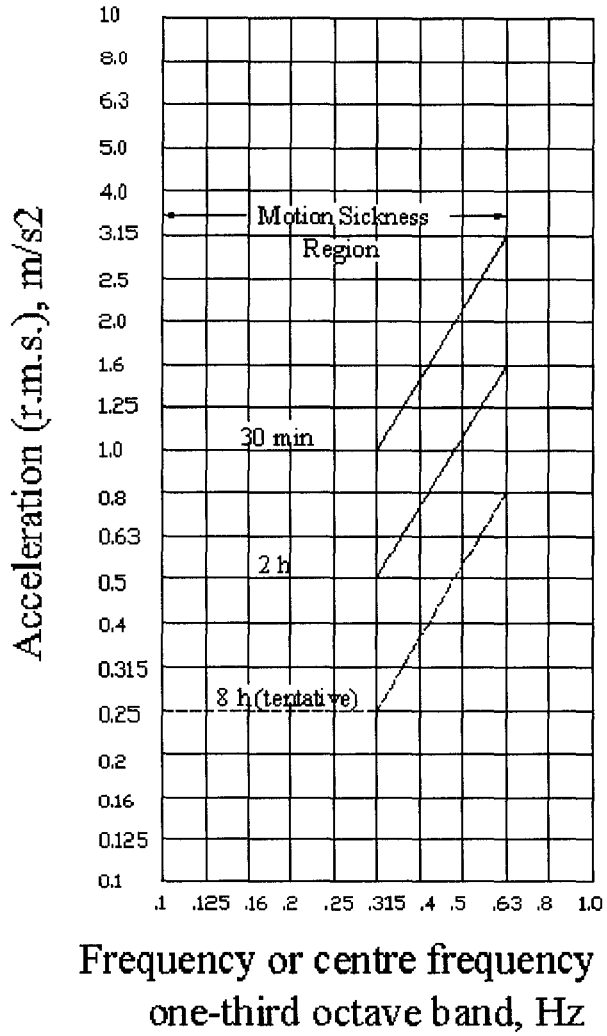

Figure 14. Severe Discomfort Boundaries for vertical acceleration (ref. ISO 2631).

The main study focused on improving the time histories in order to lessen vertical motions, and thus decrease the MSI up to tolerable levels. For this reason, conservative values of MSI, based on previous research, were adopted. Moreover, the SMS experiments no longer used *LFE* values, producing acceptable angular displacements.

Another parameter established by the group was the designation of the word Hotel for the "high frequency bow seas" and Lima for the "low frequency quartering sea"

condition. The use of these labels prevents the anticipation or expectation to experience motion sickness by the subjects [14].

With the aim of obtain enough recovering time for the subjects, 3 longitudinal MIIs per minute and 1.5 lateral MIIs per minute was assumed. The numerical simulation for MII in a time history was conducted using a nominal lateral tipping coefficient of 0.25 and a nominal longitudinal tipping coefficient of 0.17. The vertical displacement, pitch and roll were combined in the Hotel condition. This modification certainly reduced the vertical displacement of the SMS in the range of +/- 10 feet and restricted the expected occurrence of MSI to a rate of 13.1 % and 12.7 % respectively for the Hotel and Lima conditions. The results are presented in Table 8.

Characteristic	HOTEL	LIMA
Wave Multiplier	0.97	1
Vertical Acc. (Vert. Dipsp.) Multiplier	1	2
Pitch Angle Multiplier	2.5	2
Roll Angle Multiplier	2.5	2
Minute 5,6 Reduction Factor	0.84	1
No. of Predicted Lateral MIIs in 20 minutes exposure	31	28
No. of Predicted Longitudinal MIIs in 10 minutes exposure	32	35
Predicted MSI in 1 hour	13.10%	12.70%
Standard Dev. for Roll (Angle-deg)	6.06	6.89
Roll Modal Period (Toe-sec)	11.6	11.6
Standard Dev for Pitch (Angle-deg)	2.26	1.05
Pitch Modal Period (Toe-sec)	6.7	18.3
Standard Dev for Vertical Displ (Disp-ft)	2.44	3.51
Vert. Disp Modal Period (Toe-sec)	7.4	18.3
SMS Limit Roll (Angle-deg)	14.5	14.5
SMS Limit Pitch (Angle-deg)	14.5	14.5
SMS Limit Vert (Disp-ft)	9.9	10.5

Table 8. Particulars of Final MII Drive Time Histories (ABCD Group 1992).

This drive time history conditioned the vertical displacement of the SMS up to +/- 10.5 feet and thus the prediction of MIIs to a variation of 13.1% under the Hotel condition.

In consequence, the Hotel drive time history described an unrealistic combination of roll, pitch and heave component due to the limited vertical motion of the SMS. On the other hand, the Lima drive time history established more realistic values without restrictions.

Finally, the MSI caused the interruption of 22 of 77 runs. The averaged time in a run before it stopped was 29 minutes. In case of the Hotel condition the MSI represented a 30% of the general profile and in case of the Lima condition, MSI represented the 16%.

3.2.3 Analysis of the model for Tipping and Sliding MIIs:

Based on the research done by Baitis [10] the ABCD researchers established a time domain method for the estimation of the number of times that crew members lose their balance during deck operations. Every event was defined as MII: "the occasions when the ship motion induced forces introduce instabilities in a person's stance. These forces cause the person to stop their task and hold on to part of the ship or to significantly alter their posture to regain their stability." [14].

The ABCD researchers incorporated Baitis' *LFE* concept [10] as part of their experimental determination of MII. In the introduction of the present chapter *LFE* is defined. From that definition it is possible to determine the relationship between MII and *LFE*, and then calculate the latter in the frequency domain. Following Graham's [10] and Baitis' [11] results, the *LFE* concept was expanded in order to calculate MIIs in the frequency domain as well. These calculations are possible assuming a Rayleigh distribution of *LFE* amplitudes, including the non-zero vertical acceleration. As a result the symmetry condition is longer applicable and thus the estimator becomes a "General Lateral Force Estimator (*GLFE*)" [10].

The experimental analysis of MIIs in terms of *GLFE* for starboard and for port was established by means of Equations 23 and 24 (see point 2.2.1.2). The probability of occurrence of these *GLFE* was estimated by using Equation 25, which is based on the Rayleigh distribution assumption. Finally, the number of MII events in one task evolution of T_T seconds was calculated with Equation 26.

Also, in this experiment the MIIs were obtained using a "deck to shoe" friction coefficient of 0.7. This value did not take into account the fact that the experience and expertise of the subject would affect the number of MII. In the same way, the lateral tipping coefficient was set equal to 0.25 (see Equation 13).

Summarizing, the model for the determination of MIIs during the SMS experiments followed the same assumptions presented in point 2.2.1.2. Hence, the adopted model was simple, rigid and did not consider the subject capacity to change the C.G., augment the stance width, or anticipate any motion. For this reason the prediction of MII in these experiments is likely to be overestimated, based on the fact that a combination of these factors could improve the subject's stability.

3.2.4 Sources of variability in basic parameters:

Even a minor variability in the experiments affected the instance in which a subject went through an MII in response to an applied ship motion induced force. Three basic considerations that represent a source of variability in the rate of MII were:

a) The ship motion conditions.

b) The subjects.

c) The tipping and friction coefficient.

a) The ship motion conditions: Ship motion can be predicted with a high level of accuracy. However, the ship motion conditions depend on different aspects that can produce variability in the results. The conditions are related to the sea state, the selected operation condition, the location of the person on the ship and the motion response of the ship. The Sea State is a function of the geographic position where the ship is operating, the season and the local climate conditions. The operating condition selected by the crew is related to the mission profile of the ship and the ship capacity. For example, a change in speed and heading can augment the motion severities by a factor of 3 or more [14].

b) The subjects: There are different subject parameters presented in these experiments such as subjects' height, weight, shoe size, body center of gravity and static stance. All these parameters were measured without any difficulty, but the task performance of these subjects was only determined by means of the MII data. The individual degradation in every performance was quantified in terms of MSI.

c) The tipping and friction coefficient: The values of tipping coefficients were obtained from the video analysis and derived from the electronic devices. The variability in tipping coefficient as a consequence of subject body stance in experimental runs as well as variability in tipping coefficient for different subjects and sea conditions is based on the video information saved in several ASCII format files. One example of these files is presented above in Table 7, section 3.2.1.1.

3.2.5 Results and conclusions of the ABCD experiments:

Results of MII:

The total number of MII obtained from the experimental task number 1 (body lateral MIIs) up to task number 5 (body longitudinal MIIs) under the Hotel and Lime -motion profiles are presented in Table 9.

The empirical determination of the tipping coefficient was established through two approximations. One referred to a local analysis and the other to a global analysis. The first consists of the calculations of the forces affecting the subject at the time of each MII event. In the second approach, the total number of MII measured was associated with the overall motion environment.

In Table 9 it is possible to confirm that the number of longitudinal MIIs was greater than the number of lateral MIIs. The reason was the resistance of the body against tipping frontward and backwards. However, the most events for lateral MIIs were under the Hotel motion profile. In case of the longitudinal MIIs, the Lima motion profiles created the most occurrences [16].

MII	Hotel	Lima
Body Lateral MIIs	88	30
Body Longitudinal MIIs	178	234

Table 9. Total Number of MIIs observed.

In the same way, the assessment of local forces at the time of MII occurrences contributed to the identification of different types of MIIs. Table 10 presents the different types of MII as well as the total number related with each group.

Among the qualitative and quantitative groups presented in Table 10, there are two relevant results: the MII type A and MII type AC. 69% of the MII occurrences were lateral MIIs and 81% were longitudinal MIIs. The events of MII peaked when the number of local forces acting on the subject was highest. The forces for the type A were almost sinusoidal

describing a typical profile of frigate motions. However, for the type AC the profile was not smooth. For this reason the ABCD researchers were wondering if "the event of MII at an "unsmoothness" AC peak would have occurred if the peak had been smooth?" [16].

Type	Description	No. MIIs
A	MII at or near smooth peak in GL	229
B	MII in opposite direction	8
C	MII at obvious discontinuity in GL, and not near peak	27
AC	MII at or near peak, but GL not smooth	181
D	MII not explained by GL	31
E	MII too near start or end of task (+2/-1 sec)	22
F	MII already identified for current GL peak	27
X	other	5

Table 10. Classification of MII types.

Following the results of Table 10, two types of "unsmoothness" [16] were analyzed. One was associated with the SMS's physical characteristics and the other was associated with the "irregularity of motions expected in a natural seaway" [16].

Despite the fact that empirical tipping coefficients only estimated for the A and AC types combined, other types of MII are incorporated into the analysis as well. In Table 11 an analysis of the other types of MII is described.

In the same way, Table 12 presents the average results for tipping coefficients estimated by means of local and global analysis. Based on these values, variations between body lateral and body longitudinal tipping coefficients were expected by the researchers. They established that the lower values for body longitudinal MII occurred at lower levels of force than did the body lateral MII. That means that a subject was less stable when he/she was standing in the primary lateral force direction than when he/she was standing at right angles to it.

MII types	Description
B	MIIs which occur when there was no significant lateral force, but there is a peak in longitudinal force. For example in Task 1 when the subject is standing facing aft and generally experiencing large lateral motions from roll. The subject likely tipped frontward or backward.
C	MIIs which occurs at times when the local forces acting on the subject are not large, but the forces change in an "unpredictable" way. For example when the subject anticipates one type of motion but a different one occurred.
D	MIIs which occur during relatively quiescent periods, when SMS cabin is barely moving. It is possible that the subject's attention wandered, or that some other mechanism was acting, like for example motion sickness symptoms
E	MIIs which occur very near to the start or end of a task. For example just after or before changing tasks. These MIIs are discharged as the subject was likely to be still changing tasks.
F	MIIS which occurs when more than one tip or stumble is caused by a single peak in local forces. For example where the subject regains his balance for a brief period, but then stumbles again during a single motion cycle.
X	MIIs which occur after the SMS motion have stopped, but before the entire experiment protocol has finished. In this case, the MII was formally reported by either the subject or observer, but it is not interest for the current MII model.

Table 11. Classification of the other types of MII.

Analysis	Lateral MIIs	Longitudinal MIIs
Local Analysis		
Hotel Profile	0.235	0.185
Lima Profile	0.229	0.200
Global Analysis		
Hotel Profile	0.288	0.204
Lima Profile	0.294	0.221

Table 12. Empirical Tipping Coefficients.

The disparity between motion conditions for the same MII type was not relevant, though there were three of four cases in which the tipping coefficient value under the Lima profile was bigger than its correspondent in the Hotel profile. This denoted an anticipation of the person or an undemanding reaction of him/her in the low frequency profile. For that reason, a possible dependence between the tipping coefficient and the frequency was established.

The results of tipping coefficients for people of different heights to *G* are shown in Figure 15. On this graph it is possible to evaluate the spread of the data. The spread is less in the longitudinal tipping coefficient from the local analysis and is more in the body lateral tipping coefficient from both global and local analysis.

It is interesting to mention the number of subjects who did not go through any "body lateral MII". There were three volunteers that did not experience this type of MII in the Hotel profile and five in the Lima profile. Hence, the variability in the lateral tipping coefficient was not entirely identified by these experiments.

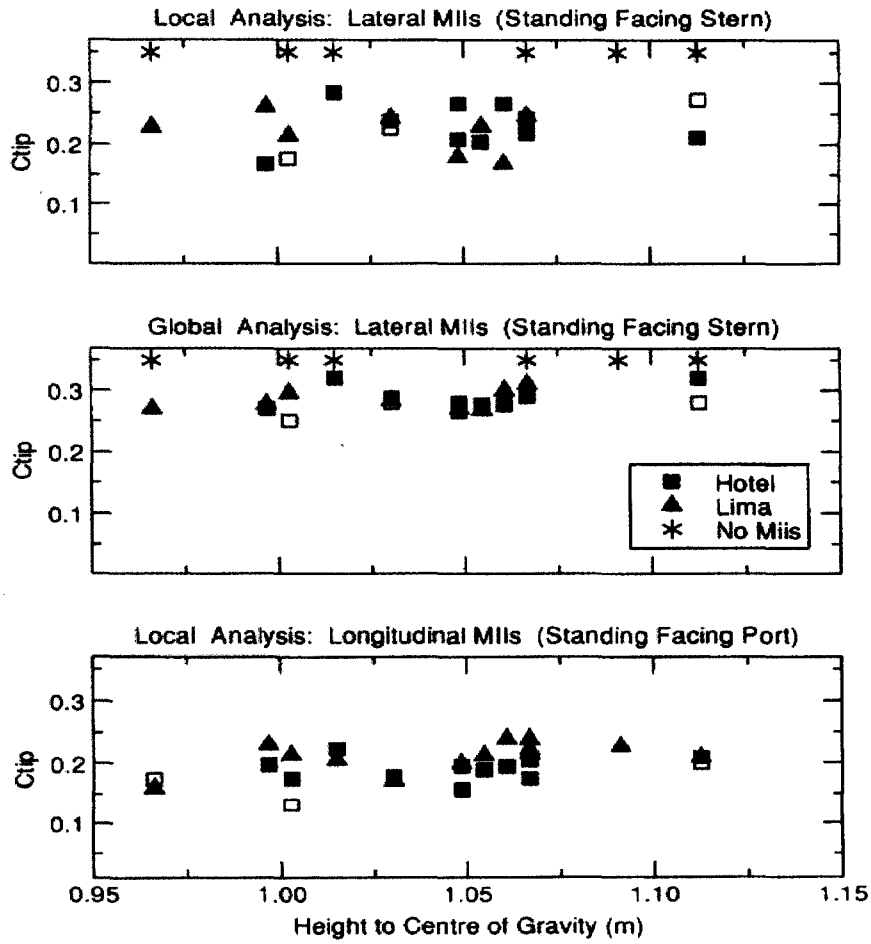

Figure 15. Sample Tipping Coefficients for Global and Local Analysis (ABCD Group).

Results of Energy Expenditure:

As discussed in point 3.2.2, the subjects' oxygen consumption was studied while they performed an arbitrary operation in both static and dynamic conditions during MII events. This experiment was based on a possible correlation between the "accumulation of effects of work done by altering posture to compensate for ship motions and the development of MIF" [16].

The results of the static and dynamic experiments are presented in Figure 15. From this graph, it is possible to infer that the person required more energy under dynamic conditions than under static conditions. However, the necessary quantity of additional energy is small. The graph shows a black bar as a reference, which represents the energy expenditure for walking on level ground at 2 miles/hr (3.2km/hr).

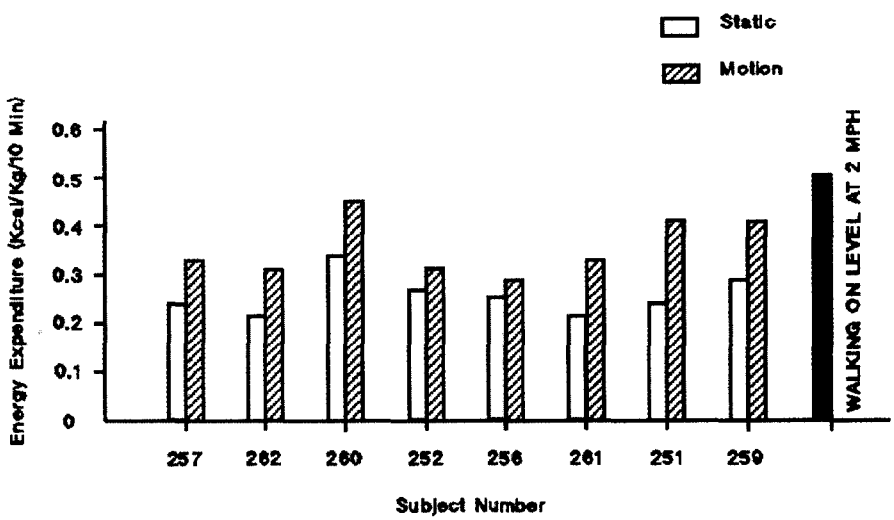

Figure 16. Energy expenditure (ABCD Group).

The ABCD researchers found a consistent method to measure the effects of the ship motions on energy expenditure. Furthermore, they expected an increase in the value of the

energy expenditure under dynamic conditions, due to long term exposure and extreme ship motions. This is the case with small fishing vessels.

Results of Cognitive Experiment:

The experiments were performed under static and dynamic conditions. Based on these results, a statistical significance test was established. The definition of the verbal meaning and the p-values was determined as follows:

$p<0.001$ = very strong evidence of difference between motion conditions

$p<0.010$ = strong evidence

$p<0.025$ = fairly strong difference

$p<0.050$ = some evidence

$p<0.100$ = slight evidence

$p<0.100$ = no real evidence

The experiments also revealed that for short exposures to motions, purely cognitive skills were not degraded. In the same way, tests that considered psychomotor skills presented significant variation. The influence of the crew's attitude and expectation with respect to the motions became significant when an external volunteer was tested. This subject experienced early MSI, while all the others did not. However, there was dissimilarity in measured cognitive and psychomotor performance and MSI as well.

Conclusion of the ABCD Experiments:

This unique and innovative research proposed a method to calculate the effects of ship motions on crew performance. Based on the experiment's collected data, the postural stability model was validated.

It was discovered that the tipping coefficients included in Graham's MII model [11] were very similar to those obtained in this experiment. Moreover, Graham's model [11] was validated almost entirely in this research.

On the other hand, the restriction in motions of the SMS such as pitch and roll maximum angles, absence of yaw, and lateral motions, contributed to the estimation of unrealistic motion time histories. Likewise, the presence of low incidence body lateral MIIs was a consequence of the need for pure linear lateral motions [16].

However, the ABCD research group encouraged the performance of additional MII experiments in order to measure the effects on the subject due to the missing ship motion components. It is expected that the motions as a result of sway and yaw on the local lateral ship motion could cause difficulties in the subject's self stabilization in controlled tasks.

One conclusion was referred to the ability of the subjects to avoid MII instead of anticipating it. That means that the subject's self stabilization had a tendency to "decrease the expected number of MII from the rigid model" [14]. Therefore, in terms of quality, the model was highly dependant on the ship's motion. It was recommended that more experiments with the aim of improving a less conservative MII prediction model. For example, the nominal values of 0.25 and 0.17 for the tipping coefficients used by naval crews were more realistic than the mean global values for tipping coefficients of 0.271 and 0.193 [14].

The last part of the experiments related with the cognitive aspects, demonstrated that these skills were not degraded during short exposures to motions. Nevertheless, the aspects related with psychomotor skills showed some dissimilarity.

3.3 Background in Wave Theory.

Since ancient times questions about the oceans and their waves were always in the mind of important philosophers and scientists like Aristotle and Da Vinci. Aristotle explained in Book III of Meteorology, written in 350 B.C., about Wind Theory and how the force of the wind influences the motions of the mass. Likewise, a second theory was written by Da Vinci at the end of the fifteenth century.

In the historical development of wave theory different approaches were taken, mostly led by several French mathematicians. One of the first was d'Alembert. He proposed a principle of dynamics of fluid particles. Later Laplace, based on this principle, published his Theory of Tides in 1775-76. This was the first description of the ocean as a perfect liquid of variable depth rotating on a uniform spheroid and being influenced by the attraction forces of the sun and the moon.

In 1781 another mathematician, Lagrange, presented the problem of water waves with an application to hydrodynamics. This work was inspired in Euler's research and became a classical theory. Many years later, the scientific community recognized Lagrange's velocity potential and Fourier's analysis of local perturbations of the fluid surface as basic theories for the study of waves. The first approach of the Classical Wave Theory appears at the beginning of the XIX century. In 1802, Stokes along with Gerstner began to study on classical solutions for finite oscillatory waves on infinitely deep water.

After the First World War, another important work was presented by Norbert Wiener in 1930, whose generalized harmonic analysis caused the appearance of the first stochastic models. This kind of model revolutionized different disciplines such as electronics, fluid mechanics, climatology, astronomy, economics and acoustics. In 1939, Jeffreys, using his powerful seismological and statistical skills, studied the generation of the waves. During the same years other scientists, like Munk, concentrated in the propagation of waves, and Neumann studied the generation of them.

Among different scientists and research studies, such as Rice (Gaussian Noise), Levy (Brownian Motion), and Tukey (Acoustics and Noise), the stochastic model was introduced in the investigation of ocean waves by Pierson within a Physical Oceanography study in 1952. After one year, in 1953, the first paper of a seakeeping study including a new stochastic model was presented by Pierson along with St. Denis. This paper, titled "On the Motions of Ships in Confused Seas," was a milestone. These two researchers introduced a measure of realism into the definition of wave excitation of ship motions, which proved a much better theory than the existing sinusoidal wave train. Pierson and St. Denis represented the seaway at a fixed point within this new concept and divided it into four cases of analysis [17]. These cases are:

1. A periodic wave system having an amplitude component at a single spectral frequency.
2. A periodic wave system having components at many discrete spectral frequencies.
3. A periodic wave system having a continuous amplitude spectrum represented by a Fourier Integral.

4. A periodic wave system represented by energy integral assuming a Gaussian distribution.

Using statistical models the concept of the seaway was introduced as the sum of an infinite number of infinitesimal regular waves. The energy spectrum is established to represent the seaway. This spectrum is the variance density of the number of waves with respect to the frequency. Based on this analysis, different responses of the ship in a seaway can be obtained. In the same way, the designers can improve the ship motion response in different environments by using the probability theory.

This was the beginning of the modern study of ocean waves. Since that time, the investigations were concentrated in the generation, the propagation, the measurement and the non-linear interaction between the waves.

3.4 Background in Ship Motions.

The study of motions started between the seventeenth and eighteenth centuries with Newton and Bernoulli. Newton postulated the Classical Dynamic Theory and Bernoulli proposed the Differential Calculus for solving compound motions. The formulation of the problem comes one century after, when Froude presented the rolling theory; after that, Krilov extended this theory, developing his "Theory of oscillating motions of the ship." This was the basis of the Froude – Krilov Hypothesis. This hypothesis is a static and simple approach to predict the motion of the ship and define that the presence of the vessel does not disturb the hydrodynamic pressure field associated with the incident waves. There is a linear Froude – Krilov theory, which takes into account an average wave cycle that affect the ship. The waves are assumed to be long and thus a flat water line affecting the vessel.

There is also a non-linear Froude Krilov theory which considers a wave profile affecting the vessel.

Thus, the Froude–Krilov forces and moments can be calculated using this hypothesis. For these calculations several assumptions were established:

1. In the linear theory the restoring forces and moments are proportional to the amplitudes of heave, pitch and roll. Therefore these forces and moments can be expressed linearly in terms of these time variables.
2. Given the Froude-Krilov forces and moments in the non-linear theory, the response of the ship due to the wave field is controlled by changes of buoyancy and changes due to wave position. These changes occur when the ship moves from the equilibrium position.

In 1950, Weinblum and St. Denis [18] contributed to the evaluation of the seagoing qualities of a ship, making the first step towards understanding the ship dynamic. They introduced an analytical method to determine, in terms of the ship form, the motions that a ship experiences when it is moving in an arbitrary direction on a seaway. They assumed that the ship is a rigid body. This study considers three basic steps:

1. Determination of the motion of the seaway itself and the forces induced by it on the ship.
2. The analysis of the properties of a ship moving in calm water.
3. The evaluation of the behaviour of a ship in a seaway.

After all these contributions, the modern study of the ship motions began, concentrating in areas like seakeeping, validation, consistency of the theory, non-linear motions and development of computational programs.

3.5 Background in Seakeeping.

Seakeeping represents measuring parameters, which are used in the design stage of any vessel to evaluate its performance in a seaway. These measures are based on different parameters, which are related to the wave field influence on the vessel motions and the crew performance. The collection of all these measurements establishes the seakeeping criteria.

The early criteria of seakeeping were based on the officer's judgement rather than on the designer's specifications. During the great wars the main concern was the involuntary loss of speed or change of course. Those decisions were based on the exclusive faculty of the commanding officer.

After World War II the ship designers began to review different norms and rules regarding the ship's behaviour together with the sea state representations. This became the base for the definition of seakeeping criteria in terms of loss of speed or change of course. As a result the ship designers concentrated on two important factors:

1. The environment (wind and waves).
2. The ship behaviour in this environment (environmental operability of the ship).

The first factor was previously predicted following the theories and methods described in points 3.4. This was the basis for the study of the second factor. With this

objective in mind, the designers began to work together with oceanographers to improve the ship's response in different environments, concentrating on wave representation and prediction, following sea state characteristics and frequencies from the statistic point of view, by means of the probability theory. The study was based on the expected probability of the occurrence of extreme conditions of wind and waves in the areas of expected operations and the occurrence of those wind and wave conditions that would reduce the ship's environmental operability in the areas of expected operation.

These two statements demonstrate the link between realistic representations of the seaway and good criteria to define the conditions of operability, survivability and habitability that the ship required. These three main aspects of the ship's characteristics become the Seakeeping criteria.

The definition of the concepts that represent the operability of a ship on a seaway is well explained by Hadler and Sarchin [19]. The first concept is the "Seaworthiness," which is related to the performance of ships and floating systems working on the sea under extreme conditions. This definition involves the safety of the cargo, the crew and the hull, representing the capability of the ship to control situations like collision, grounding, fire and heavy weather effects.

Similarly, the "Seakindliness" concept is related to the response of the ship, but under non-extreme conditions of wind and waves. It is a classical concept that the navy used as a way to measure the ability of ships to accomplish a mission, and sometimes this was an argument to decide an effective defence presence. In case of merchant vessels, these measurements resulted in providing the return of the investment. Later, in the eighties, this concept was named the 'Mission Effectiveness.' The concept is well defined by Hoffman [20] as "the ability of a vessel to respond in such manner to the action of the sea that the

amplitudes of her motions and her position never become dangerous, and the accelerations she undergoes are kept to a reasonable minimum". Seakindliness involves different issues related to economical navigation and fuel consumption, representing the speed keeping qualities, security of the cargo and equipment onboard, habitability, operational limits of equipment, components and systems.

Both concepts, "Seaworthiness" and "Seakindliness," are concerned with the security of the ship. Thus, both are defined under a single general term: the "Seakeepability." However, the modern definition of Seakeepability is "seakeeping." As a definition of environmental operability of the ship, this concept is related to the wave field condition.

Seakeeping represents several physical response characteristics of the ship itself, like ship motion, slamming, deck wetness, steering in waves, added resistance, hydrodynamic loads and transient loads. Most of the first studies in seakeeping were done in frigates and destroyers under the supervision of the navy during the cold war. In this case the focus was on loss of speed or change of course, when the ship was travelling in head seas, in order to successfully execute a mission despite rough weather.

In Kehoe [21] a comparison of Soviet destroyers and US Navy destroyers considered major seakeeping design factors, such as length, displacement and ship hull form, classified into underwater and above water characteristics. It was established that these features affect motions, manoeuvring, and stability, as well as spray and deck wetness.

Seakeeping, along with the concepts of survivability and habitability, is strongly related to the hull characteristics, the crew, the equipment and the personal judgement of the captain. They are not similar, but all are consequences of the following 12 effects [22]:

1. Averaged or characteristic motion in the six degree of freedom.
2. Characteristic accelerations in the six degree of freedom.
3. Extreme motions and accelerations.
4. Green water and Spray.
5. Slamming and slamming loads.
6. Wave induced vibrations.
7. Increase in required power.
8. Stability on course, including tendency to broach.
9. Hull girder bending moments.
10. Local sea loads.
11. Hull deflection.
12. Propeller racing and tail shaft loading.

Based on these considerations, as well as the different situations that should be included in seakeeping criteria, the naval architects established three basic steps as a norm for design [22]:

1. Definition of the environment in which the ship is expected to operate.
2. Establishment of quantitative and qualitative requirements for seakeeping performance, based on the intended mission of the ship.
3. Evaluation of the design to establish whether it meets the requirements, and to recommend modifications of the design if it should become necessary.

In order to determine quantitative and qualitative requirements for seakeeping performance, different authors proposed several criteria as a result of their experiments. In Table 13, 14 and 15 are presented classical seakeeping criteria and examples of recent seakeeping performance criteria.

Ship Subsystem	Slam	Deck wet.	Vert.acc.	Lat.acc.	Roll	Pitch	Vert.mot.	Vert.vel.	Rel. mot
Ship hull	x	x	x						
Propulsion machinery									x
Ship equipment		x	x	x	x	x			
Cargo		x	x	x	x	x			
Personnel									
effectiveness		x	x	x	x	x			
Passenger comfort			x	x	x	x			
Special operations									
helicopter					x	x	x	x	
sonar									x
lifting			x		x	x	x	x	

Table 13. Limiting Criteria versus ship subsystems (ref. 22).

Moreover, from Table 16 presented in the "Principles of Naval Architecture" Vol. III, it is possible to establish the existence of a criteria respect to the passenger comfort and that these criteria considers the influence of the vertical acceleration, lateral acceleration, roll, and pitch on the people onboard.

Likewise, the criteria described in Table 14 and 15, established by the "Nordic Co-operative Project on Seakeeping Performance of Ships" [23], limiting values of the aforementioned factors for fishing vessels are calculated.

Motion	F.P.	Bridge	At midship (Lp/2)	A.P.
Vert. acc.	0.15g	0.10g	0.15g	0.20g
Lat. acc.	0.07g	0.05g	0.07g	0.10g
Roll	4.0 deg	3.0 deg	4.0 deg	6.0 deg

F.P.: Fore perpendicular. A.P.: After perpendicular.

Table 14. General operability limiting criteria for Fishing Vessels [23].

Criterion	Hull safety	Equip. oper.	cargo safety	Personnel safety, efficiency
Vert. acceleration, FP	x		x	
Vert. acceleration, bridge		x		x
Lateral acc., bridge		x	x	x
Roll		x	x	x
Slamming	x			
Deck wetness	x			

Table 15. Points of view considered in the criteria [23].

No.	Seaway Performance Criteria	Affected Elements	Performance Degradation
a) Absolute Motion Amplitudes			
1	Roll Angle	People, Mission and Platform	Personnel injury, reduced task
2	Pitch Angle	Systems	Proficiency, mission and hull system degradation
3	Vertical displacement of points on flight deck	People Mission Systems	Injury to personnel handling aircraft Inability to safely launch or recover it
b) Absolute Velocities and Accelerations			
4	Vertical acceleration	People and	Personnel Fatigue, reduced task
5	Lateral acceleration	Mission Systems	Proficiency, and mission system degradation
6	Motion Sickness Incidence (MSI)	People	Reduced task proficiency
7	Slam acceleration (vibratory, vertical)	People, Mission and Platform Systems	Personnel fatigue, injury, reduced task proficiency and mission and hull system degradation. Preclusion of towed sonar operation
c) Motions Relative to Sea			
8	Frequency of slamming (simultaneous bow emersion and accidence of a threshold vertical velocity)	Mission Systems Platform system	Hull whipping stresses and damage to sensors on the masts Slamming damage to bottom forward hull structure
9	Frequency of emergence of a sonar dome	Mission Systems	Reduced efficiency of sonar
10	Frequency of deck wetness (submergence of the main deck forward)	People Mission Systems	Injury or drowning of personnel Damage to deck-mounted equipment
11	Probability of propeller emergence	Platform Systems	Damage to the main Propulsion
d) Motions Relative to Aircraft			
12	Vertical velocity of aircraft relative to the flight deck	Mission Systems	Damage to aircraft landing gear and/or loss of aircraft

Table 16. Twelve types of seakeeping criteria, SNAME 1987 [22].

Table 16 describes recent types of criteria established by the SNAME in 1987, which introduce the consequences on persons and systems due to wave influence. For the

first time the crew degradation, fatigue and decrease of individual performance are mentioned in seakeeping criteria.

Based on these criteria, the crew operational performance degradation (in terms of Seakeeping Performance criteria) can be measured. With the aim of including the concept of MII in the seakeeping criteria, this research attempts to assess the motions of the Newfoundland fleet's fishing vessels, as well as establish MIIs on the crew of these vessels, using the numerical MOTSIM Program.

Chapter 4

The Numerical Model

The numerical study in this investigation is based on the results of the MOTSIM program. For this reason the validation of the code using small vessels is one of the main objectives of this research. Regardless of previous validations that considered a variety of vessels types, such as the classic Series 60 hull, an ice-breaker, a trawler, a frigate, a motor yacht, and a research vessel, the code has not been validated for small vessels at full scale.

One of the difficulties of the validation process is the viscous effect. This effect is significant in roll motion and certain manoeuvres. In the case of the roll of small vessels, viscous effects maybe a more significant portion of roll damping because of the vessel's size. In order to predict the roll motions precisely, it is necessary to analyze all the collected data and measurements with a high degree of accuracy.

Seakeeping and habitability are analysed with this objective in mind. The motions and accelerations at different locations onboard a fishing vessel can be evaluated based on the motion at the C.G. This analysis is carried out simulating the vessel's behaviour in a particular Sea State, heading, and speed. Based on these results, the prediction of the influence of motions on the crew performance is investigated. This influence is quantified by means of MII criteria.

4.1 The numerical model.

To evaluate the vessel behaviour in different environmental conditions, the existing numerical model MOTSIM is used. This program incorporates the concept of MII within its code. The code's routines are written in the FORTRAN 77 language.

MOTSIM is a non-linear time domain Seakeeping code that simulates six degrees of freedom motion, with forward speed in any wave conditions [24]. The ship's geometry is defined in terms of a sequence of sections, each of which is described by a set of panels. At each time step, the code determines the intersection of these panels with the waterline and redefines the paneling describing the ship's wetted surface. The pressure forces associated with the incident waves are then numerically integrated over this surface, using second order Gaussian Quadrature. The waves are taken as second order Stokes waves.

The normal velocity distribution associated with the velocity of the vessel and the incident wave particle velocity is averaged over each panel and then a least squares fitting of this distribution based on the wetted panels belonging to a particular section is made such that a unique decomposition of the modal velocities (surge, sway, heave and roll) is obtained that most closely satisfies the body boundary condition on the section. The use of the wetted surface to determine modal velocities serves as an approximation to a non-linear body boundary condition. The code allows for more general decompositions of the velocity distribution to be made using a higher number of non-standard modes. From this decomposition, the scattering forces and moments are determined for each section based on precalculated memory functions.

The memory functions for each section are derived from added mass and damping coefficients from zero speed linear theory over a truncated semi-infinite frequency range. Their use allows for arbitrary frequency content in the scattering forces and moments. The

added mass and damping coefficients can be either 2 or 3 dimensional. Corrections are made for forward speed.

Viscous effects associated with roll damping and manoeuvring are determined using semi-empirical formulae or experimentally determined coefficients. The total forces are then used in the non-linear equations of motion to determine the motions of the vessel.

The solved equations:

The simulation of the motions is based on two reference systems. One system describes the translating earth axes x, y, and z at the C.G. of the body. These axes move at a steady forward speed. The other system consists of instantaneous axes positioned in the C.G. and moving with the body.

Along the fixed axes the displacement vector $\vec{x} = (x, y, z)$ represents the motions of the surge, sway, and heave with respect to the C.G. of the body. Around the instantaneous axes the angular velocity vector $\vec{\omega} = (\omega_1, \omega_2, \omega_3)$ is considered. For small motions these axes approximate inertial axes and the angular velocities about them correspond to the angular velocities of roll, pitch, and yaw respectively.

Modifying Euler's rotation theorem, an arbitrary rotation of the vessel may be described by three angles. A convention establishes that the rotation around the axes (x,y,z) is described by the angles (θ, ϕ, ψ) following a particular order. The order implies a first rotation by an angle ψ about the z axis (yaw), a second rotation of an angle θ about the x axis (roll) and a third rotation by an angle ϕ about the y axis (pitch).

The code solves the equations for the six degree of freedom, which include three displacements and three rotations. The first vector equation to be solved is:

$$M\ddot{\vec{x}} = \vec{F} \qquad \vec{x} = (x, y, z) \tag{28}$$

where M is the body mass matrix, $\ddot{\vec{x}}$ is the second derivative of the displacement vector, and $\vec{F}$ is the total force acting on the body in the inertial system of reference.

This equation is solved as a set of six first order differential equations. One of the advantages of this code is that all the forces are calculated at the right hand side of Equation 28. The second equation that the code solves is:

$$I\omega + \omega \times I\omega = \Gamma \qquad \omega = (\omega_1, \omega_2, \omega_3) \tag{29}$$

where I is the moment of inertia matrix relative to the principal axes of the body at the C.G. and ω is the angular acceleration in the body fixed system. The term $\omega \times I\omega$ describes the second order rotational motions of the body (useful in extreme conditions). The vector Γ is the total moment with respect to *C.G.* in the body fixed reference system. Also, this equation is solved as a set of six first order differential equations. The inertia matrix I is a 3x3 and is expressed as:

$$I = \begin{pmatrix} I_{11} & I_{12} & I_{13} \\ I_{21} & I_{22} & I_{23} \\ I_{31} & I_{32} & I_{33} \end{pmatrix} \tag{30}$$

Depending on the symmetry of the body, the terms $I_{ij} = I_{ji}$ $, i \neq j$ are generally taken as zero. In the case of small motion, linearity is assumed and the fixed axes are considered to be equal to the instantaneous axes. That means $\omega = \alpha$, and Equation 29 is:

$$I\alpha = \Gamma \tag{31}$$

The third equation gives the angular motions. The expression is the following:

$$\eta = A(\theta, \phi, \psi)\omega \tag{32}$$

where A is the transformation matrix dependent on the modified Euler angles (θ,ϕ,ψ), it is a 3x3 homogeneous coordinate transformation matrix:

$$A = \begin{bmatrix} \cos\theta & 0 & -\cos\phi\sin\theta \\ 0 & 1 & \sin\phi \\ \sin\theta & 0 & \cos\phi\cos\theta \end{bmatrix} \tag{33}$$

where θ the angle of roll, ϕ is the angle of pitch and ψ is the angle of yaw. These angles (θ,ϕ,ψ) are the modified Euler angles that represent the motions of Yaw, Roll and Pitch. Originally Euler angles were not developed for vessel rotation, thus a modification was required. In the same way, this equation is solved as a set of three first order differential equations.

4.2 The MII numerical calculation

The research objective is to assess the motions of Newfoundland fishing vessels and to establish MIIs on vessels using MOTSIM. In order to achieve this objective, the validation of the MOTSIM code by means of Sea Trials is conducted.

In order to measure MII numerically, the MII concept is introduced within the MOTSIM code. The simulations are established for five headings and two speeds in a wave field condition equivalent to a typical fishing season. These waves correspond to Sea State four, based on the World Meteorological Organization Sea State code.

Furthermore, two wave density energy spectrums describing irregular sea conditions are used to represent the waves that the vessel would encounter during its fishing

operations. The purpose of this numerical simulation is to represent a realistic response of the vessel to the wave field conditions. Therefore, the vessel's behaviour is modelled under the assumption of unidirectional and multi-directional waves.

Likewise, the collected data during Sea Trials are given as a multi-directional wave field, in terms of a non-directional spectrum and a spreading function. The Spreading Function used in this study is the following:

$$D(\omega,\mu)=\frac{1}{\pi}(0.5+r_1\cos(\mu-\mu_1)+r_2\cos 2(\mu-\mu_2)) \tag{34}$$

where ω is the wave frequency, r_1 and r_2 are frequency dependant coefficients in a second order Fourier expansion of the wave buoy spectrum. The variable μ is the direction, where μ_1 is the principal wave direction and μ_2 is the mean wave direction. These variables are all estimated by the software from the wave buoy based on the measurements of heave, roll and pitch collected by the buoy.

Based on the above statements, five small vessels are analyzed. Each one belongs to Newfoundland fishermen and each one operates in similar areas within the Newfoundland coastal region. In order to establish a wide range of observations, four length classes are selected. These lengths correspond to 35, 45, 65 and 75 feet (10.67, 13.72, 19.81 and 22.86 meters). Moreover, five locations onboard each vessel are selected in order to calculate the acceleration and number of MII per minute.

The selected points onboard the fishing vessels are presented in Table 17. The coordinates of each point are established in terms of the fraction of length (L) and determined from the C.G. (Point 1) of the vessel.

Points	Location
P1	(GX,GY,GZ)
P2	(-L/3,0,0)
P3	(L/3,0,L/5)
P4	(L/4,L/6,0)
P5	(-L/4,L/6,0)

Table 17. Selected Points on board Fishing Vessels.

4.3 Numerical simulation.

Following the sequence of the MOTSIM code, the geometry of the fishing vessel is generated. For the 35 foot vessel the definition of the geometry corresponds to the dimensions measured directly from the fishing vessel placed on a dry dock. For the other vessels, the dimensions are extracted from the lines plan. Figure 17 presents the typical geometry input.

Figure 17. Computer generated geometry of a 65 foot fishing vessel.

After the vessel geometry is generated, additional information relative to the wave field condition (Table 18), body symmetry and the position of the reference coordinate

system is introduced in the input files. Once these parameters are established, the initial conditions are determined.

An initial parameter is the position relative to the fixed axes and the vessel speed. Also, the rudder area, the autopilot, the rudder coefficients, and the propulsion coefficients can be set. There is sometimes a need to modify these parameters in order to decrease or increase the dynamic control over the vessel course. For example, the rudder coefficients and propulsion coefficients are modified if the vessel capsizes in a particular course. Usually this phenomenon occurs at a high Froude Number (Fn) and bow headings.

Likewise, smoothness in the calculation is applied whenever the speed influences the evaluation at each point in the panel. This modification takes place when the vessel capsizes or overflow situations occur. In both cases the calculation of the velocity along with the acceleration in every point are smoothed.

The wave field characteristics used in all the calculation and for all the length classes are presented in Table 18. The representation of the wave field is determined using JONSWAP, Bretschneider in uni-directional and multi-directional wave spectrum.

Irregular Wave Parameters	Value
Mean Wave Frequency	1 rad/sec
Significant wave height	2 m

Table 18. Characteristics of the Wave Field.

After setting the vessel's parameters, such as the wave field, the selection of five points in different locations onboard is established. In this investigation the criterion for the selection of the points is based on the typical working place locations in a fishing vessel.

The principal parameters of each vessel, in terms of length class, considered for the numerical simulations are presented in the following tables:

35 footer "Atlantic Swell"	
Length	10.30 m
Displacement	16.60 ton
Beam	4.20 m
Draft	1.24 m
GMT	1.35 m
$\omega\theta$	1.69 rad/sec
$\omega\Phi$	2.71 rad/sec
ωz	4.22 rad/sec

Table 19. Characteristics of the 35' Fishing Vessel "Atlantic Swell."

45 footer "Bold Wind"	
Length	14.20 m
Displacement	84.00 ton
Beam	6.26 m
Draft	2.71 m
GMT	1.59 m
$\omega\theta$	1.27 rad/sec
$\omega\Phi$	1.66 rad/sec
ωz	2.92 rad/sec

Table 20. Characteristics of the 45' Fishing Vessel "Bold Wind"

65 footer "Ocean Billow"	
Length	18.50 m
Displacement	152.00 ton
Beam	6.72 m
Draft	2.09 m
GMT	1.13 m
$\omega\theta$	1.19 rad/sec
$\omega\Phi$	2.39 rad/sec
ωz	0.96 rad/sec

Table 21. Characteristics of the 65' Fishing Vessel "Ocean Billow"

75 footer "The Shamook"	
Length	22.50 m
Displacement	199.00 tonne
Beam	6.60 m
Draft	2.72 m
GMT	0.79 m
$\omega\theta$	1.03 rad/sec
$\omega\Phi$	1.58 rad/sec
ωz	2.00 rad/sec

Table 22. Characteristics of the 75' Fishing Vessel "Shamook."

Chapter 5

Full Scale Experiment: Sea Trials

The present chapter gives a general description of the sea trials and the vessels that participate in them based on the technical Sea Trial reports ref. [26] and [27].

5.1 Fishing Vessels in Sea Trials

On October 4th and December 15th 2003, two sea trials were conducted in two vessels off the coast of Newfoundland. The first trial was carried out in a 35 foot, named as "Atlantic Swell". The second sea trial was accomplished in a 75 foot vessel, named "The Shamook". Except for the Wave Bouy, the same instrumentation, methodology and regulation were used on both sea trials.

5.1.1 Instrumentation

The following is a general description of the instrumentation used in both sea trials:
Data Acquisition System (DAS):

The DAS consists of a customized designed software package that runs in two notebooks computers. These computers were mounted on a "Daqboard" hardware (see Figure 18). This software includes the following characteristics:

- FishingVesselLogger: this is the primary program used to acquire the analog data.
- CompassPointGPS: this is a processor linked to the FishingVesselLogger that receives information from the DGPS unit and also logs all the GPS data.

- FishingVesselCal: it is used for post-calibration of the acquired data.
- CompassPointNMEA Parser: it is used to post-parse the NMEA data stream from the CompassPoint 2200 GPS unit and save the resulting parsed data in ASCII format.

Additionally, the system incorporates other devices, such as:

- CompassPoint 2200 GPS: gives vessel's position and heading, rate of turn, etc.
- IOTech Daqbook 2000: provides ana-digit conversion for analog signals of rudder angle, MotionPak, accelerometers and inclinometers.
- Signal Conditioning and interfacing hardware for analog channels.
- Uninterruptible Power Supply (UPS).

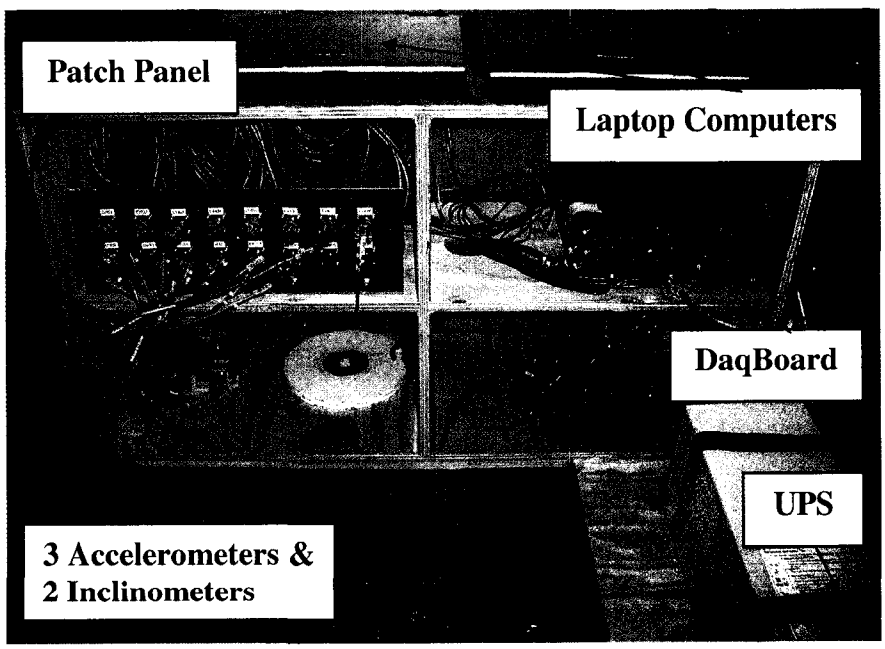

Figure 18. Data Acquisition System (DAS) [27].

Rudder Angle Measurements:

The rudder angle was determined by means of a winding cable with a wax string extension. The angle was measured from a 10 inch yo-yo type potentiometer linear displacement transducer installed around a groove cut in a circular ½ inch (1.27 cm) thick Plexiglas plate (see Figure 19). The rudder angle was calibrated about a protractor fixed to the top of the circular plate according to an estimate of zero degrees rudder angle information given by the vessel's captain.

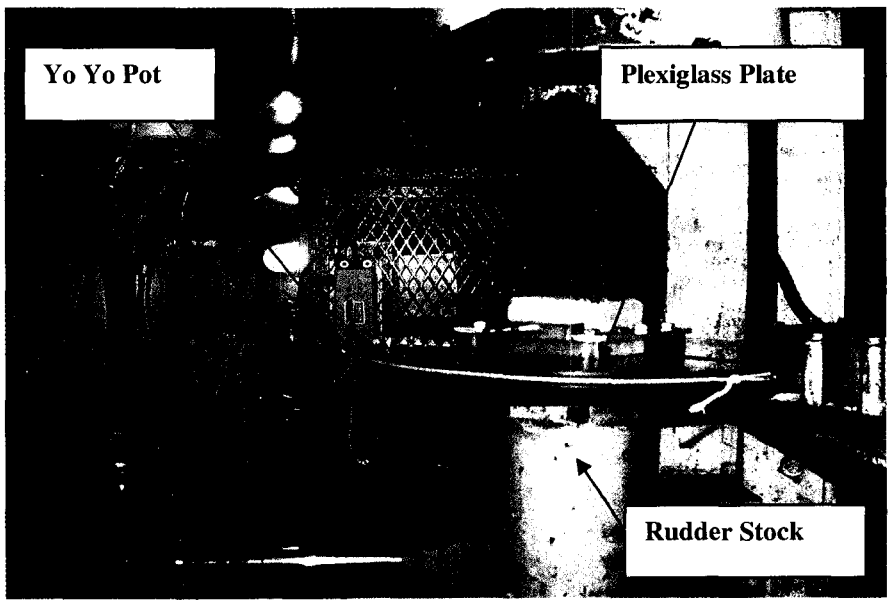

Figure 19. Rudder Angle Measurements [27].

The MotionPak:

A MotionPak was used to measure ship motions in the six degrees of freedom (see Figure 20). This instrument was positioned in the fish hold of the vessel and outputs the following channels:

- Roll rate
- Pitch rate
- Yaw rate
- Surge Acceleration
- Sway Acceleration
- Heave Acceleration

From these six channels the MotionPak software was used to derive the following 18 channels in either an earth or body coordinate system and move the motions to any point on a rigid platform fixed to the forward bulkhead. The channels were the following:

- Roll Angle, Rate and Acceleration
- Pitch Angle, Rate and Acceleration
- Yaw Angle, Rate and Acceleration
- Surge Displacement, Rate and Acceleration
- Sway Displacement, Rate and Acceleration
- Heave Displacement, Rate and Acceleration

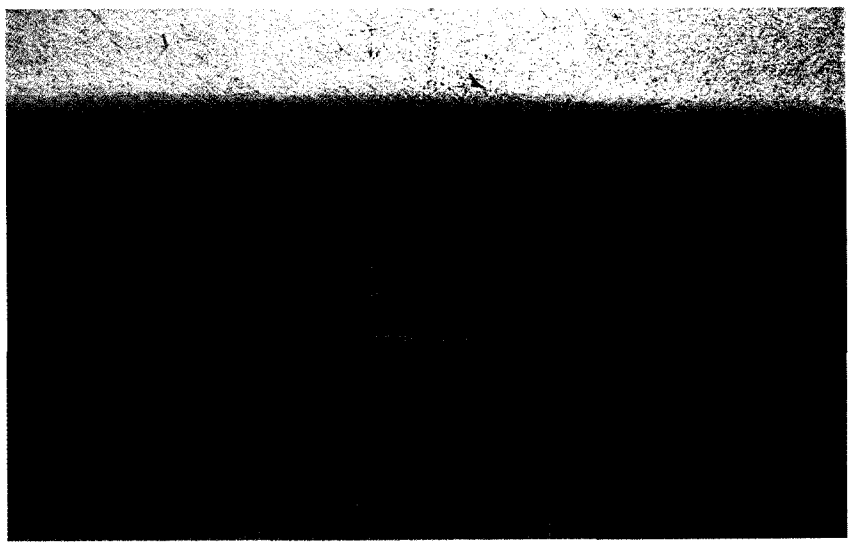

Figure 20. MotionPak Installation [26]at Nominal CG .

Furthermore, orthogonal linear accelerations of sway, surge and heave were analyzed in the vicinity of the DAS. This instrument was used to validate data collected by the MotionPak. Moreover, two inclinometers, also located near the DAS, were used to determine the pitch and roll angles.

Differential Global Positioning System (DGPS) Data:

This standard tool for marine navigation gives world wide three dimensional position coverage in real time by means of 24 satellites. Despite the fact that the GPS is operated by the US Defence Department, it is the most accurate technology available now for civilian application.

This system provides information about the vessel's position, speed and course. A Differential GPS (DGPS) increases the accuracy of the information obtained with standard GPS, including error corrections by means of a GPS signal transmitted via HF from a receiver located on pre-established positions on land.

In order to include the DGPS error corrections in the sea trials, a CompassPoint 2200 GPS was fixed on top of the deckhouse. The antenna was aligned with the vessel's centre line over the C.G. The DGPS correction signal was obtained from the Canadian Coast Guard station in Cape Race, NL.

Propeller Shaft Speed:

The propeller shaft speed was determined using an optical sensor that acts on a piece of reflective tape added on the propeller shaft at the bottom of the fish hold. The pulse train received from the optical source was fed to a custom designed frequency-to-voltage

(F/V) circuit that transformed the digital pulse train into a linear DC voltage proportional to the shaft RPM.

Additional instrumentation such as wind anemometer, sea water temperature/density measure, propane generators and signal cabling was included in the two sea trials.

Directional buoys:

The Directional Wave Buoy used in the sea trial of the 35' "Atlantic Swell" was a discus shaped (0.75 m of diameter, 15.7 kg) directional wave buoy (see Figure 21). It was used to collect information of the wave field conditions during the sea trials. The buoy configuration established the acquisition of data for 17.07 minutes every half hour. It could process and store the information as ASCII file on an internal non-volatile flash disk. The communication between the vessel and the buoy was possible using a radio modem. The buoy assembly was composing of the following components:

- Instrument housing: it is a sealed aluminium cylinder with connections for antenna and on/off plug on top. It contains the instrumentation package, onboard computer and onboard radio modem. The instrumentation package include sensors to measure all components of the motions. It was required to transform the buoy-fixed acceleration into an earth-fixed coordinate system (vertical, east-west and north-south) using these sensors. The uni-directional as well as multi-directional wave information was established by means of the earth-fixed accelerations.
- Battery housing: composed of a small sealed aluminium cylinder installed below the instrument housing that include the battery pack with 27 disposable Dcell alkaline

batteries that give a 1 to 2 week of lifetime, maintaining the data collection every half hour.

- Flotation assembly: consist on a rugged urethane foam and aluminium cage that generates enough buoyancy for the instrument and battery housing.
- On shore modem: the communication between the laptop computer onboard and the wave buoy was possible by means of a modem with power supply and antenna. The buoy manufacturer provided a windows based user friendly software package that executed the communication. The data can be recovered using an umbilical connection to the buoy.
- Mooring assembly: personnel from the Memorial University Physical Oceanography Group designed a 165 m depth mooring system. The deployment of the buoy was accomplished by the Coast Guard vessel "Shamook".

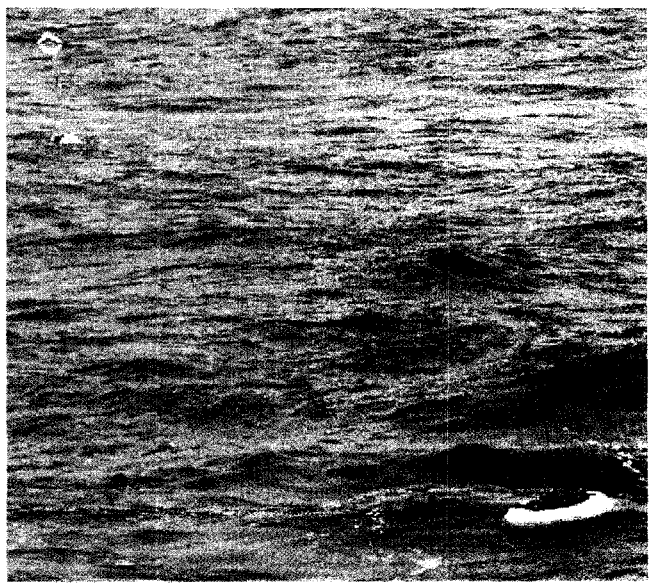

Figure 21. Wave Sentry Buoy and Radar Reflector [26].

Unfortunately, the discus shaped directional buoy was not available for the second sea trial. Therefore, during the sea trial of the 75' ("The Shamook"), a Datawell Waverider Mark II wave buoy was used. This buoy was leased from Oceans Ltd. Of St. John's, NL and they conducted the launch and recovery operation as well as the data collection and the generation of the final data product.

This wave buoy was deployed in 165 m of water at 10 nm east of St. John's approximately. The data were collected every one hour and transmitted to the vessel at a frequency of 29.760 MHz with an output power of 150-200 mW, (see Figure 22).

The personnel of Oceans provide a single point mooring in order to ensure adequate symmetrical horizontal buoy response with low stiffness enable the buoy to follow waves up to a wave height of 40 m with a resolution of 1 cm and wave periods of 1.6 to 30 s. The wave direction resolution was determined in 1.5° and the wave frequency resolution was establish in 0.005 Hz for frequencies less than 0.1 Hz and 0.01 Hz otherwise. The weight of the buoy is 212 kg and was anchored with railway train wheels given a total weight of 635 kg (1400 lbs.). The following is the instrumentation integrated in the buoy:

- Hippy-40 pitch angle/roll angle/heave displacement.
- Three axis flux gate compass.
- Two fixed X and Y linear accelerometers.
- Sea temperature sensor.
- Micro-processor.

Onboard "The Shamook' was a receiving system mounted. It included a passive 3 m long whip antenna installed on the port side above the wheelhouse. Also, a laptop computer

for storing and displaying the data collected from the buoy was used as interface. The receiver was configured to receive information at 38.760 MHz and an IOT UPS provided power supply for the laptop and for the receiver.

Figure 22. Datawell Wave Buoy Deployed [27].

5.1.2 Sea Trials

The 35 foot "Atlantic Swell":

This typical 35 foot fibreglass fishing vessel (see Figure 23) was built in King's Boat Building (St. Jones Within) in 2001. The main activity of the vessel is the inshore crab fishery. When the market conditions change, this vessel is also able to fish Capelin and Codfish.

The storage capacity of the vessel is 20,000 lbs (9,100 kg) of Codfish and 12,500 lbs (5,450 kg) of snow crab in a single trip. This dissimilarity in capacity is due to the difference in weight densities and storage methods between species.

The sea trial was conducted at 10 nm east of St. John's following the ITTC Recommended Run Pattern, Figure 25. Prior to sea trial departure, several hydrostatic characteristics such as natural period and GMT at zero speed were calculated by means of an inclining experiment. The water temperature and salinity was recorded as well as the instrumentation was inspected and calibrated. Also, the vessel's draft was estimated at the bow and at the stern.

The wave buoy was located at the position 47° 34' 21'' North and 52° 26' 45'' West. Once the "Atlantic Swell" arrived at this position the wave conditions were optimal. Based on the data given by the wave buoy, the significant wave height was about 2 meters with a dominant direction of 148 degrees True North. The wind velocity was estimated as 10 - 12 knots.

Following the ITTC patterns, ten forward speed runs were conducted; five at 4 knots in head, following, bow, beam and quartering seas, and five at 8 knots in similar headings. Between these two sets of runs, an additional drift test was carried out at zero speed. The aim was to determine the magnitude and direction of the resultant wind, wave and current vector acting on the vessel.

The 75 foot "Shamook":

This 75 foot vessel was built by the Georgetown Shipyard in Georgetown, Prince Edward Island in 1975 (see Figure 24). It is a long inshore fisheries research vessel currently operated by the Canadian Coast Guard (CCG) in the St. John's Harbour. Usually the "Shamook" is used by scientists of Memorial University and the Federal Department of Fisheries and Oceans for scientific research. Although, it is not a typical fishing vessel,

"Shamook" is a suitable subject vessel at the upper end of the fishing vessel length range (75 feet).

The sea trial was carried out on December 15, 2003 at 10 nm due east of St. John's. The water depth in that position is 165 m. Before the departure the draft at the bow and stern of the vessel was measured. This operation was carried out with the wave buoy and mooring/anchor onboard, therefore another measure was taken after the incline experiment at the end of the trial. The instrumentation was examined and calibrated as well. In order to determine the natural period of the vessel, a 10 minute zero speed run was performed in the St. John's harbour prior to the start of the sea trial.

Once the vessel reached the predetermined location, personnel from Oceans Ltd. launched the directional buoy at location 47° 34' 17'' North and 52° 26' 13'' West. The significant wave height was measured at a nominal 2 meters with winds of 10-15 knots coming from the west. Based on the information collected from the buoy, the dominant direction of the waves was north.

Following the recommended ITTC test pattern (Figure 25) a total of ten forward speed runs were carried out. Five runs were evaluated at 4 knots in head sea, following sea, bow sea, beam sea, and quartering sea. The other five tests were accomplished at 8 knots in the same directions. Between these two experiments at different speeds, an additional run was carried out at zero speed. A drift test was also conducted in order to determine response of the vessel in a zero speed trial.

Proceeding of the Runs:

1. The vessel was positioned in the vicinity of the wave buoy.

2. The head sea direction in degrees magnetic was corrected based on the wave buoy data. The correction value was estimated in 21 degrees. This value was used to establish the direction relative to the true north.

3. Two operations were conducted in order to achieve the course and speed. The first was the selection of the speed over ground and the heading (head sea run). Then, the adjustment of throttles and set of course were carried out. Once the steady state conditions of the sea were presented, the data collection began.

4. The desire course during the runs was established manually. However, it was difficult to keep a steady course, especially at low speed. The value of rudder deflection under these conditions was approximately 20 degrees.

5. The data acquisition ended after 25 minutes of steady course.

6. The vessel position was rotated 180 degrees with the aim of established the "following sea" condition. Also, the shaft RPM were set to obtain a constant speed over the ground and therefore, a patron of comparison between runs. This adjustment was established in all the courses. The collection of data on this course was completed after 40 minutes.

7. Likewise, the course arrangement of 135 degrees was conducted following the ITTC pattern, see Figure 25.

8. This run was scheduled to collect 25 minutes of data.

9. The next run continued in Beam Sea at 90 degrees. After 25 minutes the acquisition of data finished.

10. The course modification of 45 degrees was established to be consistent with the ITTC pattern. After 25 minutes the acquisition of data finished.

11. Once the first five runs were finished, the information of the wave buoy was analyzed again. This operation was conducted with the purpose of confirm the wave direction and to verify that correct operation of the buoy before the second set of runs begin.

Figure 23. The 35 feet "Atlantic Swell" [26].

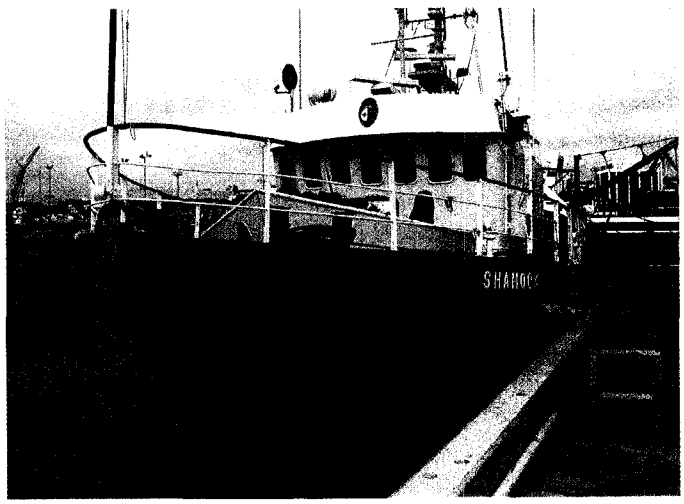

Figure 24. The 65 feet "The Shamook" [27].

The test plan in the sea trial was based on the procedures described below:

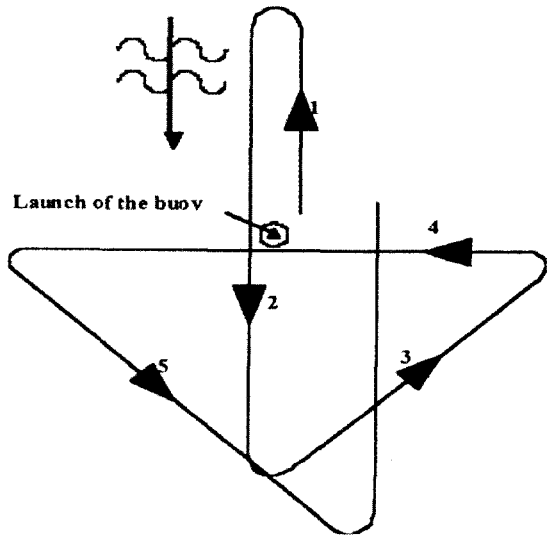

Figure 25. ITTC Recommended Run Pattern, ITTC Procedures Book, 22nd ITTC, Sept 1999 where Run 1 is Head Sea, Run 2 is Following Sea, Run 3 is Bow Sea, Run 4 is Beam Sea and Run 5 is Quartering Sea.

5.1.3 Sea trial data evaluation

Online data analysis:

With the purpose of ensuring that all the instrumentation was operating correctly an online evaluation was performed. The Data Acquisition System consisted in a network of two laptop computers. Two computers were used in order to prevent overloading of the system with the collection of the data. One computer used the software FishingVesselCal to record the raw data from the data stream. Principally, this computer converted the data format into a standard format. The other computer was utilized for the data analysis of the preceding run and also for contact with the wave buoy.

Wave data analysis:

Directional wave data were calculated from the motion of the wave buoy. Motions in the six degree of freedom were collected by sensors positioned in different locations onboard the vessel. These devices measured the angular and vertical accelerations of each motion.

Particularly in the sea trial of the 35', within the wave buoy the sea direction was measured with flux gate compass. Therefore, the data were generated in degrees magnetic. The city of St. John's has a magnetic deviation of 21.1 degrees west approximately. This value was added to obtain the wave direction in degrees true.

Raw data analysis:

The data collected by the instruments onboard was recorded originally as a voltage differential. Then, using the software FishingVesselCal a calibration file was applied to the raw data. This file consisted of a five point linear regression of each instrument. The calibration was finished in the labs of the Institute of Ocean Technology (IOT).

Ship motion analysis:

The motions on the 75' length class were calculated at two locations on the vessel: the vessel's centre of gravity and the position of the MotionPak installed close to the centre of gravity. In the case of the 35' length class the motions were measured at the vessel's centre of gravity and at Master's steering position.

For these measurements, specific software was used to evaluate the MotionPak data. This program allowed the translation of the accelerations collected to any location onboard

avoiding the use of sensors. Thus, the measured of data at the Master's steering position was accomplished without any sensors there.

Roll and Pitch analysis:

In order to established the roll and pitch period, a variance spectral analysis was performed on roll and pitch data for zero speed. The experiment at zero speed was conducted in the St. John's harbour before the sea trial begun. The output values of the spectral peak are presented in Table 23.

Period	"Atlantic Swell"	"The Shamook"
Roll	3.2226 s	6.0750 s
Pitch	2.5726 s	3.9405 s

Table 23. Period of Roll and Pitch.

Validation of MotionPak Software and Instrumentation:

In order to verify the MotionPak algorithms, the vessel's motions were translated from the original position of the MotionPak to the accelerometers positioned close to the DAS in the wheelhouse. Then, all the motions were evaluated in the body-fixed coordinate system.

5.2 Comparison between Sea Trials and Numerical Results

This section presents a comparison between the full scale vessel's motion and the numerical simulations. The full scale data are collected onboard the vessels along with the buoys on the wave field. Consequently, the significant amplitude of motion in all headings is estimated considering the sea state measured by the buoy in the testing day. The collected

data during the Sea Trials are in the time-range from 7:30 am to 10:00 am. Hence, the wave conditions are changing during the trials with new data for the waves generated by the buoy every 30 minutes, (17.07 minutes for the "Atlantic Swell").

At first, the simulations are performed in MOTSIM using the wave conditions at the time of a corresponding heading. For example, the wave at 9:30 am is used for the 65 degree of heading, since that was the time at which this heading was tested

Subsequently, and in order to determine possible variation of the results due to wave field conditions, the numerical simulations are repeated considering each wave condition estimated by the buoy. For example, the wave spectra at 7:30 am is used for all headings, and similarly the wave at 8:00 am, 8:30 am, up to 10:00 am.

In this set of simulations the same number of frequencies were used for all the headings (35) and all the wave conditions. In the original set of simulations the number varied according to the particular set of wave data (varied between 35 and 40).

It is important to mention that the spectra obtained every 30 minutes from the buoy is plotted in the charts below using a pink line and the data collected from the Sea Trial is presented by means of a dark line.

Likewise, the results presented in this chapter are calculated with the program MOTSIM based on the same considerations for both vessels at two speeds, 4 kt and 8 kt. Because the wave buoy failed due to low battery problems after 10:00 am during the Sea Trial of the "Atlantic Swell", the simulations were conducted only at low speed for this vessel.

The 35' "Atlantic Swell" at low speed:

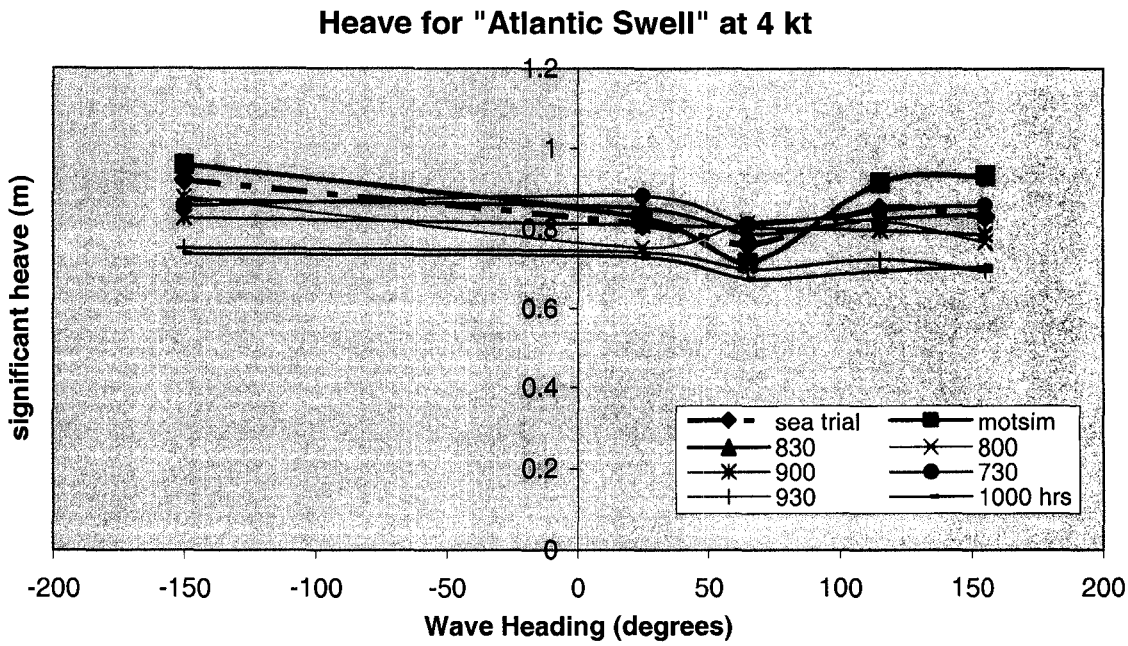

Figure 26.

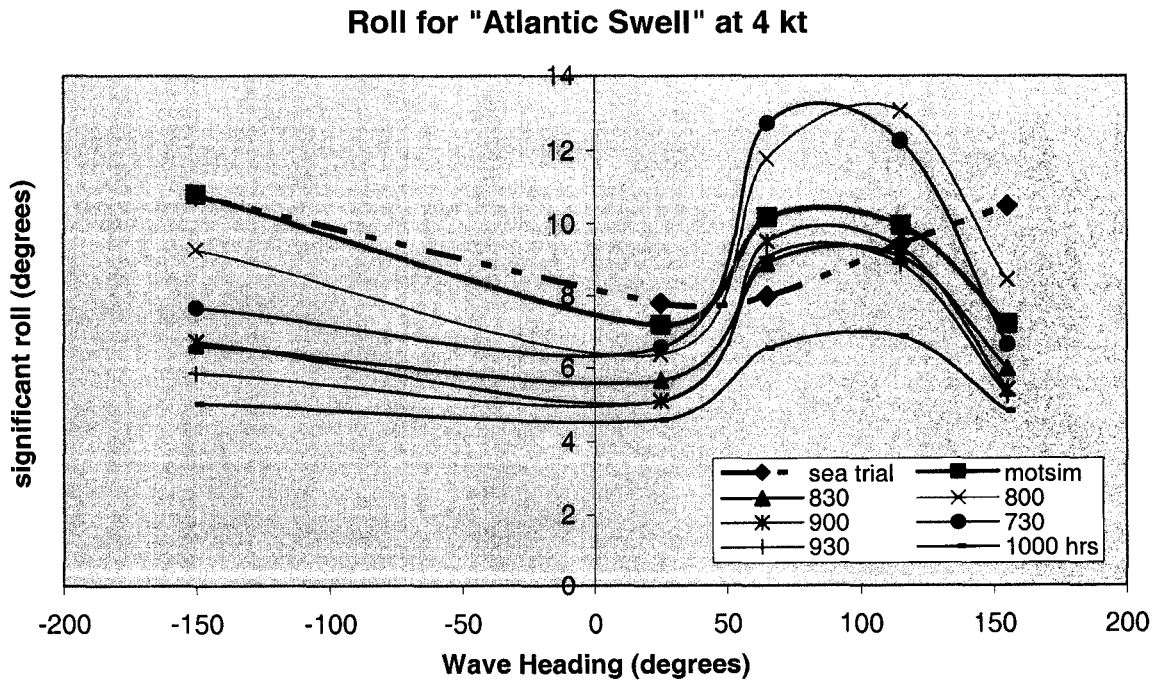

Figure 27.

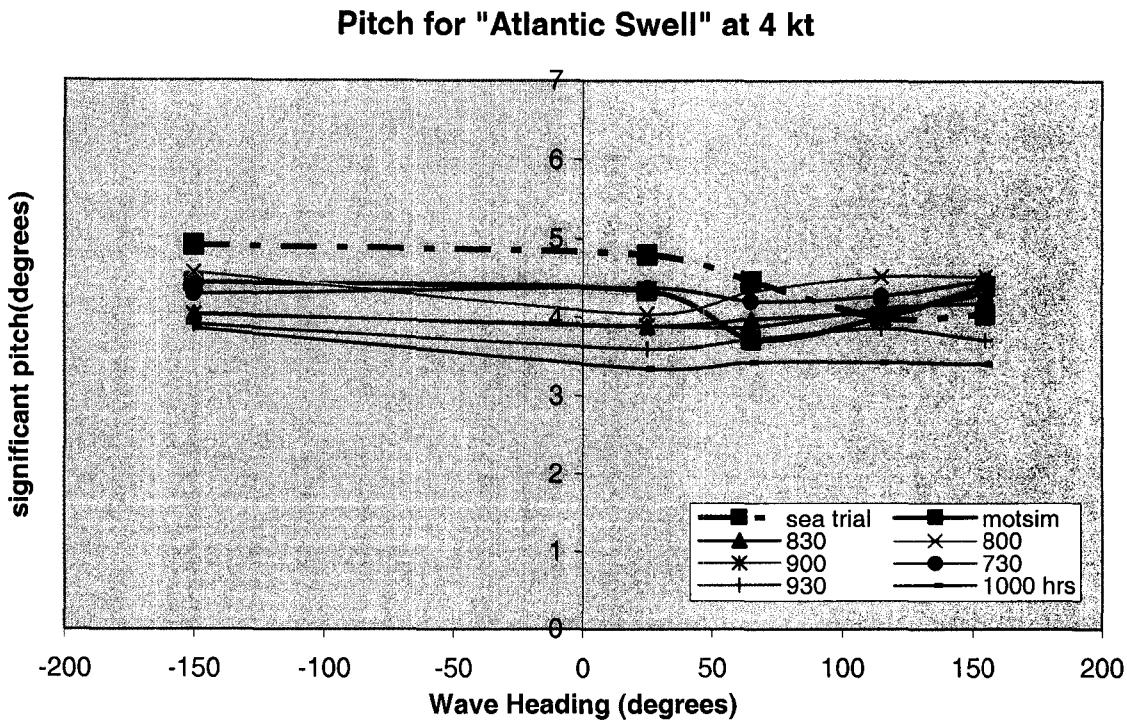

Figure 28.

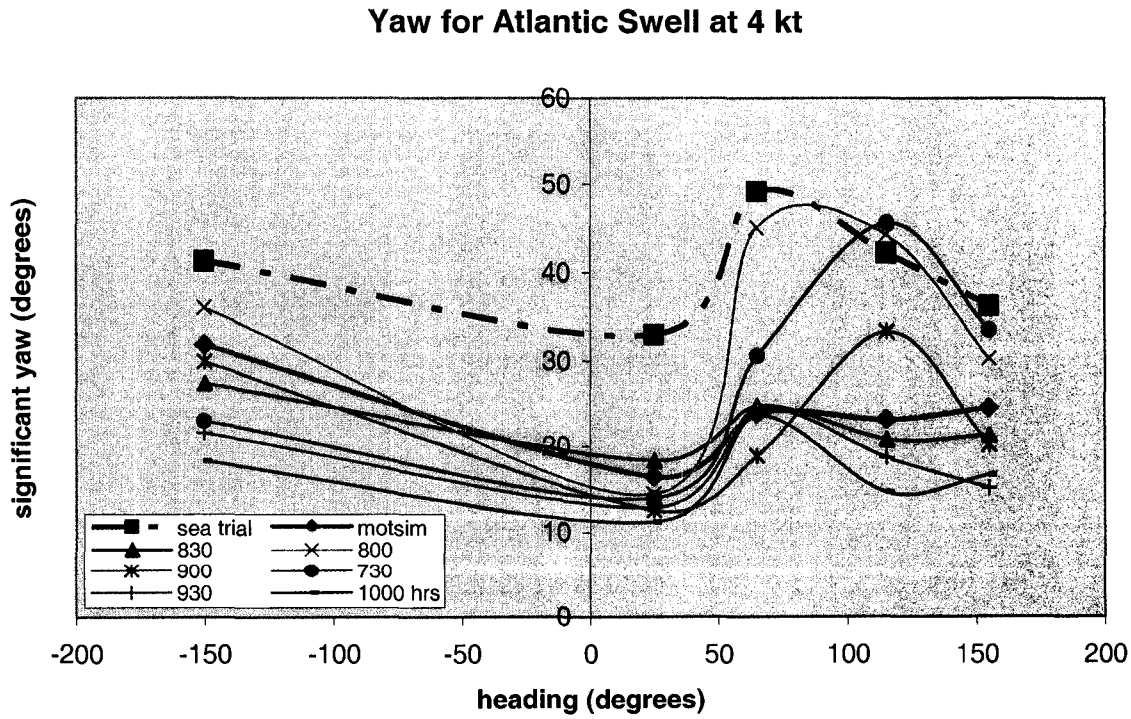

Figure 29.

The 65' "Shamook" at low speed:

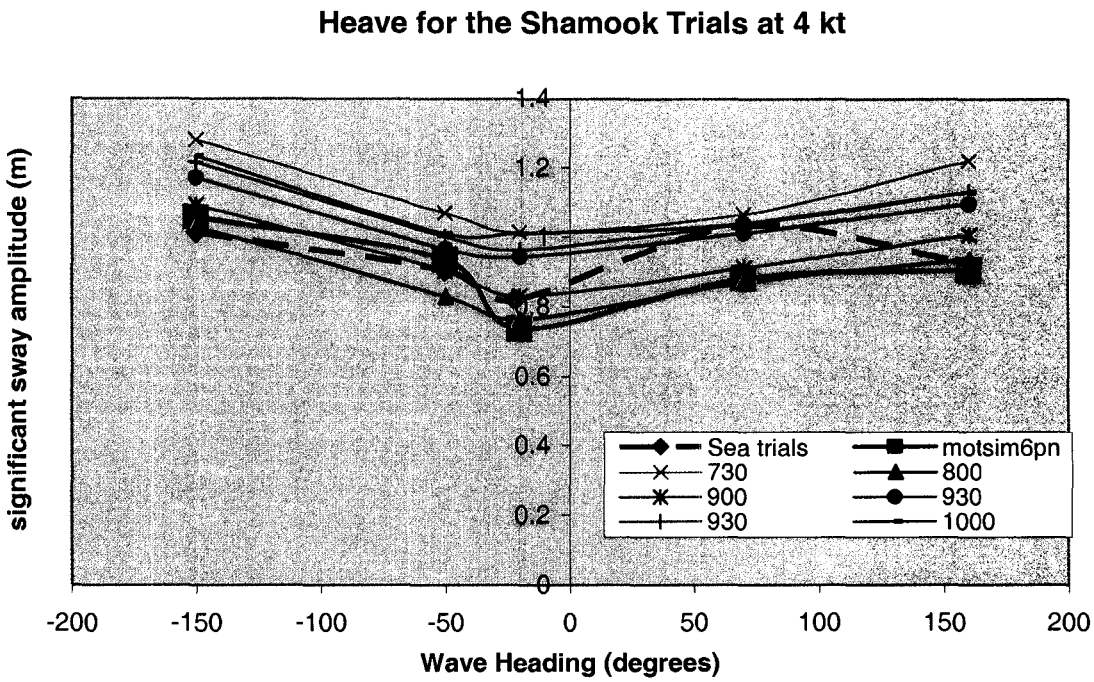

Figure 30.

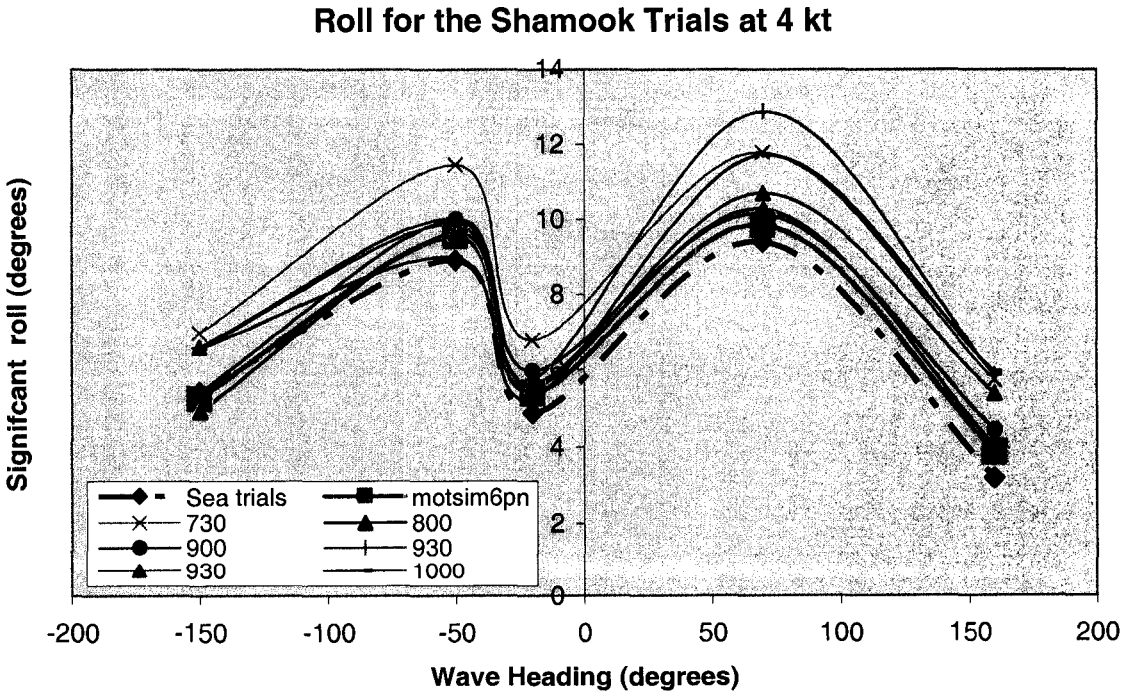

Figure 31.

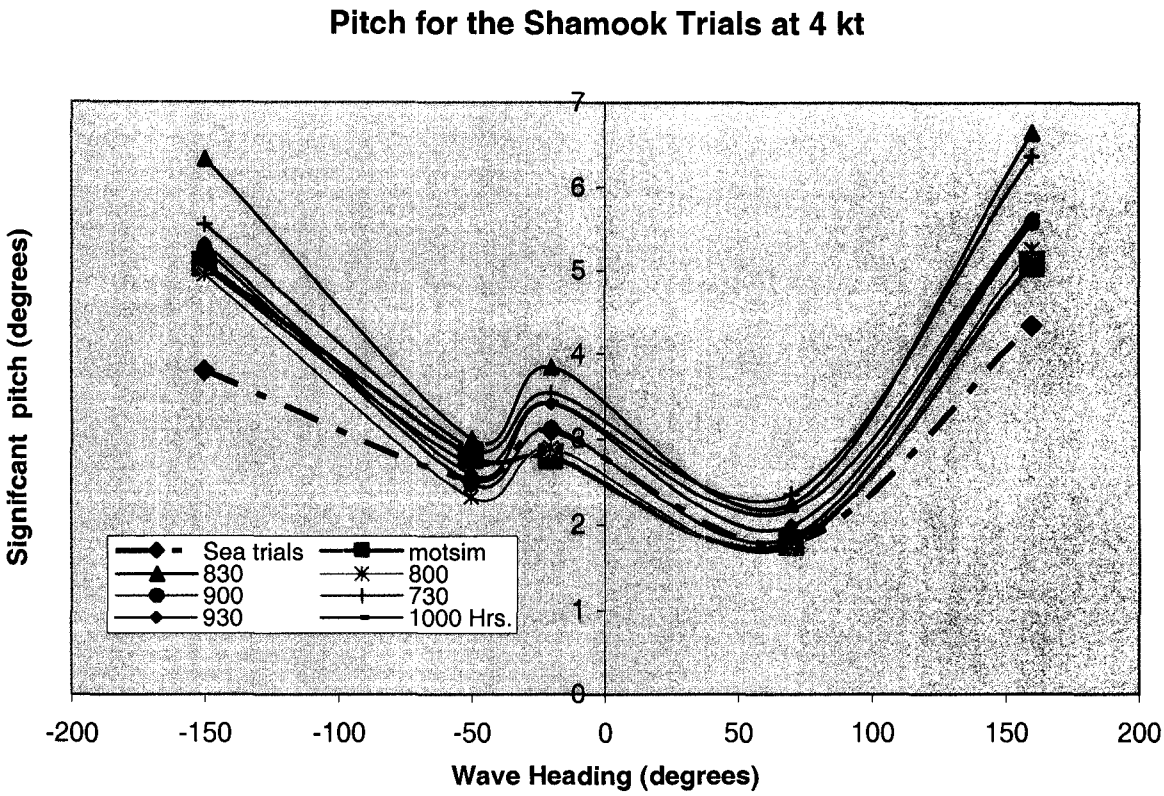

Figure 32.

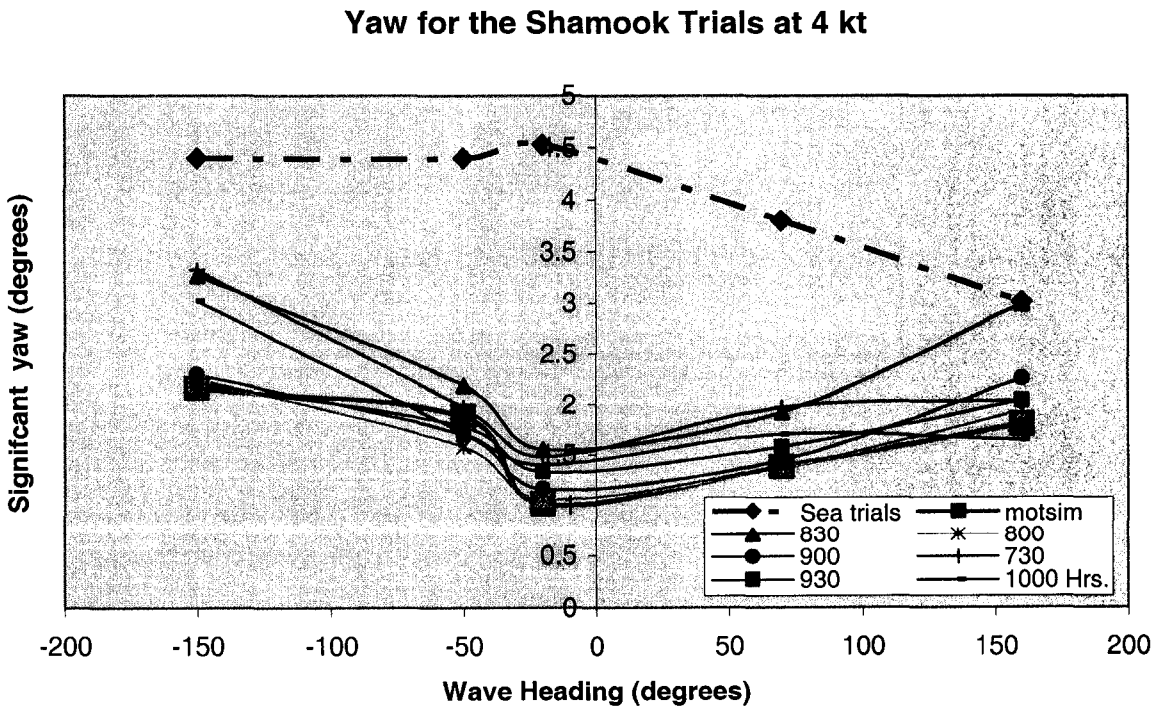

Figure 33.

The 65' "Shamook" at high speed:

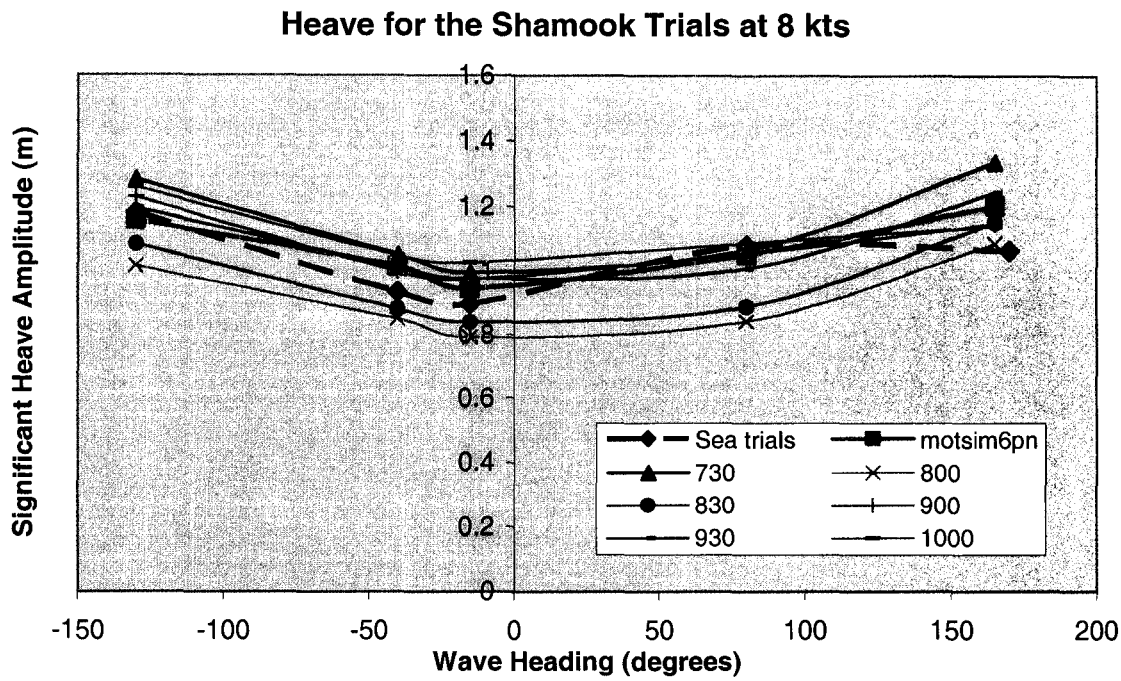

Figure 34.

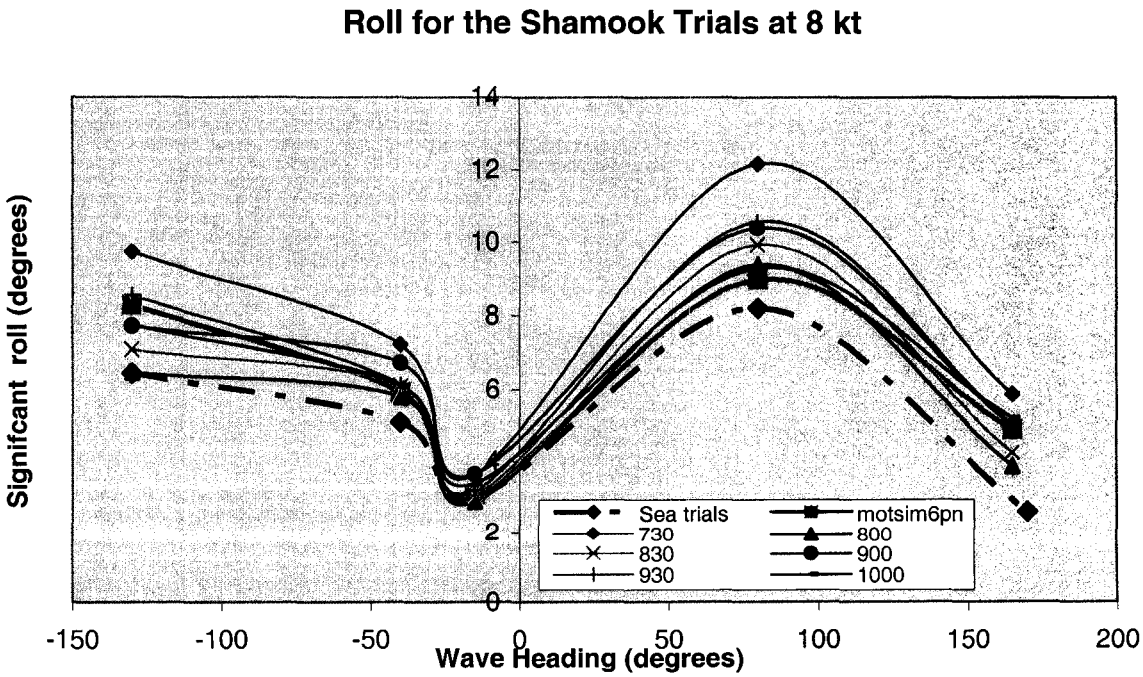

Figure 35.

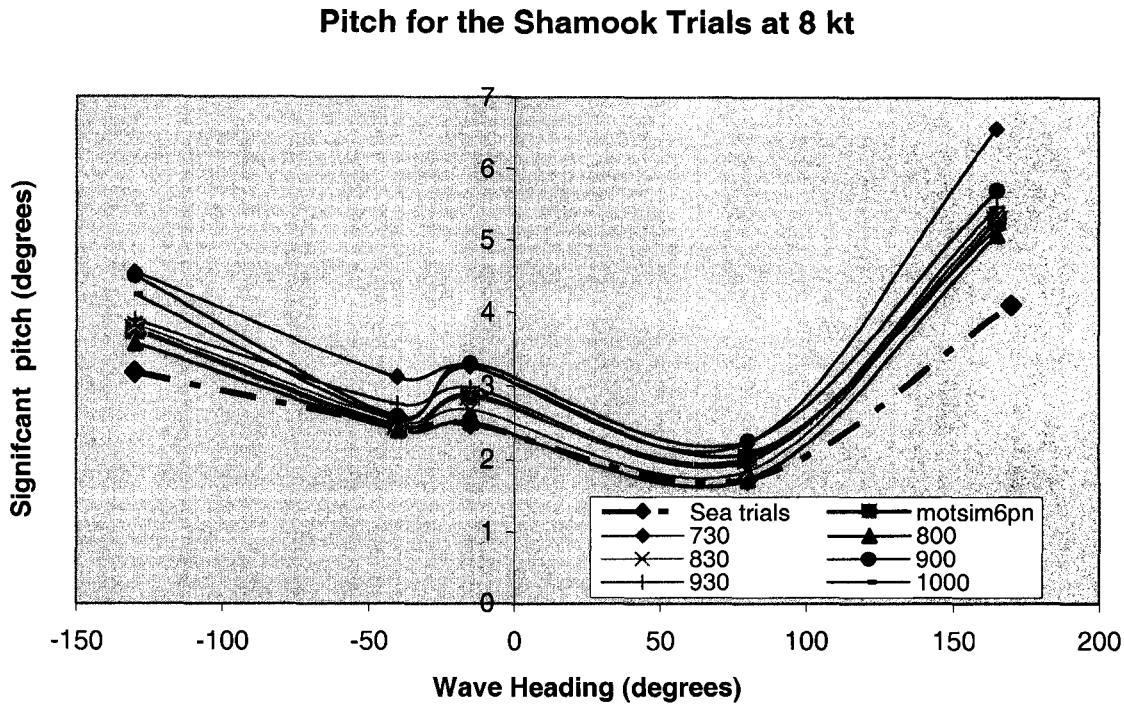

Figure 36.

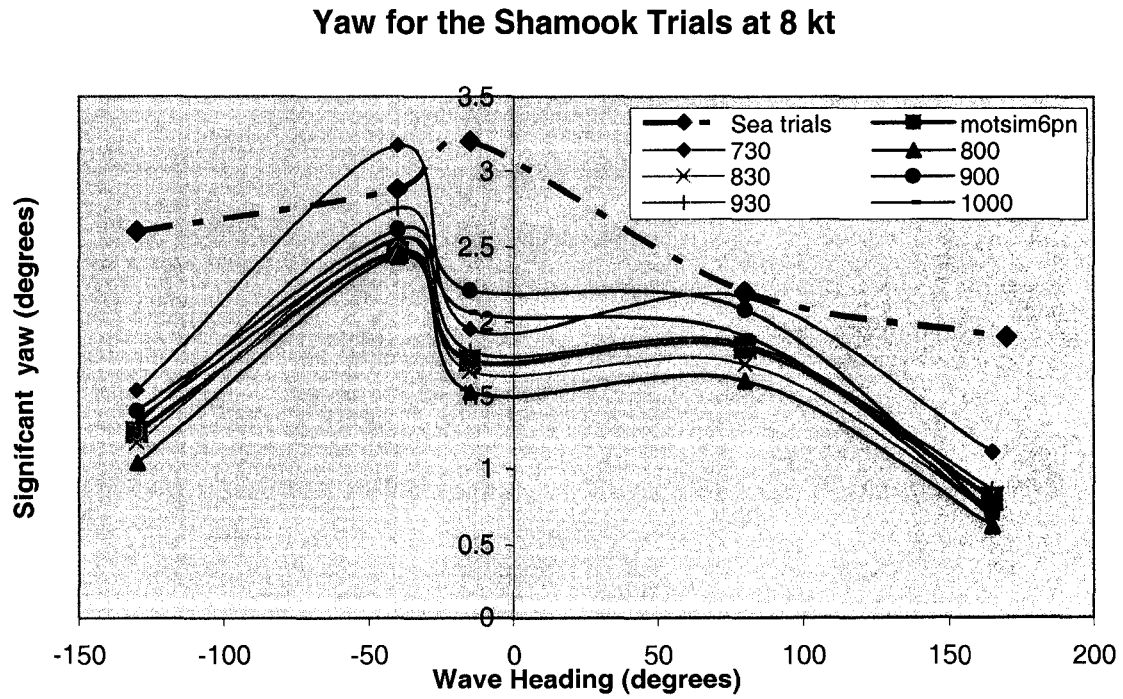

Figure 37.

5.3 Analysis

The numerical results of the motions compared with the findings obtained in the Sea Trials in a small vessel and a large vessel (35' and 65'), present a good relationship in the motions of Heave, Roll and Pitch.

The Yaw motion depends very much on the course keeping and captain skills to avoid wave encounter in order to control the Roll motion. On the other hand, the numerical code includes an auto pilot for the control of heading. Because of the absence of this instrument on board "Atlantic Swell" during the seakeeping trials, the Yaw is not perfectly established and thus a difference between the results exists.

The dissimilarity in the results of Yaw motion is less significant when the main wave direction comes from Head Sea in both vessels at low speed. Under the other conditions, following, beam and quarter Sea, is difficult to maintain a straight course, basically because the mulidirectionality of the waves produces constant changes in the course and the Roll motion tends to increase.

Chapter 6

Numerical Results

The present chapter introduces the numerical results for Motions and MII of four fishing vessels. The numerical analysis is conducted at two vessel speeds that are represented in terms of the Froude Number ($Fn = V/\sqrt{gL}$) and four wave field conditions. Each vessel is evaluated in JONSWAP and Bretschneider spectra considering the uni-directionality of the sea as well as the multi-directionality of the sea.

This analysis establishes a particular motion profile for each length class using the wave parameters given in Table 16. Likewise, a comparison between the MII at critical points on board and angles of heading at different vessel speeds is established.

6.1 Motions Results.

The analysis of the results obtained from the motion simulations is established using four different energy wave spectra; JONSWAP, Bretschneider, Multi-directional JONSWAP and Multi-directional Bretschneider. It is assumed the motions of Heave, Roll and Pitch are the most representative. The vessel's motions are considered over five Headings at Fn=0.2 and Fn=0.4 vessel's speed. In terms of MII, it is determined that the influences of Beam, Quartering and Head Sea are the most significant. A complete description of the motion results for each length class is presented in Appendix A.

In the following graphs significant motion amplitudes are averaged over bow headings (90°-180°) and presented in terms of the vessel's length is introduced. This

evaluation is established in order to determine the influence of the size in the occurrence of MII due to waves coming from the bow, in four different sea conditions and at two significant speeds. One velocity represents the trawling speed (low) and the other one represents the speed that vessel uses when it returns to home port (high).

Low Speed, Fn= 0.2:

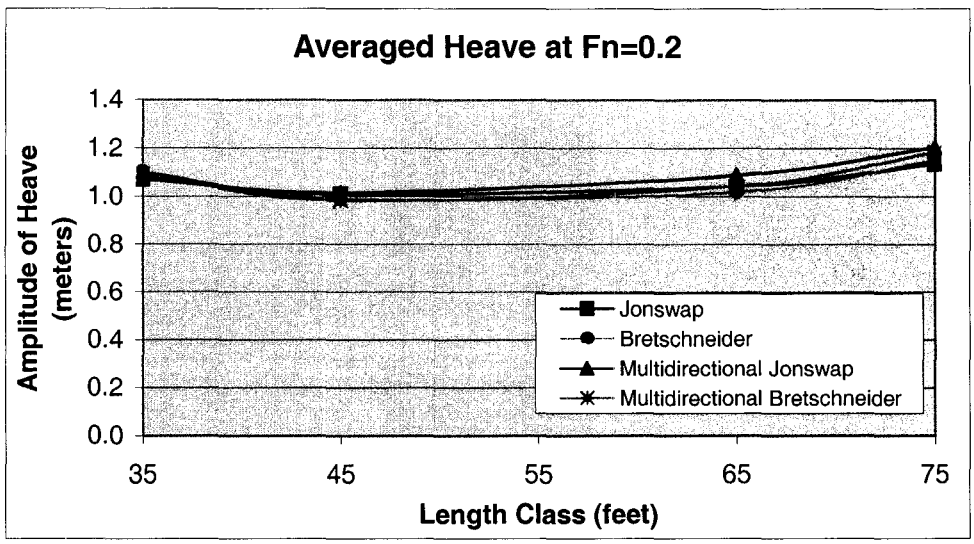

Figure 38.

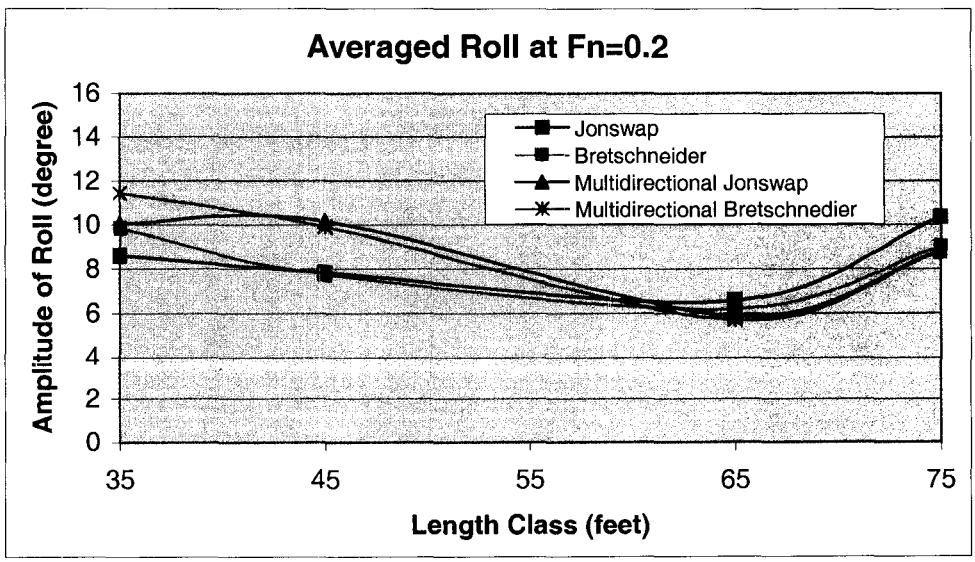

Figure 39.

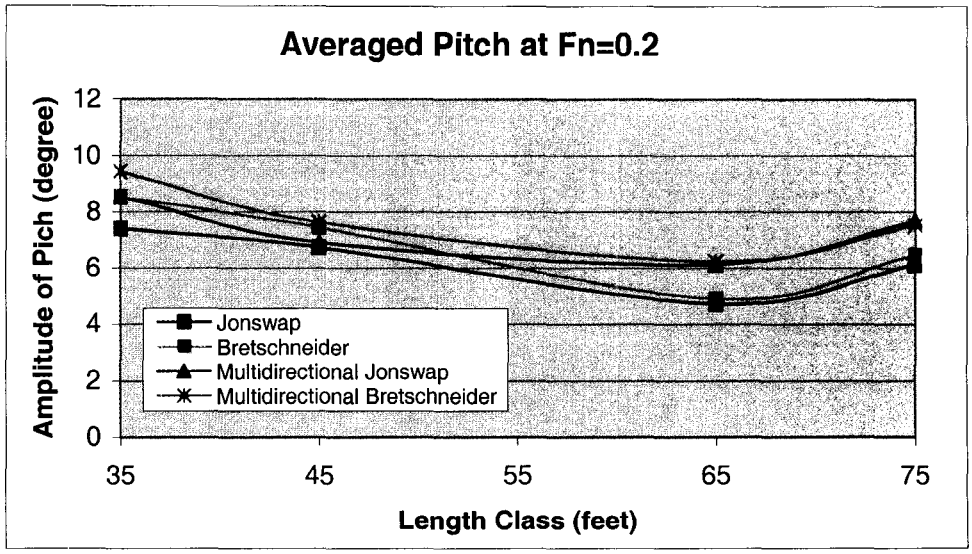

Figure 40.

High Speed at Fn= 0.4:

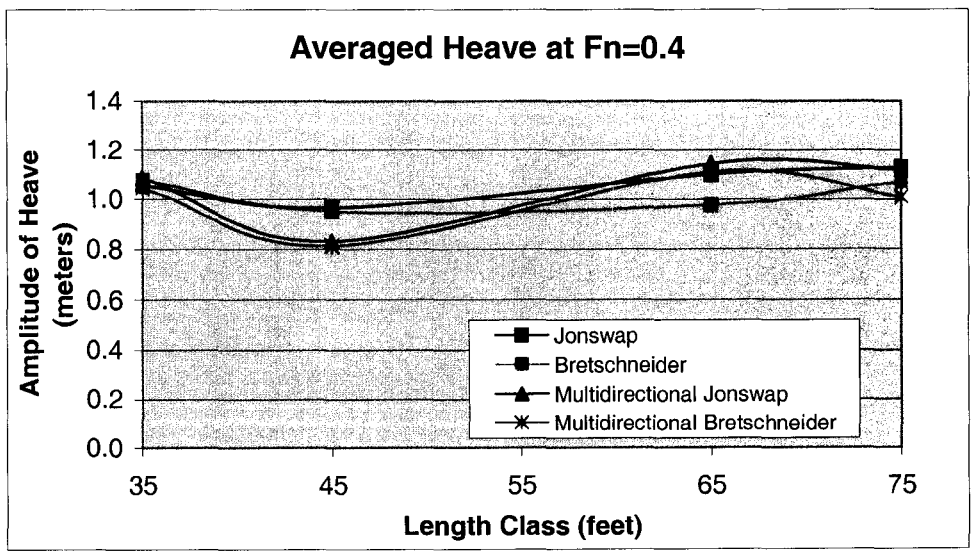

Figure 41.

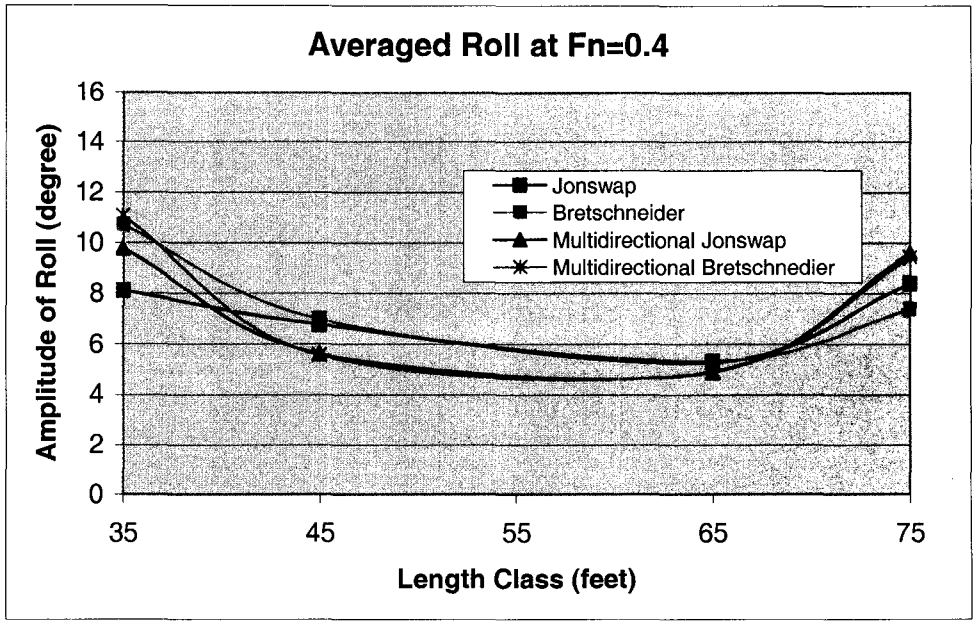

Figure 42.

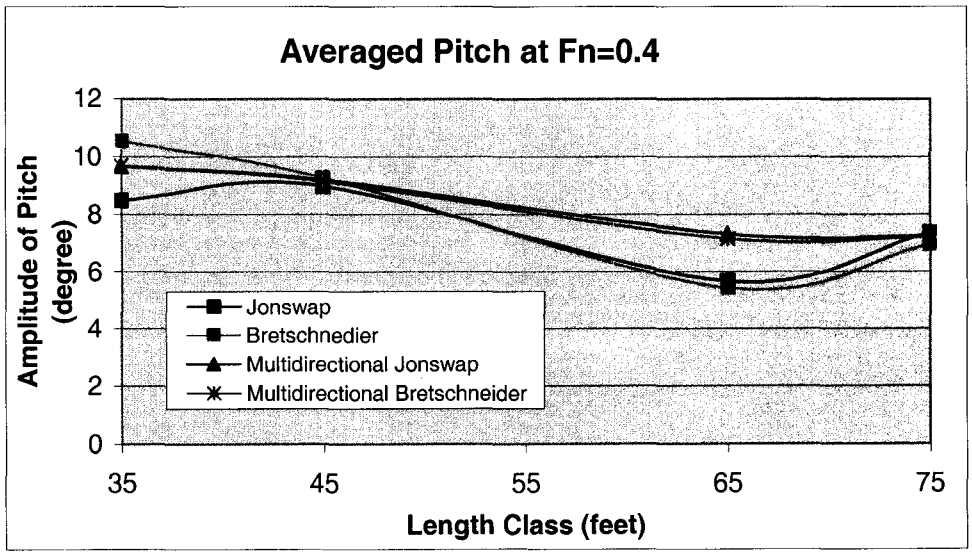

Figure 43.

6.2 Analysis of Motions

With the aim of presenting a complete analysis about the behaviour of the vessels in all the sea conditions, the motion response of Heave, Roll and Pitch are explained individually at low and high speed.

Heave Motion

At low speed all the classes performed in a similar way. The values of significant amplitudes of Heave in all the length classes are less than 1m for small vessels and less than 1.2 m for large vessels, respectively, under the same wave field conditions (see Figure 34).

Likewise, at high speed, the behaviour follows the same pattern. Moreover, the maximum value of significant amplitude of Heave is also less than 1.2 m. However, it is possible to distinguish a difference between directional and multi-directional waves in the 45' and the 65' length class. In the first case, a minimum value of significant amplitude in the two multi-directional wave spectra (JONSWAP and Bretschneider) is presented. In the second case, the 65', the amplitude shows a maximum value as a consequence of the multi-directional wave spectrum and the JONSWAP uni-directional wave spectrum (see Figure 37).

Roll Motion

In this motion, the small vessels (35' and 45') perform at the maximum values of roll amplitude. The 35' presents the highest value of significant roll amplitude in multi-directional Bretschneider spectrum (11.5 deg). Also, within the same wave spectrum the 65' presents the minimum value of roll amplitude at low speed (5.73 deg). The only length

class that shows dissimilarity between wave fields is the 45' length class. Here there is a difference of approximately 2 deg among the uni-directional and multi-directional wave field pairs.

Once the speed increases, no significant increment in the amplitude of roll is observed. However, there is a similar value of minimum amplitudes of Roll described by the multi-directional spectrum that follows the same pattern in the range of 45' to 65'. On the other hand, the only dissimilarity at high speed is observed in the smallest vessel, as well as in the largest one. In this case, maximum values of roll amplitude are established.

Pitch Motion

In the case of small vessels (35' and 45'), there are similar angles of significant amplitude of Pitch at both speeds. Except for the uni-directional JONSWAP wave field, these angles are between 8.7 deg and 10.5 deg in all the sea states.

The large vessels (65'and 75') behave similarly in each pair of wave conditions. At low speed, the difference between the values coming from the uni-directional and multi-directional sea state are, on average, 1.5 deg, always obtaining the smallest value in the pair of uni-directional wave conditions. However, at high speed, a difference in the sea states appears only in the 65' length class.

6.3 The MII Results.

The following graphs represent an average value of MII due to bow headings in four wave field conditions and at low and high speed. From the five points selected onboard, only point number 3 is above the deck, inside the wheelhouse. For these reason the other four are considered as "deck points". An average over bow headings calculated in order to

establish the number of MII per minute for each length class in any wave direction is included in the following charts. The complete results of MII are presented in Appedix B.

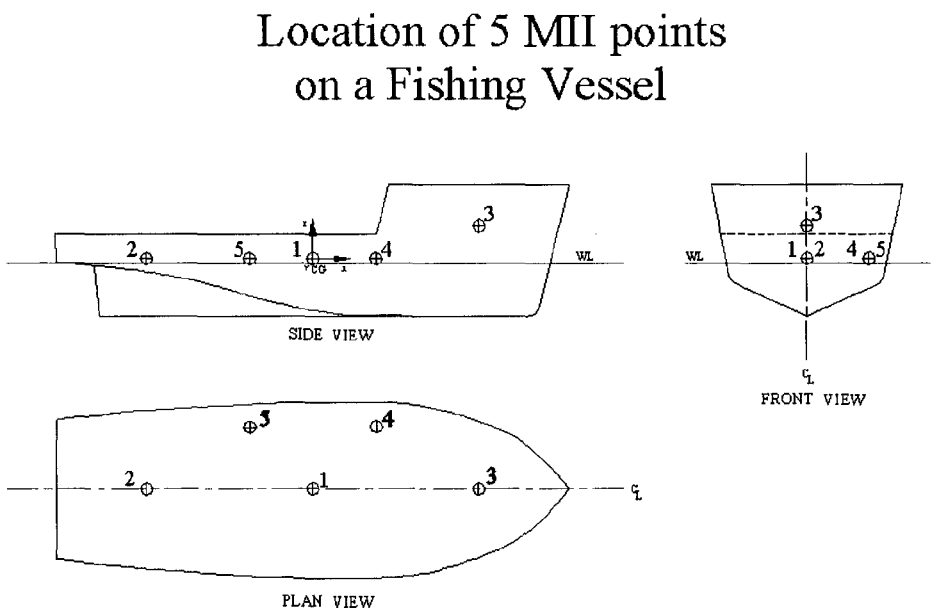

Figure 44. Selected locations on board.

6.3.1 Averaged MII for Bow Headings:

The findings of MII events are quantified considering an average over the four energy spectra. Furthermore, the occurrence of MII in the experiments obtained from the numerical simulations is significantly influenced by bow headings. These are represented by the beam, bow and head sea. Therefore, the average MII in the following charts is established only within this range of headings.

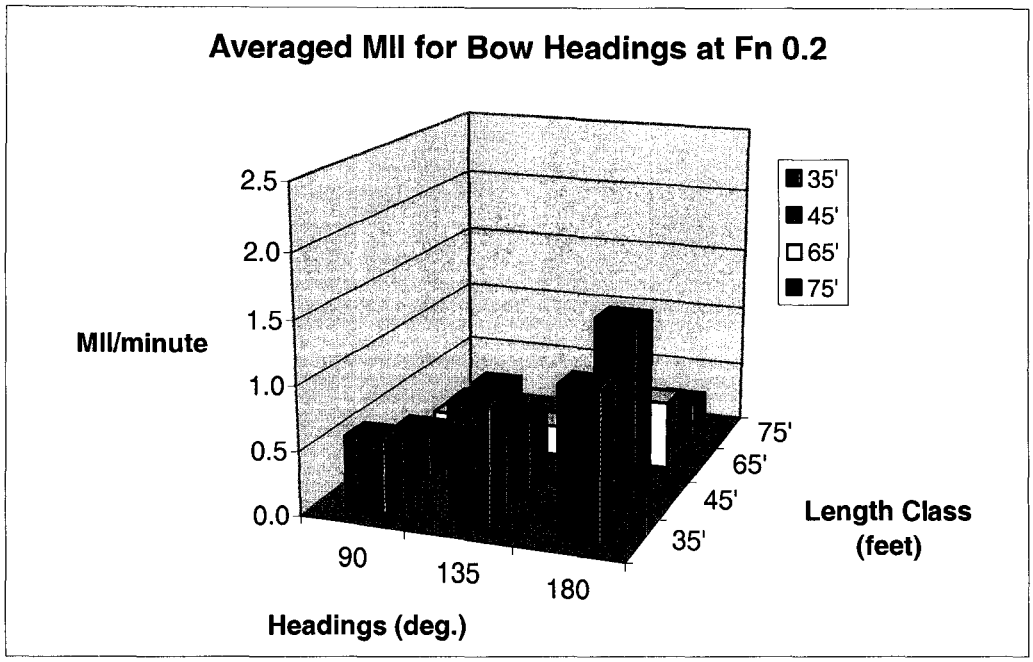

Figure 45.

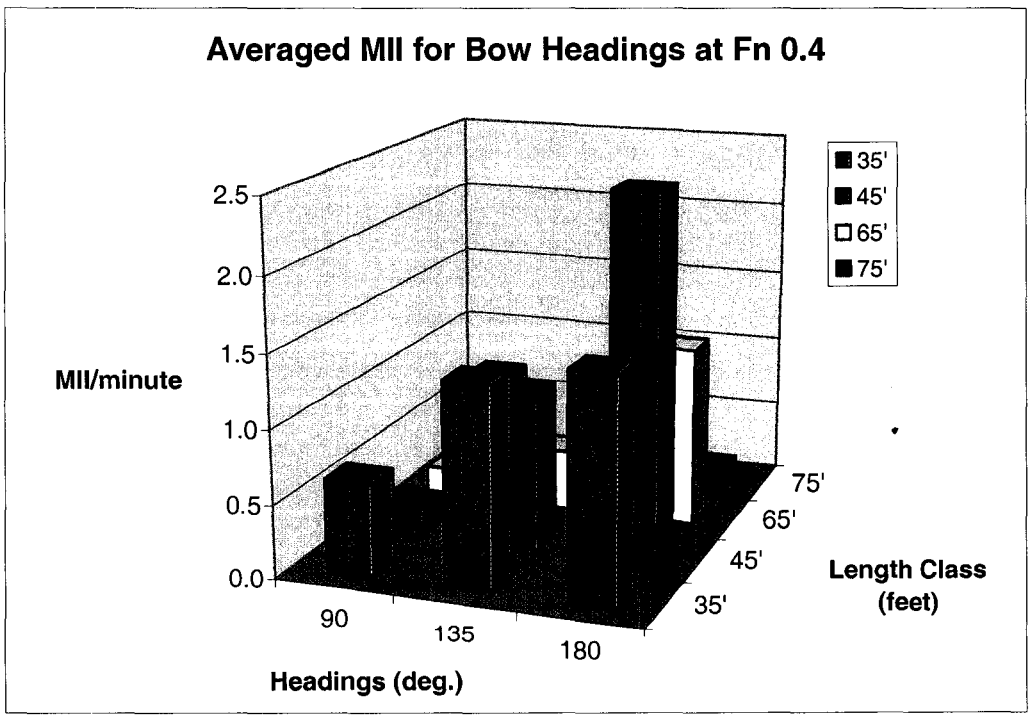

Figure 46.

6.3.2 Average values of MII:

Two conditions are determined by means of describing the influence of the wave field's representations in the number of MII events. One condition considers MII due to the JONSWAP and the Bretschneider spectrum averaged over three bow headings at two vessel speed: Fn=0.2 and Fn=0.4. The other condition is based on a similar pattern, but using uni-directional and multi-directional wave conditions. With the aim of establishing a criteria of expected values of MII per minute in each length class considering both conditions an Averaged Motion Interruption (AMI) value is introduced. This index symbolized the averaged events of MII in each length class including the four wave fields at two speeds. This index is subdivided in AMI_p, AMI_{bhMax} and AMI_{dpMax}, defined as:

AMI_p : is the Averaged Motion Interruption of Points and corresponds to the over all mean value. In other words, the AMI_p described the MII averaged over all points, bow headings and wave fields.

AMI_{bhMax}: is the Averaged Motion Interruption of all the MII values resulting from bow headings considering only the average of its maximum values.

AMI_{dpMax}: is the Averaged Motion Interruption of all the MII values resulting from deck points in bow headings including the average of its maximum values. The deck points include points: P1, P2, P4, and P5.

From the perspective of the safety conditions, and based on the results presented in this chapter, it is possible to analyze the optimal and the worst condition for each length class considering selected locations on board, headings, wave field conditions and vessel speeds. With the purpose of establishing an answer to the questions what length class

performed the worse at low and high speed?, what is the maximum MII expected in a particular length class?, which is the worst point on board?, which is the worst heading?, which is the worst wave field?, and which is the worst speed?, several comparisons are estimated. These plots compare the values of AMI_p with the values of the other two indices and also with the maximum values of MII in individuals point at Fn=0.2 and Fn=0.4 respectively.

The following tables include the results of MII for all length classes at two speeds considering bow headings and four wave conditions.

At Fn = 0.2:

35' Length Class at FN = 0.2					
Wave Field	Point	90 deg	135 deg	180 deg	
JONSWAP	1	0.2	0.5	0.3	
	2	0	0.2	0.6	
	3	1.8	2	2.5	
	4	0.3	0.9	0.4	
	5	0	0.3	0.3	
Bretschneider	1	0.8	0.9	0.7	
	2	0.2	0.4	0.9	
	3	3.5	3	4.2	
	4	1.1	1.5	0.8	
	5	0.3	0.5	0.7	
Multi-JONSWAP	1	0	0.2	0.4	
	2	0	0.2	0.8	
	3	0.7	1.5	2.4	
	4	0.1	0.6	0.7	
	5	0	0.3	0.8	
Multi-Bretsch.	1	0.2	0.6	0.5	
	2	0	0.4	1	
	3	1.9	2.6	3.2	
	4	0.2	1.2	0.8	
	5	0	0.7	0.9	
AMI p		0.57	0.93	1.15	0.88
AMI bhMax		3.5	3	4.2	3.57
AMI dpMax		1.1	1.5	1	1.20

Table 24.

45' Length Class at Fn 0.2					
Wave Field	Point	90 deg	135 deg	180 deg	
JONSWAP	1	0	0	0.47	
	2	0	0.446	2.01	
	3	0.95	1.563	3.55	
	4	0.1	0	0.24	
	5	0.1	0.112	1.89	
Bretschneider	1	0.19	0.112	1.07	
	2	0.1	0.781	3.08	
	3	1.62	2.344	5.56	
	4	0.1	0.112	0.47	
	5	0.19	0.335	2.72	
Multi-JONSWAP	1	0	0	0	
	2	0	0.446	1.182	
	3	1.143	0.893	0.946	
	4	0	0	0	
	5	0	0.446	0.946	
Multi-Bretsch.	1	0.381	0	0.236	
	2	0	0.893	1.182	
	3	1.905	2.009	1.891	
	4	0.381	0	0.236	
	5	0	0.893	0.946	
AMI p		0.36	0.57	1.43	0.79
AMI bhMax		1.91	2.344	5.56	3.27
AMI dpMax		0.38	0.893	3.08	1.45

Table 25.

65' Length Class at Fn 0.2					
Wave Field	Point	90 deg	135 deg	180 deg	
JONSWAP	1	0	0	0	
	2	0	0	0	
	3	1.24	1.03	0.36	
	4	0	0	0	
	5	0	0	0	
Bretschneider	1	0.09	0	0	
	2	0	0	0.12	
	3	2	1.48	1.82	
	4	0	0	0	
	5	0	0	0	
Multi-JONSWAP	1	0	0	0.12	
	2	0	0	0.73	
	3	0.57	0.68	1.95	
	4	0	0	0.12	
	5	0	0.11	0.36	
Multi-Bretsch.	1	0	0	0.36	
	2	0	0	0.73	
	3	0.95	1.48	3.16	
	4	0	0	0.49	
	5	0	0	0.49	
AMI p		0.24	0.24	0.54	0.34
AMI bhMax		2	1.48	3.16	2.21
AMI dpMax		0.09	0.11	0.73	0.31

Table 26.

75' Length Class at Fn 0.2					
Wave Field	Point	90 deg	135 deg	180 deg	
JONSWAP	1	2	0	0	
	2	1.72	0	0	
	3	4.01	0.69	0.37	
	4	2.19	0	0	
	5	2.19	0	0	
Bretschneider	1	1.05	0	0	
	2	0.86	0	0	
	3	3.43	2.08	1.16	
	4	1.14	0	0	
	5	1.24	0	0	
Multi-JONSWAP	1	0.19	0	0	
	2	0.19	0	0	
	3	1.71	1.16	1.12	
	4	0.19	0	0	
	5	0.19	0	0	
Multi-Bretsch.	1	0.19	0	0.12	
	2	0.19	0	0.12	
	3	1.72	1.16	2.24	
	4	0.19	0	0.25	
	5	0.19	0	0.25	
AMI p		1.24	0.25	0.28	0.27
AMI bhMax		4.01	2.08	2.24	2.16
AMI dpMax		2.19	0	0.25	0.13

Table 27.

At Fn =0.4:

35' Length Class at Fn .4					
Wave Field	Point	90 deg	135 deg	180 deg	
JONSWAP	1	0.1	0.2	0.5	
	2	0	0.5	1.1	
	3	0.9	1.4	1.8	
	4	0.4	0.6	0.6	
	5	0	0.8	0.8	
Bretschneider	1	0.2	0.5	0.6	
	2	0.1	0.9	1.3	
	3	1.5	1.9	2.4	
	4	0.6	1.2	0.8	
	5	0.1	1.3	1.3	
Multi-JONSWAP	1	0.2	0.4	0.6	
	2	0.3	0.7	1.8	
	3	1.2	3.5	3.2	
	4	0.6	1.9	1.7	
	5	0.4	1.8	2.2	
Multi-Bretsch.	1	0.7	1.3	0.6	
	2	0.4	0.9	1.6	
	3	2.7	3.4	4.6	
	4	1.1	2.4	1.1	
	5	1	1.8	1.8	
AMI p		0.63	1.37	1.52	1.17
AMI bhMax		2.7	3.5	4.6	3.60
AMI dpMax		1.1	2.4	2.2	1.90

Table 28.

45' Length Class at Fn .4					
Wave Field	Point	90 deg	135 deg	180 deg	
JONSWAP	1	0.1	0	0.42	
	2	0.1	1.02	3.11	
	3	0.76	3.58	6.08	
	4	0.1	0.51	0.42	
	5	0.19	0.77	2.54	
Bretschneider	1	0.19	0.13	0.57	
	2	0.38	2.05	3.67	
	3	1.62	4.6	8.2	
	4	0.1	1.02	0.28	
	5	0.48	1.54	2.97	
Multi-JONSWAP	1	0	0	0.56	
	2	0	0.38	2.97	
	3	0.09	1.02	5.65	
	4	0	0.13	0.28	
	5	0	0.26	0.28	
Multi-Bretsch.	1	0	0	0.71	
	2	0	0.64	3.25	
	3	0	3.07	6.64	
	4	0	0.26	0.42	
	5	0	0.38	0.42	
AVI p		0.2	1.07	2.47	1.25
AMI bhMax		1.62	4.6	8.2	4.81
AMI dpMax		0.48	2.05	3.67	2.07

Table 29.

65' Length Class at Fn .4					
Wave Field	Point	90 deg	135 deg	180 deg	
JONSWAP	1	0	0	0	
	2	0	0	0.15	
	3	0.86	2.12	3.99	
	4	0	0	0	
	5	0	0	0.15	
Bretschneider	1	0	0	0	
	2	0	0	0.29	
	3	1.81	2.12	3.55	
	4	0	0	0	
	5	0	0	0.29	
Multi-JONSWAP	1	0	0	0	
	2	0	0.13	1.33	
	3	0.29	1.19	5.03	
	4	0	0	0	
	5	0	0	0.74	
Multi-Bretsch.	1	0	0	0.44	
	2	0	0	1.48	
	3	0.76	2.91	5.77	
	4	0	0	0.44	
	5	0	0	1.18	
AMI p		0.19	0.42	1.24	0.62
AMI bhMax		1.81	2.91	5.77	3.50
AMI dpMax		0	0.13	1.48	0.54

Table 30.

75' Length Class at Fn .4					
Wave Field	Point	90 deg	135 deg	180 deg	
JONSWAP	1	0.86	0	0	
	2	0.76	0	0	
	3	3.43	0.55	0.61	
	4	0.86	0	0	
	5	0.86	0	0	
Bretschneider	1	0.67	0	0	
	2	0.57	0	0	
	3	2.77	1.09	1.07	
	4	0.57	0	0	
	5	0.67	0	0	
Multi-JONSWAP	1	0.29	0	0	
	2	0.19	0	0	
	3	1.43	8.72	0.31	
	4	0.19	0.28	0	
	5	0.19	0	0	
Multi-Bretsch.	1	0.09	0	0	
	2	0.19	0	0	
	3	1.24	2.98	0.61	
	4	0.09	0	0	
	5	0.09	0	0	
AMI p		0.8	0.68	0.13	0.41
AMI bhMax		0.86	4.36	1.07	2.72
AMI dpMax		0.86	0.28	0	0.14

Table 31.

Comparison 1. To answer the question what length class present the worst performance at low and high speed, the index AMI_p is plotted, in Figure 46 and Figure 47, for each length class and compare with AMI_{bhMax} and AMI_{dpMax} for all the length classes. In order to verify the MII data for the length classes considering bow headings at two speeds several tables are plotted. For example the 45' length class at Fn=0.4 has a AMI_p=1.25. The average of the maximum value of MII in each bow heading is 1.62, 4.60 and 8.20 respectively, see Table 29. The average of these values is 4.81 MII/minutes, see Table 33. Likewise, considering only deck points, the values of maximum MIIs in each bow heading are 0.48, 2.05 and 3.67 respectively. The average of these MIIs is 2.07, see Table 33. Then, the AMI_p=1.25 is compared with averaged values of 4.81 and 2.07 MII/minutes in Figure 48.

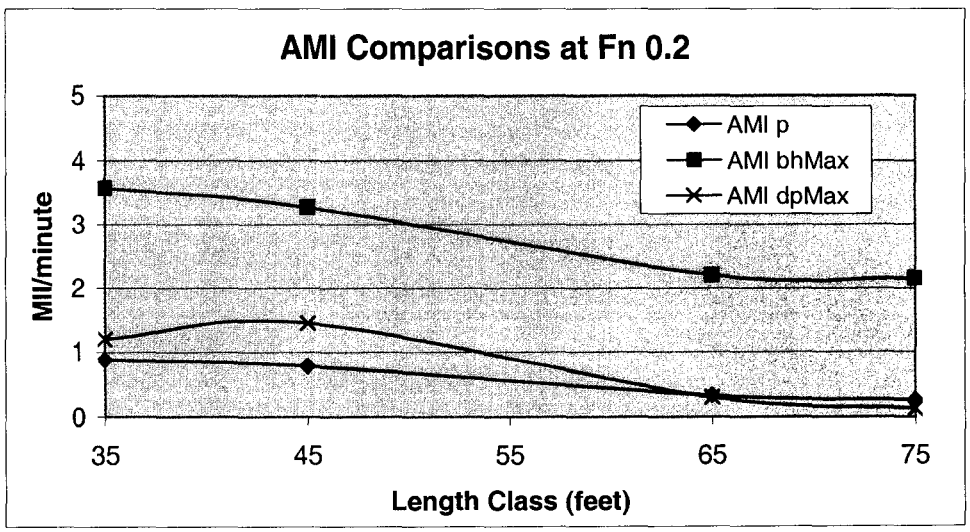

Figure 47.

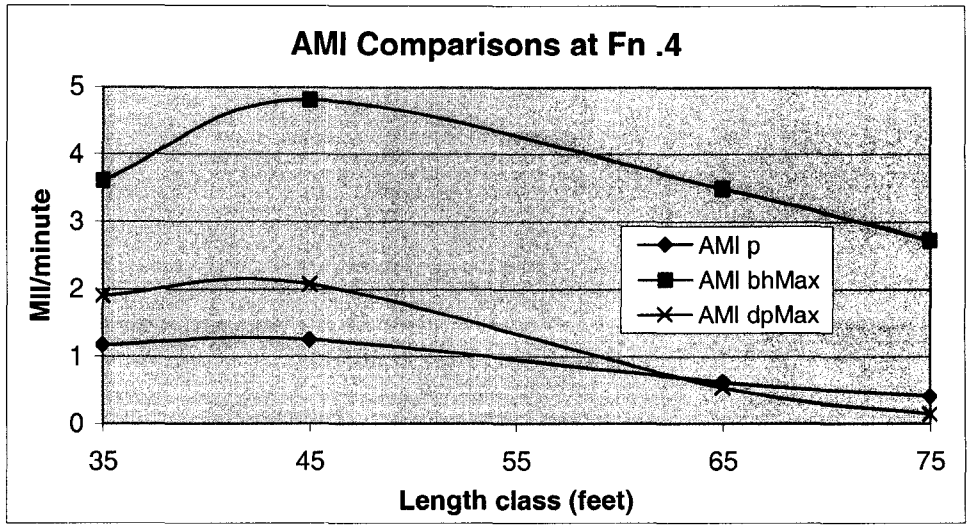

Figure 48.

Tables:

AMI at Fn=0.2				
Length Class	35'	45'	65'	75'
AMI p	0.88	0.79	0.34	0.27
AMI bhMax	3.57	3.27	2.21	2.16
AMI dpMax	1.20	1.45	0.31	0.13

Table 32.

AMI at Fn 0.4			
Length Class	AMI p	AMI bh	AMI dp
35'	1.17	3.60	1.90
45'	1.25	4.81	2.07
65'	0.62	3.49	0.54
75'	0.41	2.72	0.14

Table 33.

Comments:

Based on the first comparison, it is possible to observe (Fn = 0.4), significant values of AMI at high speed from all points in bow headings and also from deck points. One exception is the 35' length class, which presents at high and low speed the same amount of

AMI over bow headings. Also, the 75' length class at both speeds shows the same values for AMI over deck points.

Comparison 2. To answer the question of what is the maximum AMI_p expected in a particular length class; the index AMI_p is estimated for each length class and compared with maximum values over wave fields in bow headings (Max at bh) as well as compared with the values considering only deck points (Max at dp), see Figure 49 and Figure 50. For example, the 35' length class at Fn=0.4 has an AMI_p = 1.17. The maximum value of MII/minute considering deck points is 2.4 and the MII/minute in bow headings (including all points) is 4.6, (see Table 28 and 35). These three values are compared in the following charts.

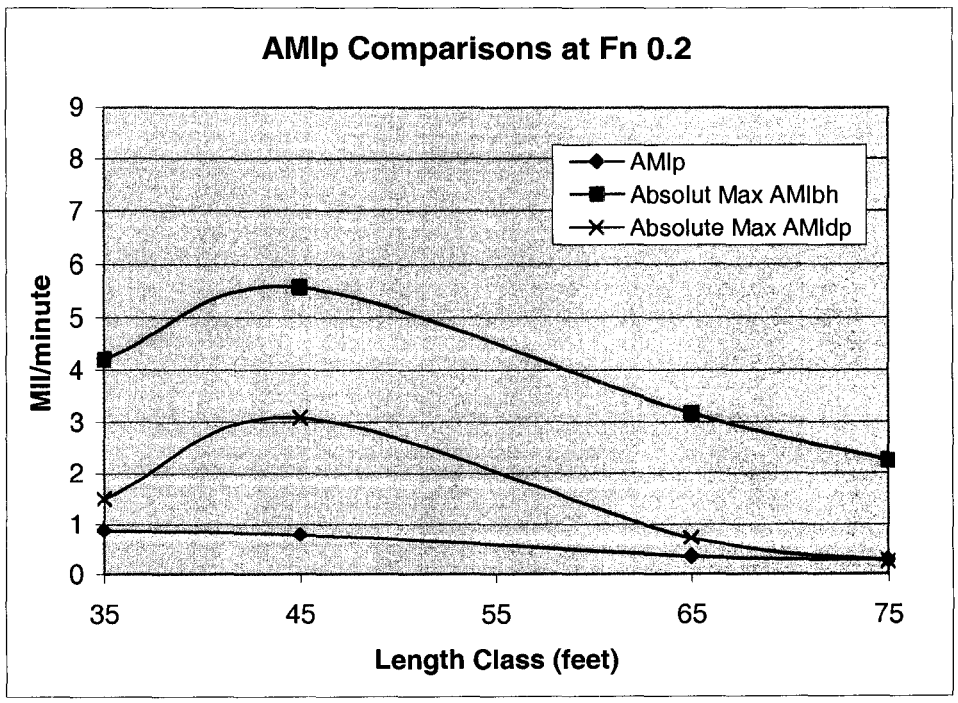

Figure 49.

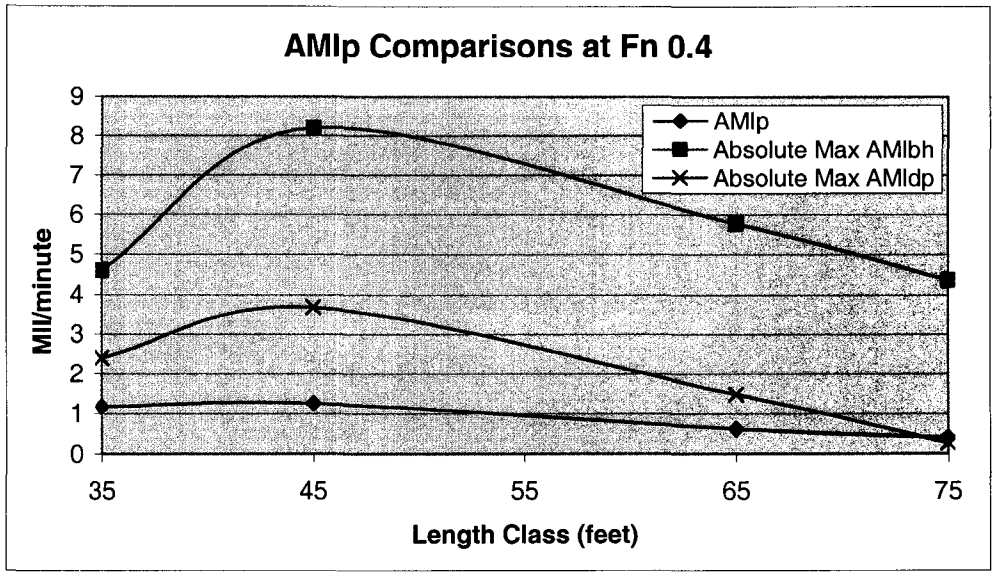

Figure 50.

Tables:

Maximum Individual Values at Fn 0.2			
Length Class	AMIp	Max at bh	Max at dp
35'	0.88	4.20	1.50
45'	0.79	5.56	3.08
65'	0.34	3.16	0.73
75'	0.27	2.24	0.25

Table 34.

Maximum Individual Values at Fn 0.4			
Length Class	AMIp	Max at bh	Max at dp
35'	1.17	4.60	2.40
45'	1.25	8.20	3.67
65'	0.62	5.77	1.48
75'	0.41	4.36	0.28

Table 35.

Comments:

In the case of maximum individual values of MII, estimated in Comparison 2, the highest value occurs in bow headings and in deck points arises at high speed, see Table 34 and Table 35.

Comparison 3. In order to estimate the worst point on board, the values of AMI_p are compare with the maximum values in each point averaged over bow headings, see Figure 51 and Figure 52. For example, point 3 in the 75' length class has a maximum value of MII at Fn=0.4 of: 3.43, 8.72 and 1.07 in bow headings (see Table 31). The average of this value is 4.2 (see Table 37). The results are plotted in Figure 53 and 54. The average value (AMI_p) of all the MIIs in point 3 in all the wave fields is 1.99 (see Table 37); this calculations are presented in Figures 51 and 52.

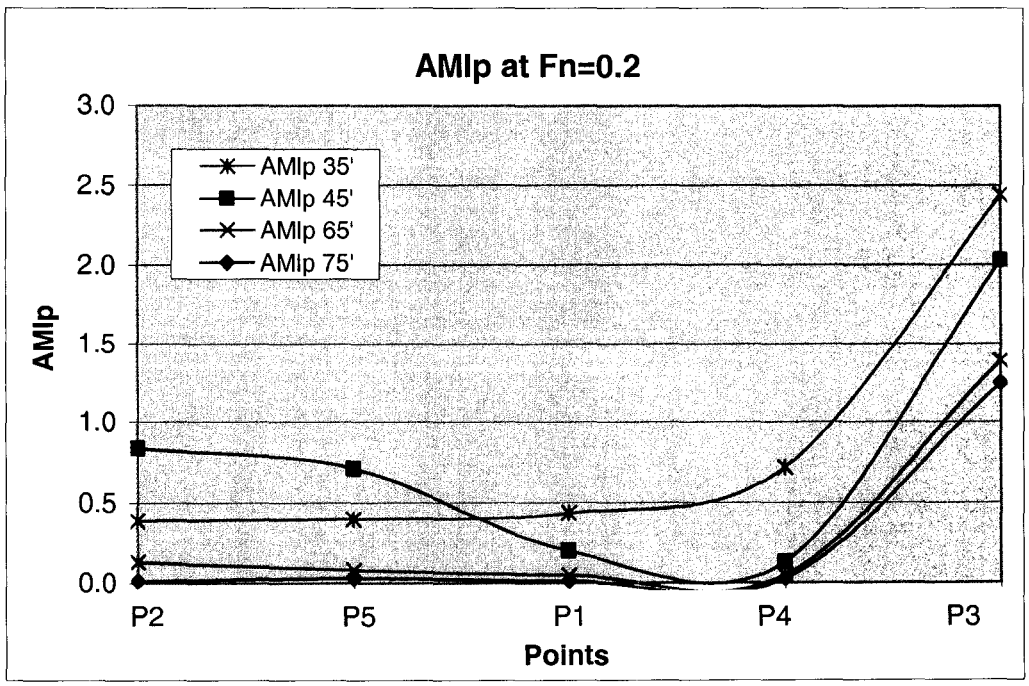

Figure 51.

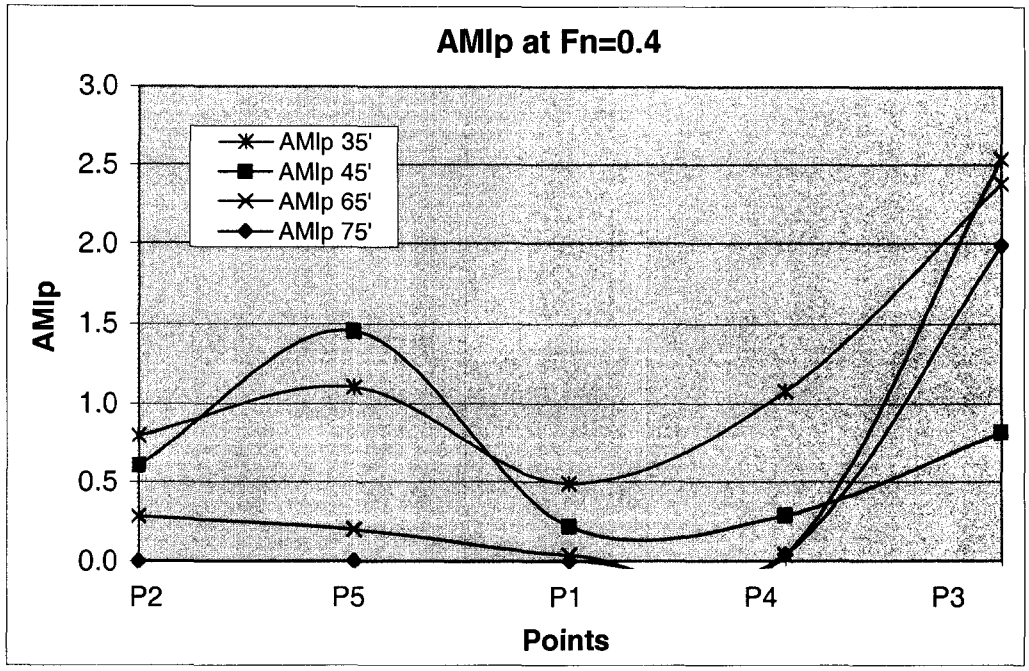

Figure 52.

Tables:

Fn .2								
Point	35' AMI	35' Max MII	45' AMI	45' Max MII	65' AMI	65' Max MII	75' AMI	75' Max MII
P1	0.440	0.900	0.205	0.381	0.048	0.360	0.508	2.000
P2	0.390	0.400	0.843	3.080	0.132	0.730	0.015	1.720
P3	2.440	4.200	2.031	5.560	1.393	3.160	1.249	4.010
P4	0.720	1.500	0.136	0.470	0.051	1.500	0.031	2.190
P5	0.400	0.900	0.715	2.720	0.080	0.490	0.031	2.190

Table 36.

Fn .4								
Point	35' AMIp	35' Max MII	45' AMIp	45' Max MII	65' AMIp	65' Max MII	75' AMIp	75' Max MII
P1	0.490	1.300	0.220	0.710	0.037	0.440	0.000	0.900
P2	0.800	1.800	1.460	3.670	0.282	1.480	0.000	0.400
P3	2.380	4.600	3.440	8.200	2.533	5.770	1.990	4.200
P4	1.080	2.400	0.290	1.020	0.037	0.440	0.040	1.500
P5	1.108	2.200	0.819	2.970	0.197	1.180	0.000	0.900

Table 37.

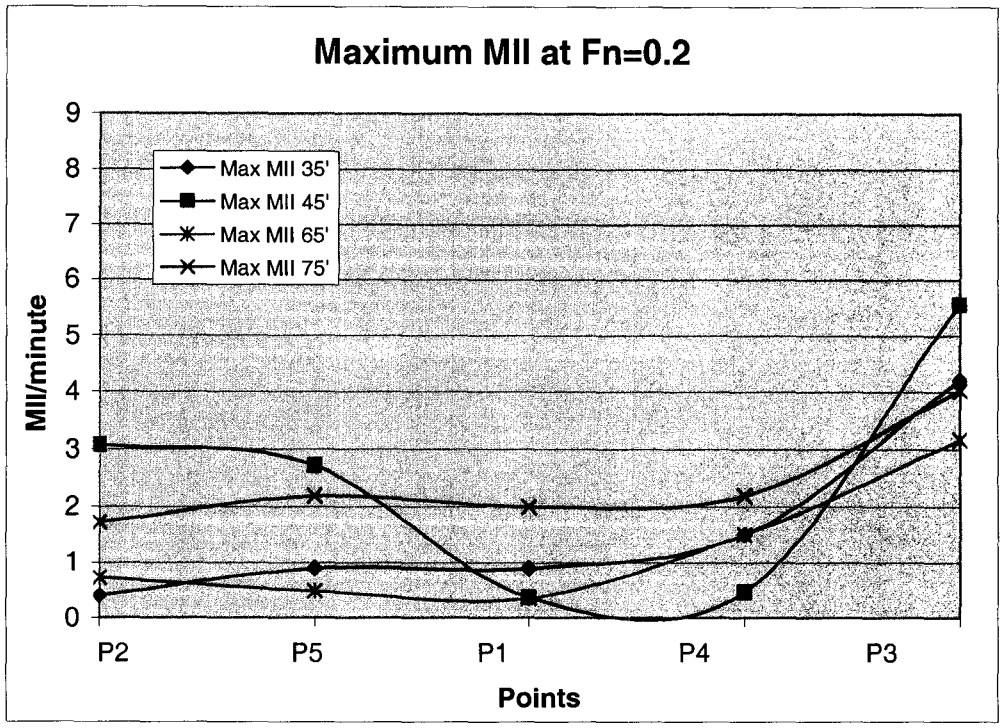

Figure 53.

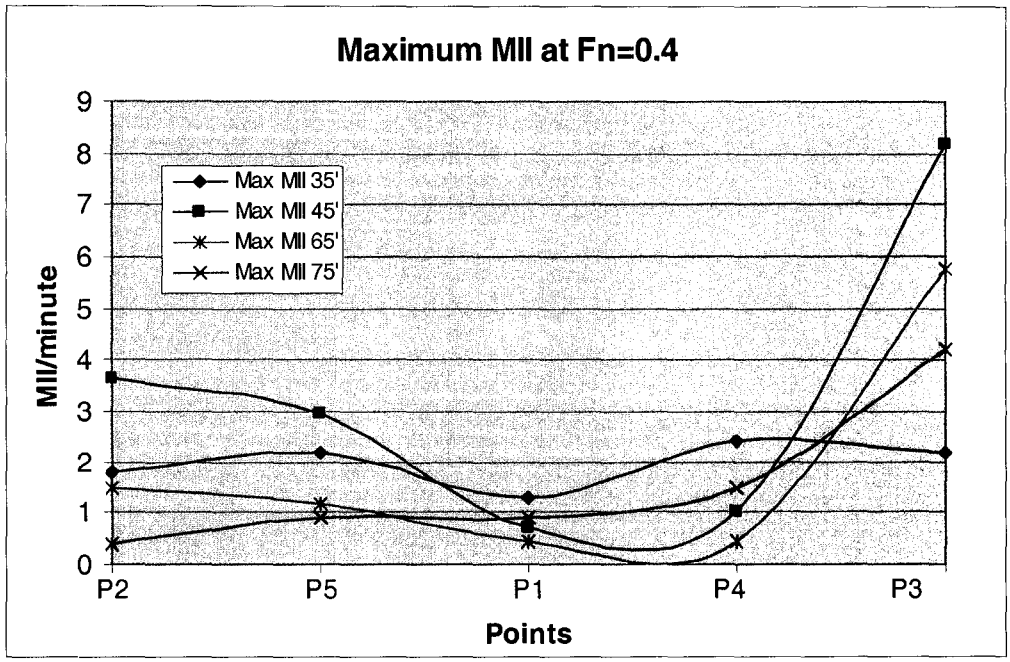

Figure 54.

Comments:

According to comparison 3, individual points are evaluated for each length class in order to establish the dangerous locations on board. The values of MII for each class averaged over bow headings and wave field including the maximum are presented in Tables 36 and Table 37.

The present analysis is performed considering all the points. The values observed in point 3 are certainly high. The reason for this is that this particular point is located in the wheel house at (L/3, 0, L/5), usually presenting extremely high values of MII compared to the other points. The main characteristic of this position is that it is located inside the vessel, at distance L/5 elevated over the main deck, see Figure 44. Although the person on the wheelhouse is not fishing on an open deck, he experiences greater acceleration than a person standing on deck.

Following the criteria of risk levels in MII presented by other authors in the past, Table 38 and Table 39 described the risk of MII in different locations on board.

Locations at Fn .2				
Risk	AMIp 35'	AMIp 45'	AMIp 65'	AMIp 75'
High	P4=0.72	P2=0.84	P2=0.13	P1=0.51
Low	P2=0.39	P4=0.14	P1=0.05	P2=0.02

Table 38.

Locations at Fn .4				
Risk	AMIp 35'	AMIp 45'	AMIp 65'	AMIp 75'
High	P5=1.11	P2=1.46	P2=0.28	P4=0.04
Low	P1=0.49	P1=0.22	P1,P4=0.44	P1,P2,P5=0

Table 39.

Based on the above tables, P2 at stern position (-L/3, 0, 0) in the center line is predominantly a dangerous location at low and high speed. In the same way, at both speeds, the small 35' length class exhibits high levels of AMI_p at the vessel side in P5 and P4 at both speeds. On the other hand, the low risk position is always the P1 located at the *C.G.* in each vessel at high speed.

The locations on board are represented by points. The arrangement of the points in the previous charts follows an order from the stern to the bow along the vessel.

Comparison 4. With the objective to find the worst heading the following graphs, Figure 50 and Figure 51, describes AMI_p (MII/minute averaged over points and wave fields) in each length class and all headings. The values of AMI_p are presented in Tables 40 and 41.

AMIp at Fn .2					
Length Class	0 deg	45 deg	90 deg	135 deg	180 deg
35'	0.00	0.09	0.57	0.93	1.15
45'	0.01	0.00	0.36	0.57	1.43
65'	0.03	0.03	0.24	0.24	0.54
75'	0.01	0.04	1.24	0.25	0.28

Table 40.

AMIp at Fn .4					
Length Class	0 deg	45 deg	90 deg	135 deg	180 deg
35'	0.79	0.70	0.63	1.37	1.52
45'	0.00	0.00	0.20	1.07	2.47
65'	0	0	0.19	0.42	1.24
75'	0	0.03	0.8	0.68	0.13

Table 41.

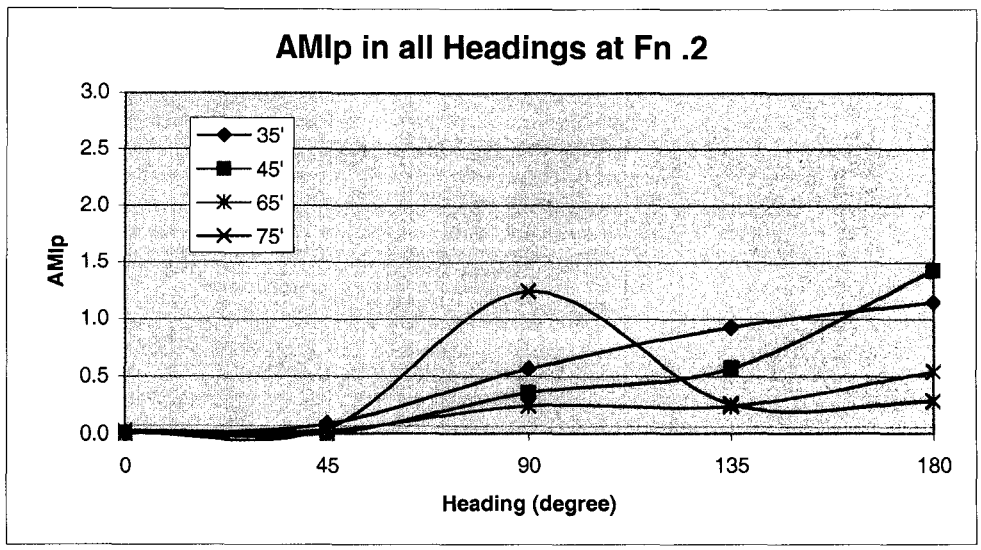

Figure 55.

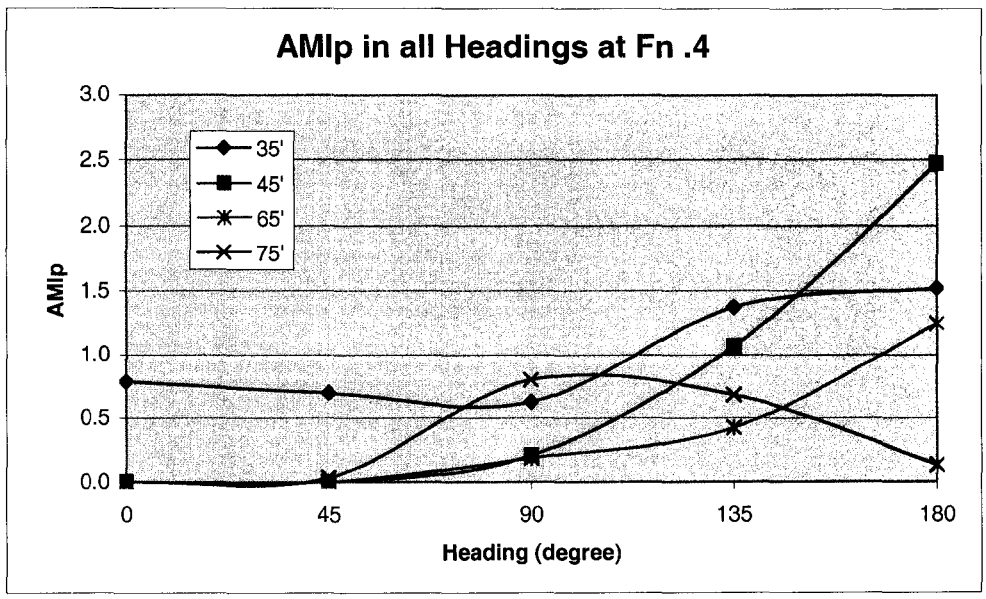

Figure 56.

Comments:

The most adverse wave direction for each vessel is tested in Comparison 4, see Table 40 and Table 41. From this evaluation, it is important to comment on the following:

- Bow Sea (μ=135°) and Head Sea (μ=180°) are always the worst sea conditions at low and high speeds in most length classes but for the 75 footer.

- Beam Sea (μ=90°) are the worst sea conditions for the 75 foot vessel at low speed. A phenomenon of resonance occurs in the 75' length class. This particular problem appears because the mean wave frequency of 1 rad/sec and the vessel's natural frequency of roll, 1.03 rad/sec, have approximately the same value. This problem is basically a consequence of the characteristics of the hull. The 75' is a steel vessel; therefore, its displacement is bigger than the other three fibre glass vessels. Consequently, this factor influences a lower value of GMT ($GMT_{75'}$=0.79 m).

Comparison 5. With the aim of representing the worse wave field condition in bow seas Figure 57 and Figure 58, based on Table 42, describes the AMI_p of each length class for the four wave fields.

Speed	Wave Field	AMIp 35'	AMIp 45'	AMIp 65'	AMIp 75'
Fn .2	JONSWAP	0.420	0.457	0.105	0.527
	Bretschneider	0.796	0.751	0.241	0.442
	Multi-JONSWAP	0.360	0.243	0.186	0.21
	Multi-Bretsch.	0.600	0.444	0.33	0.282
Fn .4	JONSWAP	0.540	0.788	0.291	0.317
	Bretschneider	0.791	1.044	0.341	0.322
	Multi-JONSWAP	1.152	0.465	0.348	0.479
	Multi-Bretsch.	1.376	0.634	0.519	0.222

Table 42.

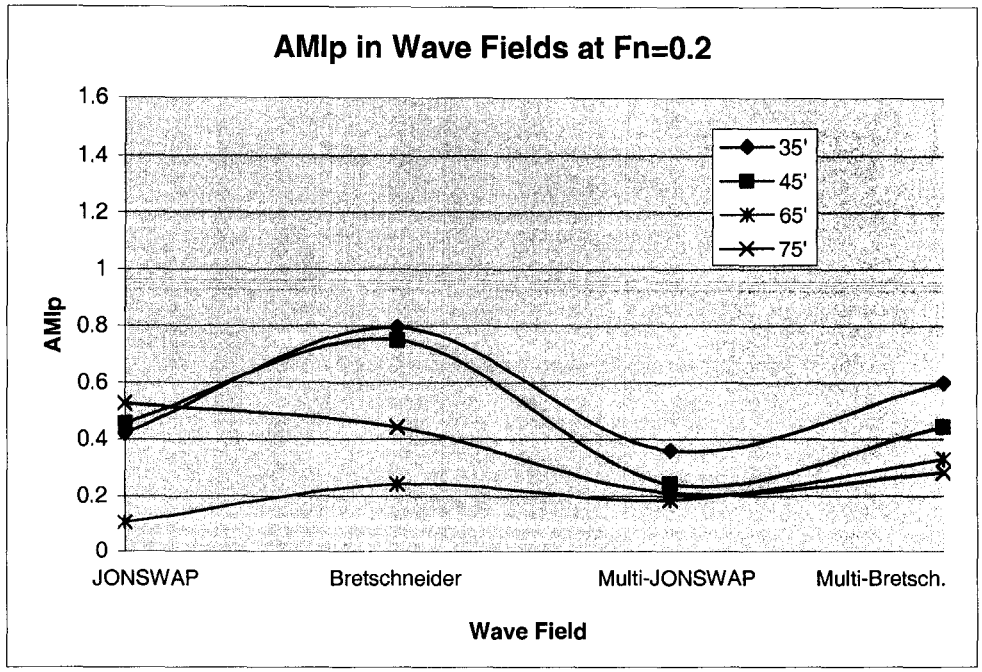

Figure 57.

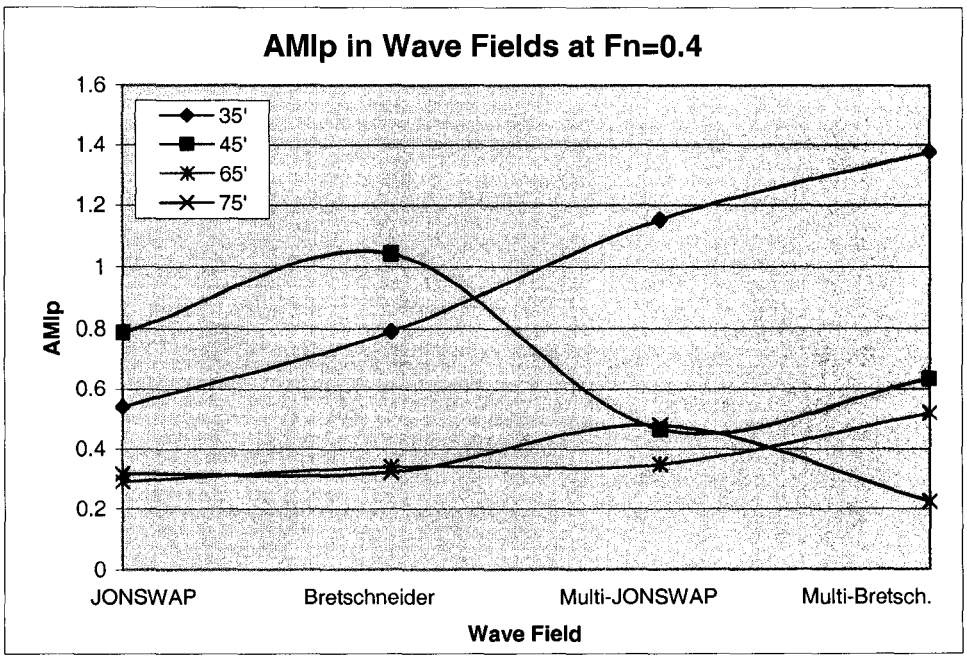

Figure 58.

Comments:

The uni-directional wave field conditions produce significant MIIs in small vessels at low and high speed, particularly the uni-directional Bretschneider spectrum. However, the small vessel (35') presents highest MII values in multi-directional waves at high speed. All the other length classes have low MIIs in this wave field.

On the other hand, the wave field with the least number of MII is the uni-directional JONSWAP in all the length classes, except for the 75'. This energy spectrum produces a significant number of MII in the larger vessel at low speed. The JONSWAP energy spectrum involves a narrower band of frequencies than Bretschneider spectrum (broad band of frequencies). Therefore, the latter implies that a vessel is more vulnerable to MII events.

Comparison 6. With the purpose of evaluate the worse speed of two values of Froude Numbers (Fn), the response of each length class is compared with the AMI_p at different length class, see Table 43. The over all mean value AMI_p is considered only in bow headings. Figure 59 presents the comparison at two speeds.

AMIp				
Speed	35'	45'	65'	75'
Fn .2	0.54	0.47	0.22	0.37
Fn .4	1.00	0.75	0.37	0.33

Table 43.

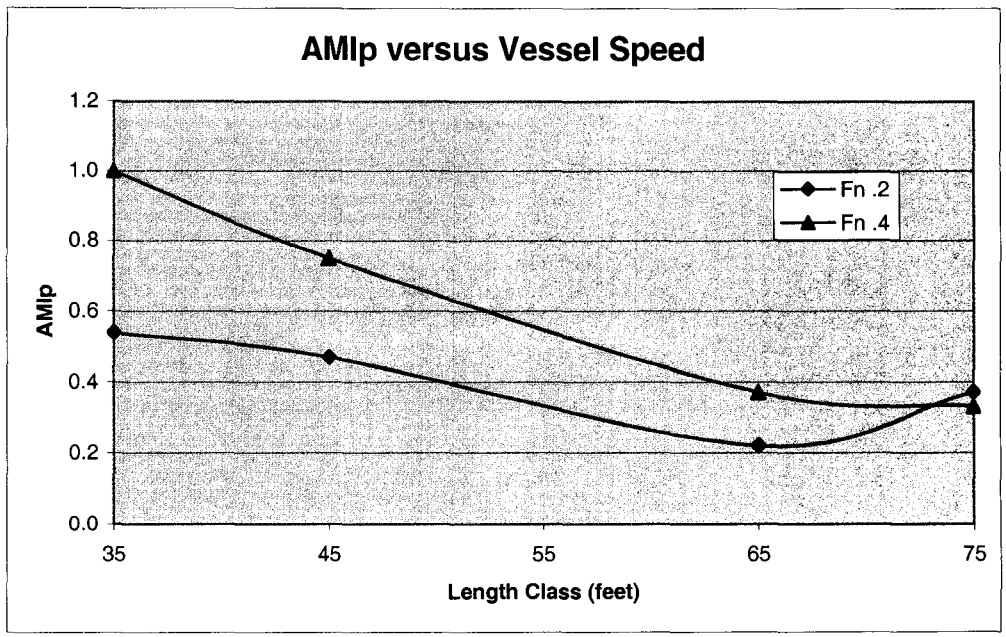

Figure 59.

Comments:

According to Comparison 6, the highest values of AMIp occur at high speed. The only exception is in the 75' length class, which is affected by high AMIp at low speed. This is a consequence of the resonance effect.

Chapter 7

Analysis of Wave Conditions

With the aim of establishing the response of the vessel due to the change in significant parameters, several results are plotted. Parameters like wave length, wave period and wave frequency have been modified in the numerical code and the effect they have in different locations onboard has been evaluated.

In order to determine the behaviour of the vessel operating during a normal fishing season off the North-east of Newfoundland, a 5 day trip is used and waves over 10 year statistic of the sea conditions are estimated. This condition is compared with the waves of the South-east coast of Newfoundland considering the same period of time.

7.1 Wave Conditions

The data show that waves in the North-east coast of Newfoundland during the last 10 years have followed similar distribution during a typical fishing season. In Newfoundland, a fishing season starts in April and it extends until November. The following chart in Figure 60 presents an average of the Significant Wave Height (SWH) in each month [28].

During the summer the sea is relatively calm and thus the SWH is less than 2 m. Once the fall begins, the wind appears and the SWH increases rapidly up to more than 2 m. However, the total average of the SWH over the last 10 fishing seasons is 2 m. Therefore, numerical calculation using three different values of SWH in each length class will be assumed. The parameters are: 2 m with a period of 6.3 sec, and 2.5 m and 3 m, with a

period of 8 sec. The levels represent the minimum, medium and maximum values of waves in the numerical experiment. Hence, a five day trip is established based on these SWH levels, see Figure 61.

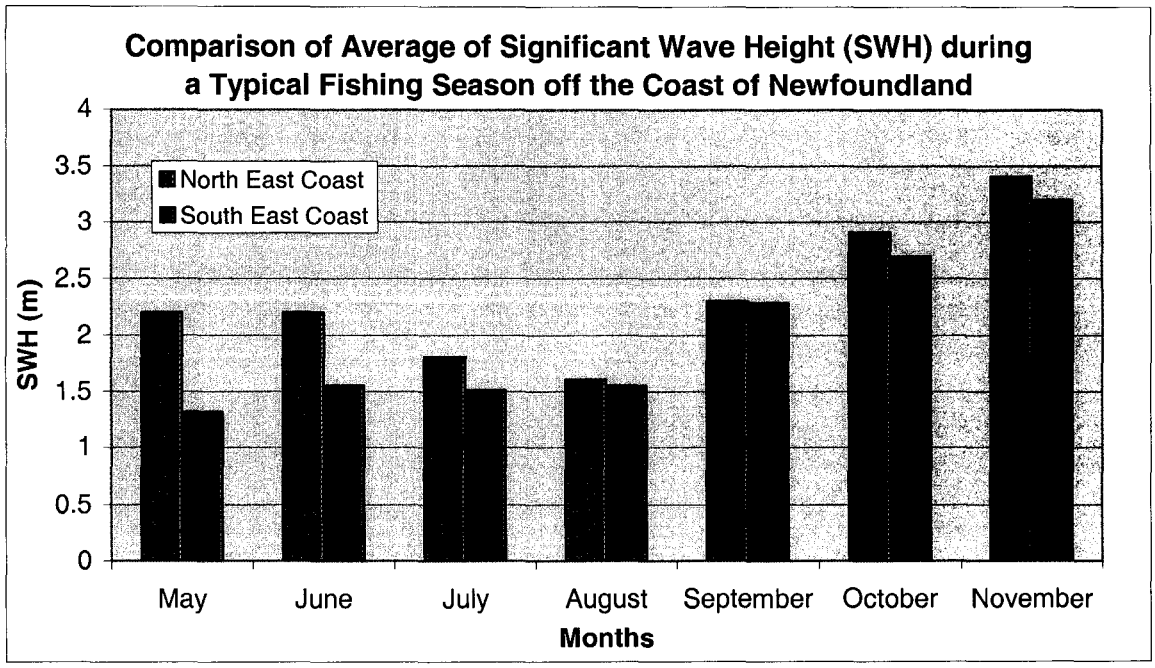

Figure 60.

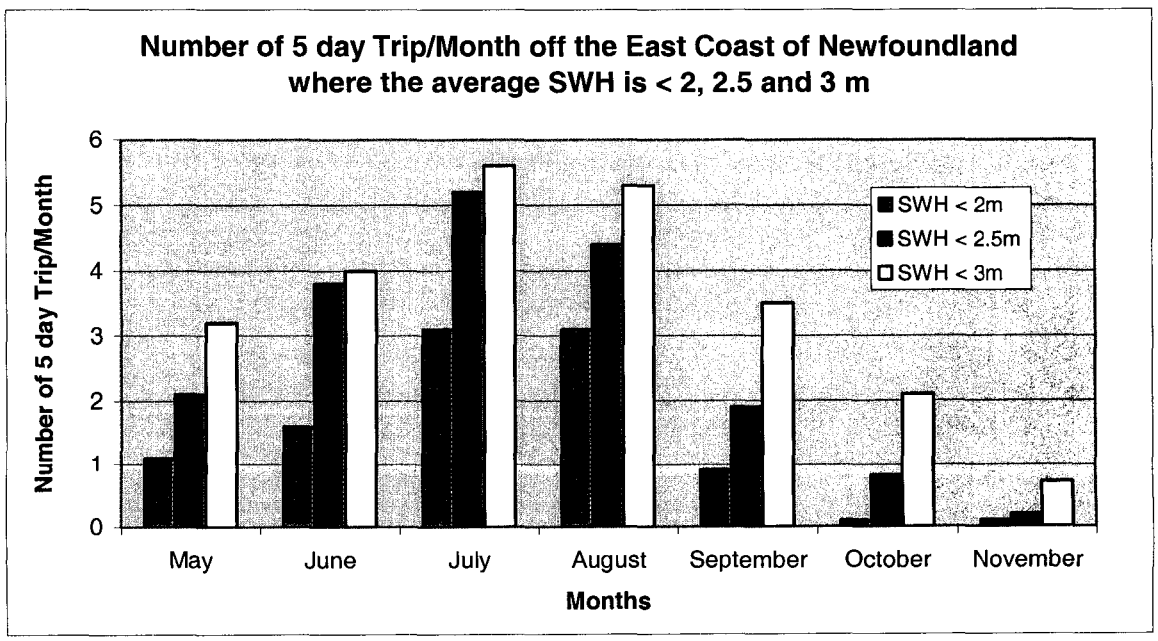

Figure 61.

From the statistics presented in Figure 60, it is possible to infer that in all the months the presence of SWH less than 2 m is not common. Hence, if the crew is expecting to sail in calm waters (SWH<2 m), they can go out only two times during the period July-August, one time during the month of June and just a few days (< 5 days) during the rest of the season.

In the same way, if the crew wants to operate the vessel in a medium level of waves, (e.g. < 2.5 m of SWH), the number of days increases. Under this condition, the vessel can sail in the south east coast up to four 5 day trips in July, three in August, two in June, one in May and September and less than five days during the rest of the season. From the chart it is possible to establish that waves of SWH between 2 m and 2.5 m are very usual during the summer.

However, despite the calm wind during this season, most of the waves are higher than 2.5 m. Therefore, the crew has the opportunity to fish more times in high SWH than in small SWH conditions. For example, in July the vessel is able to sail almost the whole month with SWH less than 3 m. That means it can go out five times for 5 days in a month without exceeding the 3 m of SWH. In June and August the vessel can go out up to four times sailing in a 5 day trip. During May and September the number of trips is less and the crew can perform only two 5 day trips in that month. As soon as the fall comes, the waves increase in height and the opportunities to fish become less. For this reason, in November it is almost impossible to go out for more than 5 days with wave heights less than 3 m.

7.2 Motion Stress Profile

Based on the wave conditions established in 7.1, it is interesting to evaluate the behaviour of the vessel under the same parameters. This analysis considered the MIIs that

were determined in the numerical simulation in different SWHs for unidirectional wave field conditions and averaged over five points on board. For this reason, the performance of each length class is calculated considering a specific bow heading of 135 deg (between beam and head sea) at low and high speed. The values of MII in this heading are presented in terms of the index AMIp.

The analysis determines the values of AMIp in each location under the three levels of SWH. Hence, the results shown on the charts are presented for three levels of SWH, see Figures 62-65.

Finally, it is possible to obtain the Stress Motion Profile for each length class. This profile gives the information about the values of AMIp in a particular bow heading under different SWHs. Also, with this profile it is possible to predict the value of AMIp expected to occur in 5 day trips per month for different length classes.

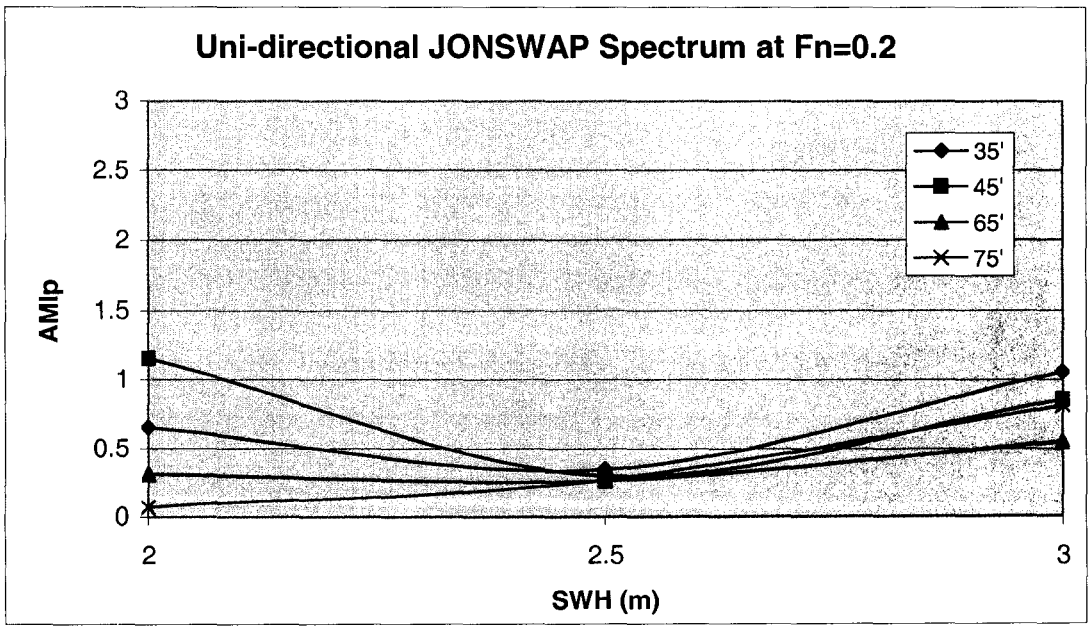

Figure 62.

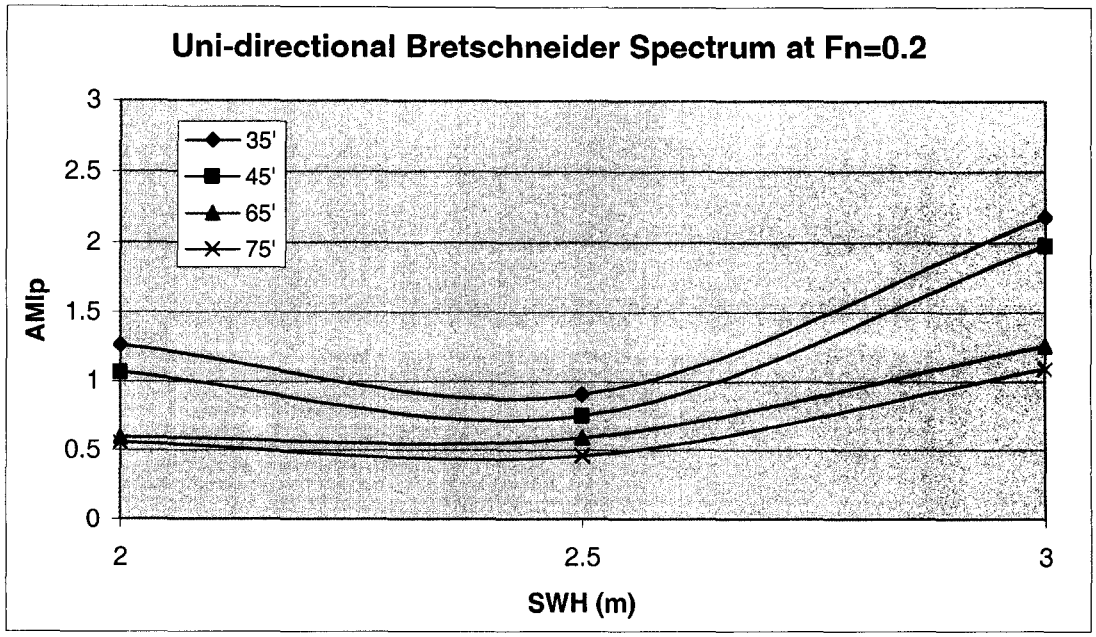

Figure 63.

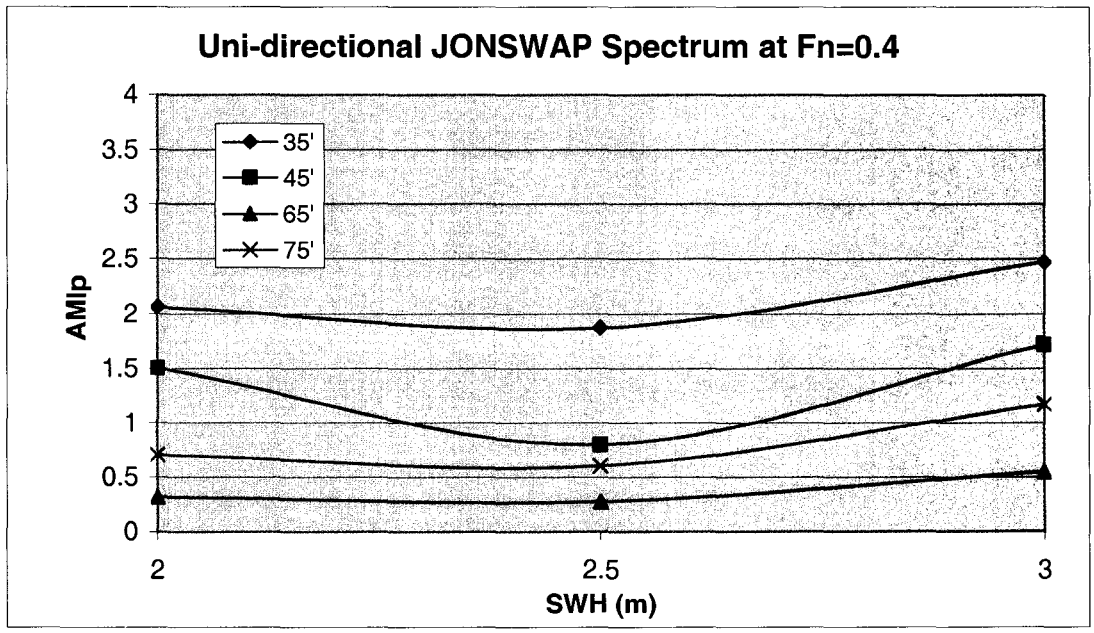

Figure 64.

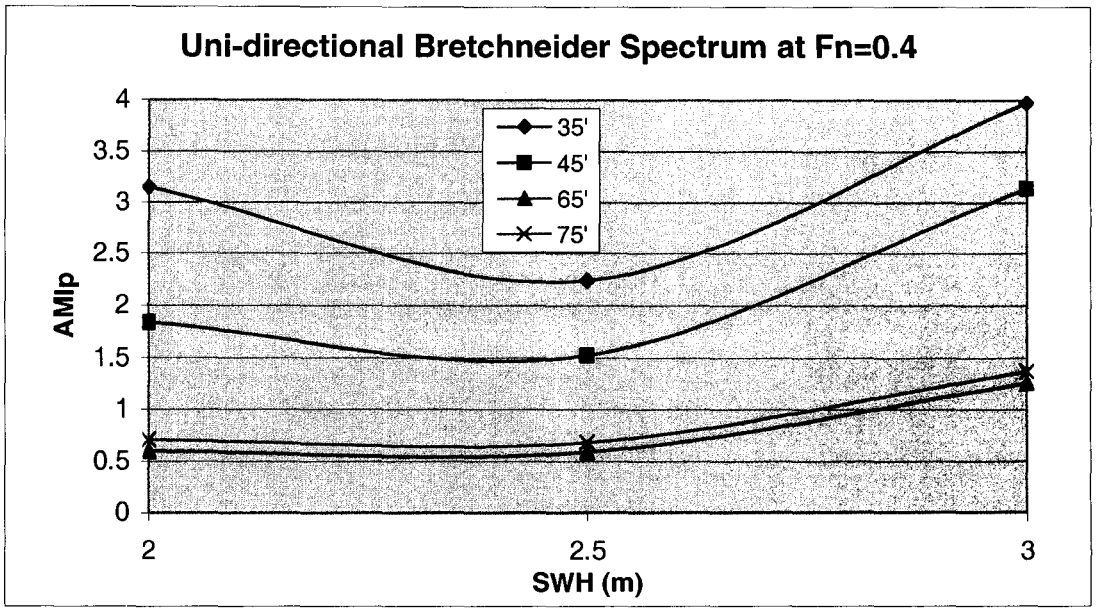

Figure 65.

Comments:

The response of all the length classes at low speed is similar. It deepens on the range of frequencies under the selected energy spectrum. In this case, the uni-directional Bretschneider spectrum presents higher AMIp values in the small vessel. However, the SWH of 3m is always a risk condition. The Bretschenider spectrum considered a spread range of frequencies; therefore the response of the vessels is very similar under this spectrum, even in different wave parameters.

In the case of high speed the difference between SWHs is significant. The AMIp increases rapidly with the wave height while the length decreases. Therefore, it is clear that the small vessels are expected to encounter high number of AMIp and thus MIIs with wave heights more than 3 m in average.

All the curves showed a decrease in the amount of AMIp when the SWH=2.5m. The reason is the change in the wave parameters. The SWH=2m has a period of 6.3 sec and the other waves, SWH=2.5m and SWH=3m, have a period of 8 sec.

In the case of the 75' length class the influence of the resonance effect in roll motion at low and high speed is significant, see in Appendix A: Figures 86 and Figure 87. This condition appears in beam sea (angle of heading = 90 deg) and affects the response of the vessels at heading angle = 135 deg. Therefore, this length class presents higher AMIp than the 65' length class in most of the results.

Chapter 8

Conclusions

A complete assessment of the motions of small fishing vessels is evaluated in the previous chapters. Several conclusions can be established from this analysis:

1. In general, the small vessels were likely to be affected by most of the factors considered in the present research. At the same time, these length classes were the most difficult to analyze in terms of prediction of motion. Therefore, the importance of the accuracy in the collection of the data was high.

2. Primarily, the high speed factor influenced the appearance of a high number of Motion Induced Interruptions (MIIs) in the small vessels. However, at high vessel speed, the multi-directionality of the wave substantially affected the occurrence of MIIs in the small length class. On the other hand, the number of events of MIIs in large vessels was less influenced by the high speed.

In the same way, it is possible to conclude that high speeds combined with multi-directional waves are relevant factors that make a significant impact to the safety on small vessels. Furthermore, once the length of the vessel started to increase while maintaining high speed, the number of MIIs increased as well. However, in this case, the uni-directional wave became the most important factor.

3. The combination of low speed and uni-directional waves had an effect on the small vessel. Particularly, the large vessels experienced increases in MIIs due to the relationship between low speed and uni-directional waves.

Therefore, it can be determined that low speed influences the appearance of high numbers of MIIs in most of the lengths, but only in the presence of uni-directional waves. This situation is not representative of real wave conditions, though it does give an approach of the response of a vessel under ideal conditions.

4. The heading was one of the significant factors that influenced the occurrence of MIIs in this experiment. Principally, the bow headings produced higher MIIs in all the vessels. This phenomenon was independent of the speed and included all of the wave field conditions.

Hence, the difficult in keeping the course, while at the same time avoiding accidents on board, is related to the direction of the encounter wave. As expected, more events of MIIs and potentially more accidents happened while traveling in head, bow or beam sea than in following or quartering sea.

It is important to mention that the numerical simulations only considered waves coming to the starboard. However, in the simulations the waves were symmetric and thus the yaw motion was not affected by this condition. In the case of the Sea trial, the condition was different, because the waves were not symmetric. Therefore, the prediction of yaw motion was affected significantly. Problems with auto-pilots was also a significant factor.

5. The two energy spectra used in these experiments followed almost the same pattern, obtaining similar responses from the vessels in each wave direction. This means that the vessels had similar responses in uni-directional waves under JONSWAP and Bretschneider and likewise, similar responses in multi-directional waves using both spectra at both speeds.

In contrast, these spectra (JONSWAP and Bretschneider) caused high values of MIIs in the small vessels using multi-directional waves. Thus, it is possible to establish that the energy spectra only impacts small vessel in multi-directional waves. It is important to remark too, that when the speed is increased in the numerical simulation, the energy spectra caused high MIIs in both small vessels.

From the point of view of MIIs, the conclusion that arose from evaluating the energy spectra is that for small vessels, the difference between uni-directional JONSWAP and Bretschneider spectra is not important. Both spectra had the same influence, especially at low speed, where the vessel had less control against waves coming from different directions and with different lengths and frequencies. On the other hand, once the length started to increase, the influence of each energy spectra separately became more significant.

From the point of view of the motions, the both energy spectra follow the same pattern in terms of multi-directional and uni-directional waves.

6. The numerical code is based on the potential theory and panel method. Hence, the number of sections, points and panels included in the geometry of the vessel generated by the computer increase the accuracy of the results significantly.

Also, the increase in the number of panels produces less control problems of the vessel avoiding capsizing and overflow at high speed and high waves.

This situation was presented during the simulations of the small vessels. In this case, modification of control coefficients was required. The increase and decrease of the propulsion coefficient was always related with the variation of the manoeuvrability conditions. Frequently, the modifications were conducted with high values of SWH in order to give the vessel more freedom to return to its original course and more speed to maintain the course avoiding the rapidly increase in yaw motion.

7. The results of motions given by the numerical code MOTSIM are well establish and validated by means of the Sea Trials. The absence of an auto pilot in one of the vessels was the main reason of the lack of precision in the prediction of motions of "The Atlantic Swell". This condition affected essentially the prediction of yaw motion.

However, it is expect to continue with sea trials and numerical simulations during the next year. Also, several model tests will be conducted for the small length classes in the towing tank of the Institute of Ocean Technology (IOT).

The results presented in this thesis combined with future estimations will provide a better validation to the numerical code for all fishing vessel length classes.

List of References

[1] Pillay, A. and Wang, J., "Technology and Safety of Marine Systems."

[2] International Maritime Organization IMO, "Code of Safety for Fishermen and Fishing Vessels," Part A, London, May 1982.

[3] Maritime Search and Rescue Newfoundland Region, "Fishing Vessel Safety Review (less than 65 feet)," November 2000.

[4] Marine Investigation of Transport Canada, "West Coast Fishing Vessels Casualties Inquiry," Ottawa, March 1975.

[5] Newsletter of Oceanic Consulting Corporation, "Making Waves," September 2003.

[6] A.R.J.M. Lloyd, "Seakeeping, Ship Behaviour in Rough Weather."

[7] F. Veenstra and J. Stoop, "BEAMER 2000, Safety – integrated (re-)designing: THE KINDUNOS METHOD," Agricultural Research Dept., Netherlands Institute for Fisheries Research and Department of Safety Studies, Technical University Delft, July 1992.

[8] American Bureau of Shipping, ABS "Guide for Crew Habitability on Ships," December 2001.

[9] Graham, R. Baitis, A.E. and Meyers, W.G., "A Frequency-Domain Method for Estimating the Incidence and Severity of Sliding," DTRC/SHD-1361-01, August 1991.

[10] Baitis, A.E., Applebee, T.R. and McNamara, T.M, "Human Factors Considerations applied to Operations of the FFG-8 and Lamps MK III," Naval; Engineers Journal, May 1984.

[11] Graham, R., "Motion-Induced Interruption as Ship Operability Criteria," Naval Engineers Journal, March 1990.

[12] Graham, R., Baitis, A.E. and Meyers, W.G., "On the Development of Seakeeping Criteria," Naval Engineers Journal, May 1992.

[13] Baitis, A.E., Bales, S.L., McCreight, W.R and Meyers, W.G., "Prediction of Extreme Ammunition Cargo Forces at Sea," DTNSRDC Report SPD-704-01, 1976.

[14] Baitis, A.E., Holcombe, F.D., Conwell, S.L., Crossland, P., Colwell, J., Pattison, J.H., Strong, R., "1991-1992 Motion Induced Interruption (MII) and Motion Induced Fatigue (MIF) Experiments at the Naval Biodynamic Laboratory," Carderock Division, Naval Surface Warfare Center Report CRDKNSWC-HD-1423-01, Bethesda, Maryland, September 1995

[15] International Standard Organization, ISO, "Evaluation of Human Exposure to Whole-body vibration" – Part 3: Evaluation of Exposure to Whole-Body z-axis vertical vibration in the frequency range 0.1 to 0.63 Hz", ISO 2631/3 – 1985 (E)

[16] Crossland, P., Colwell, J.L., Baitis, A.E., Holcome, F.D., and Strong, R., "Quantifying Human Performance Degradation in a Ship Motion Environment: Experiments at the US Naval Biodynamics Laboratory," Proceedings of the International Seminar on Comfort on Board and Operability evaluation of High Speed Marine Vehicles, Cetena, Genoa, November 1994.

[17] St. Denis, M and Pierson, W.J., "On the Motions of Ship's in Confused Seas," Trans. SNAME, New York 1953.

[18] Weinblum, G. and St. Denis, M., "On the Motions of Ships at Sea," Trans. SNAME, New York 1950.

[19] Hadler, J.B. and Sarchin, T.H., "Seakeeping Criteria and Specifications," Technical & Research Symposium S-3: Seakeeping 1953-1973.

[20] Hoffman, D. and Marks, W., "Applications of Wave inputs to Seakeeping," Technical & Research Symposium S-3: Seakeeping 1953-1973.

[21] Kehoe, J., "Destroyer Seakeeping: Ours and Theirs," U.S. Naval Institute Proceedings, November 1973.

[22] Lewis, E., "Principles of Naval Architecture: Motion in Waves and Controllability," Vol. III, SNAME 1989

[23] Nordic Co-operative Organization for Applied Research, "Assessment of Ship Performance in a Seaway, the Nordic Co-operative Project: Seakeeping Performance of Ships", NORDFORSK 1987.

[24] Pawlowski, J.S., Bass, D.W., "Theoretical and Numerical Study of Ship Motions in Heavy Seas", Trans. SNAME Vol. 99, New York, October 1991.

[25] Bass, D.W., Cumming, D., "Experimental and Numerical Study of Water Trapped on Deck", STAB 2000, Tasmania, Australia, Feb. 2000.

[26] Barrett, J., Cumming, D., and Hopkins, D., "Description of Seakeeping Trials carried out on CCGA Atlantic Swell-October 2003", NRC-TR-2003-28, December 2003.

[27] Barrett, J., Cumming, D., and Hopkins, D., "Description of Seakeeping Trials carried out on CCGA Shamook-December 2003", NRC-TR-2004-01, January 2003.

[28] Fisheries and Oceans Canada, information obtained in November 2004 available on: http://www.meds-sdmm.dfo-mpo.gc.ca/meds/Home_e.htm

Appendix A

Numerical results of amplitudes of motion for each length class.

The 35' Length Class.

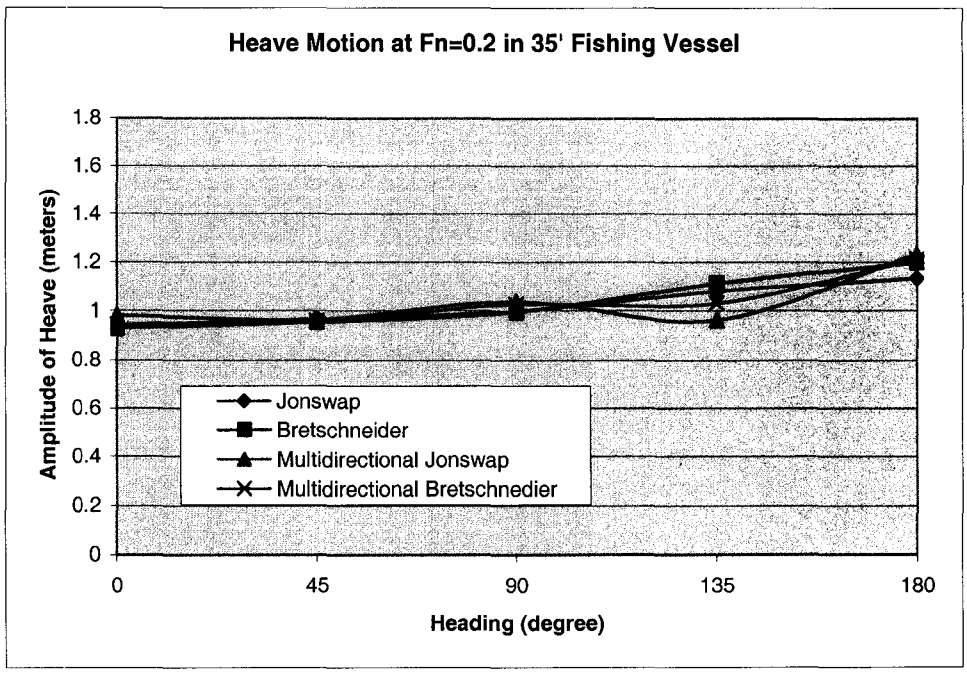

Figure 66.

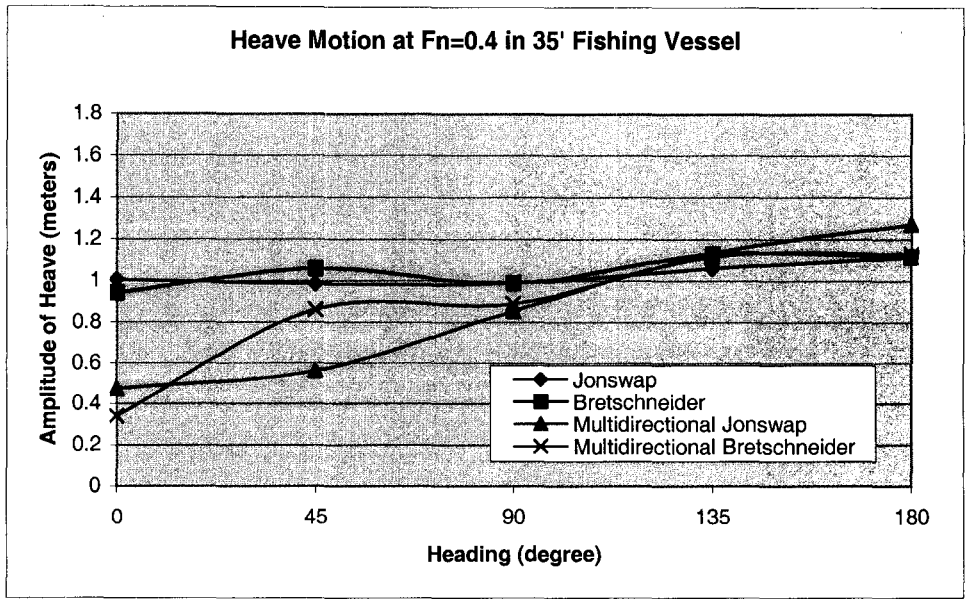

Figure 67.

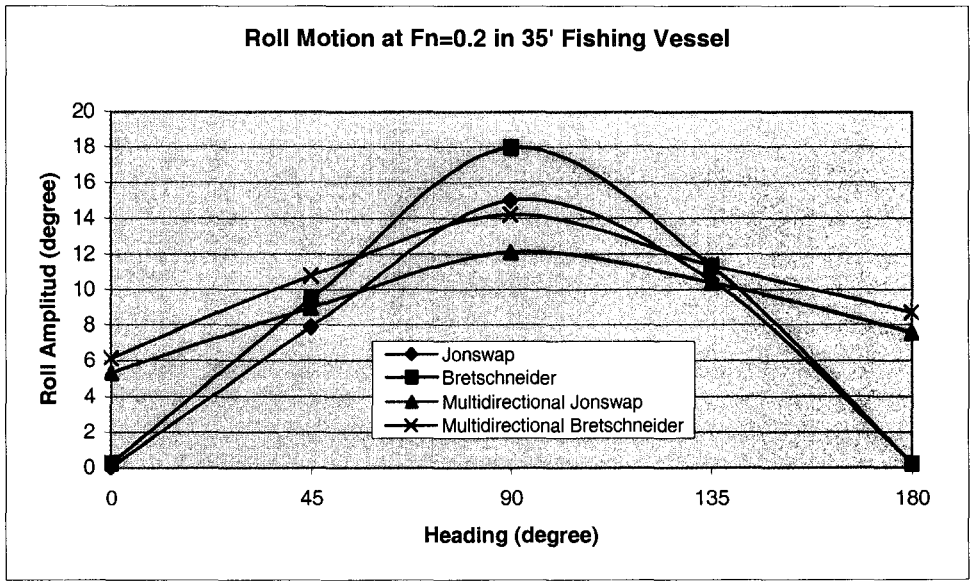

Figure 68.

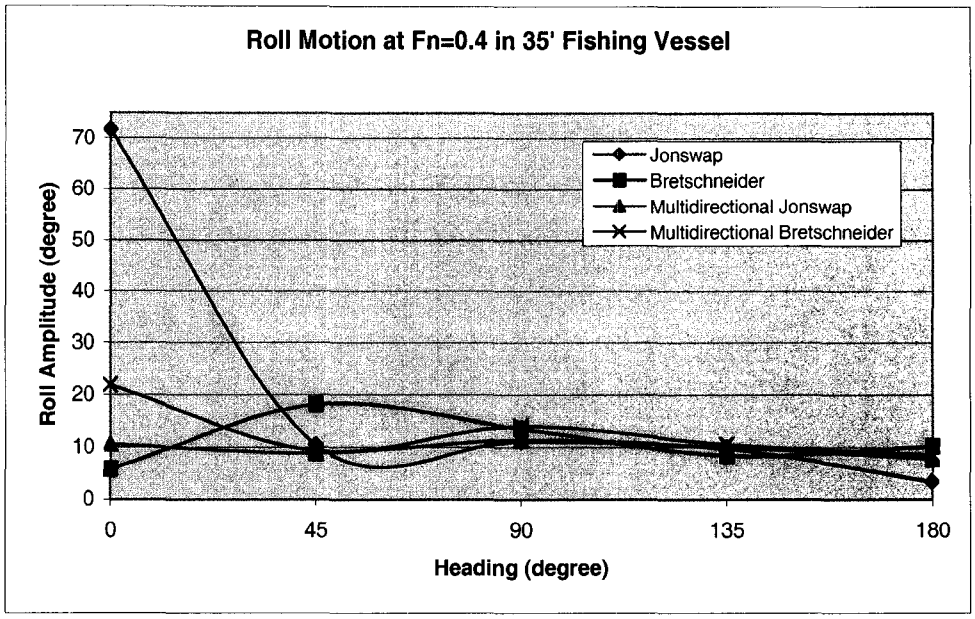

Figure 69.

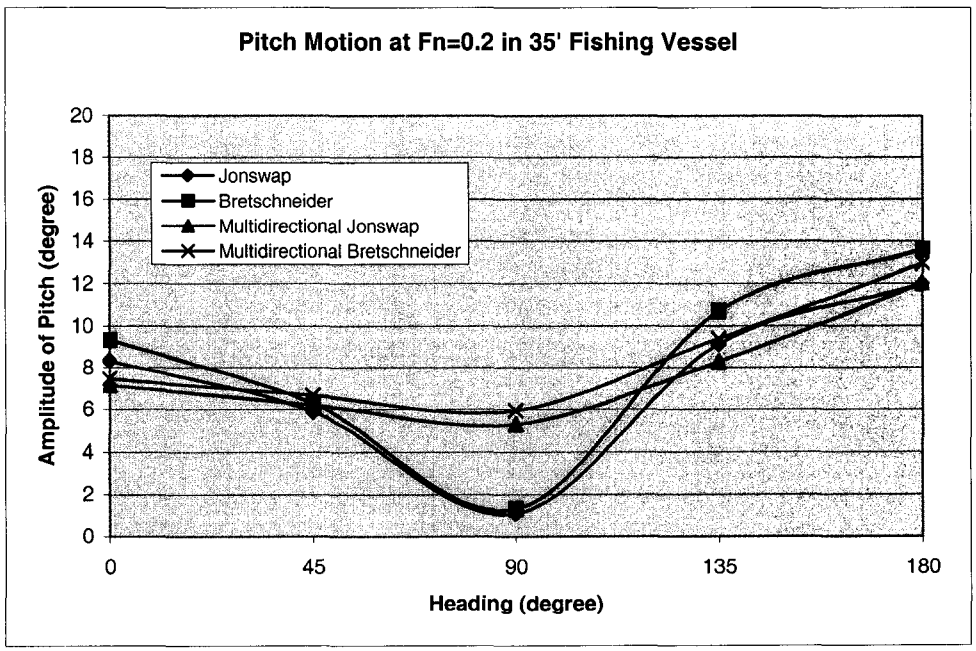

Figure 70.

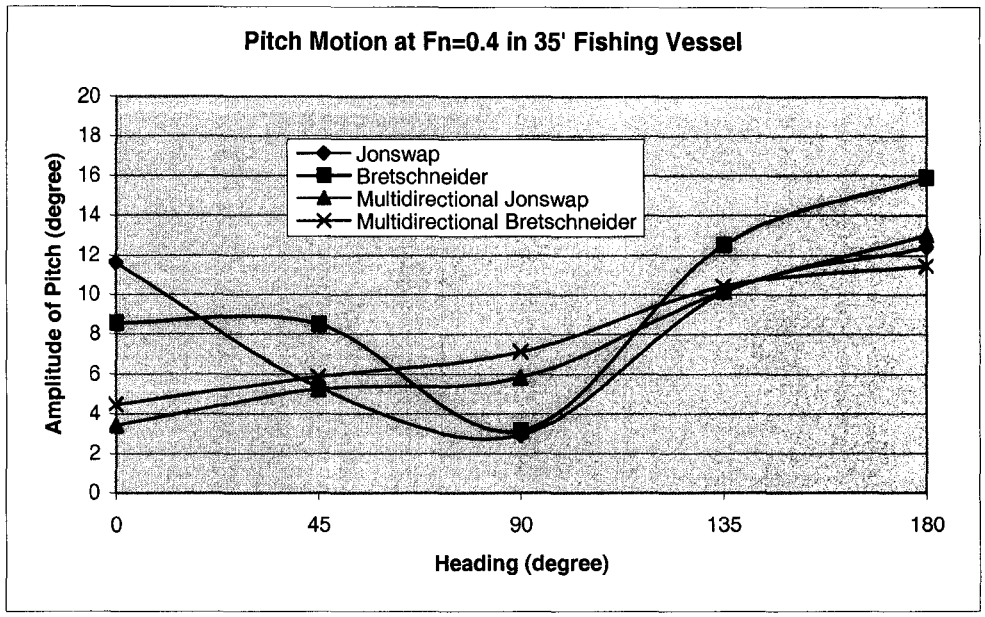

Figure 71.

The 45' Length Class.

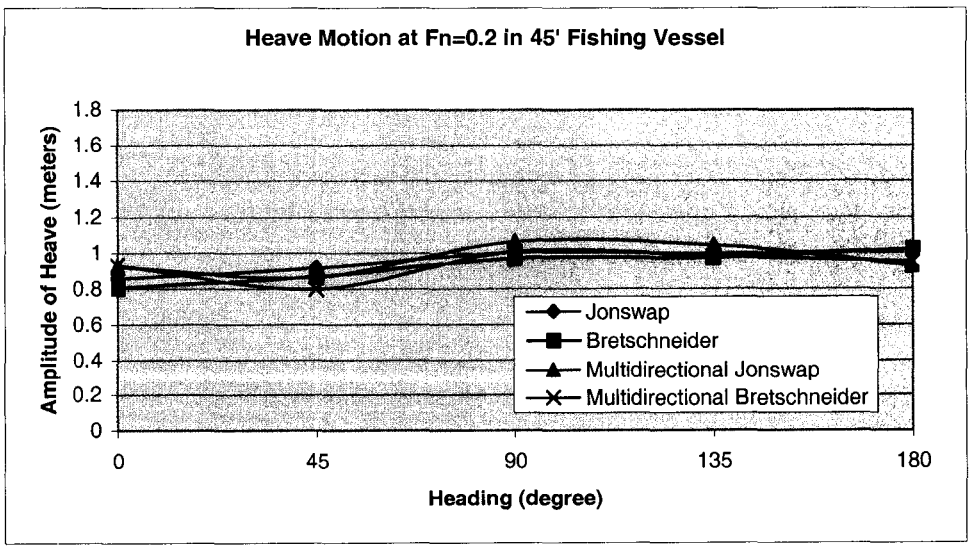

Figure 72.

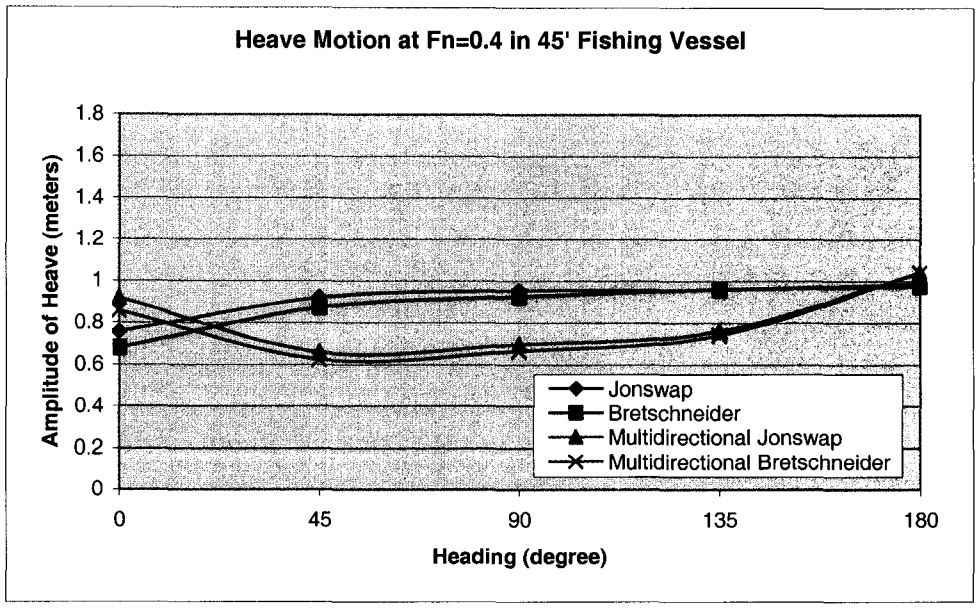

Figure 73.

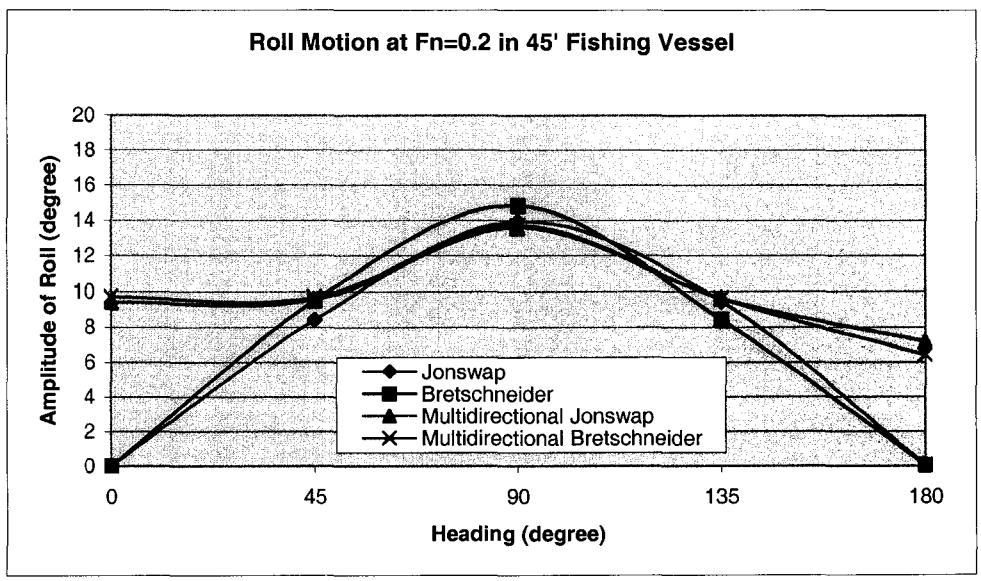

Figure 74.

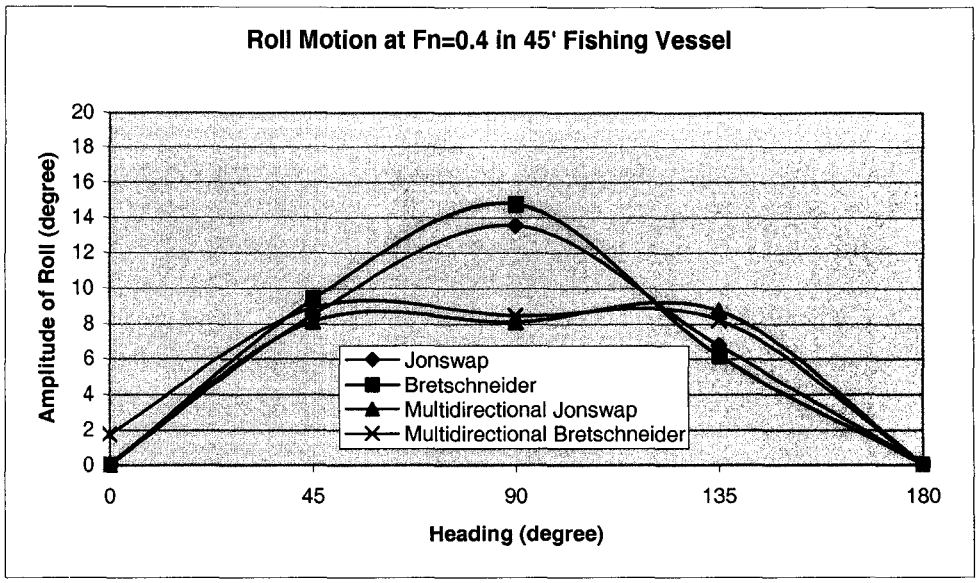

Figure 75.

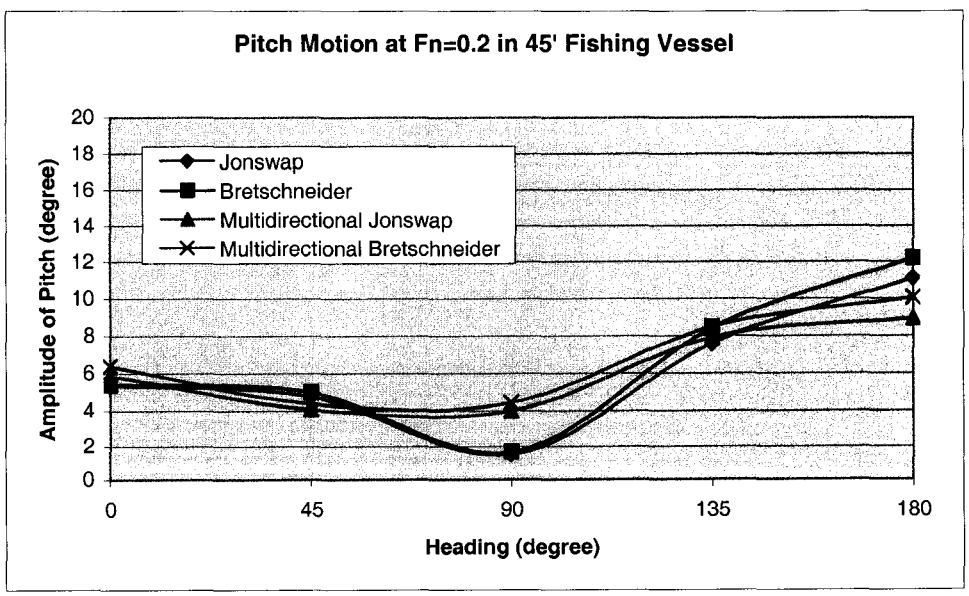

Figure 76.

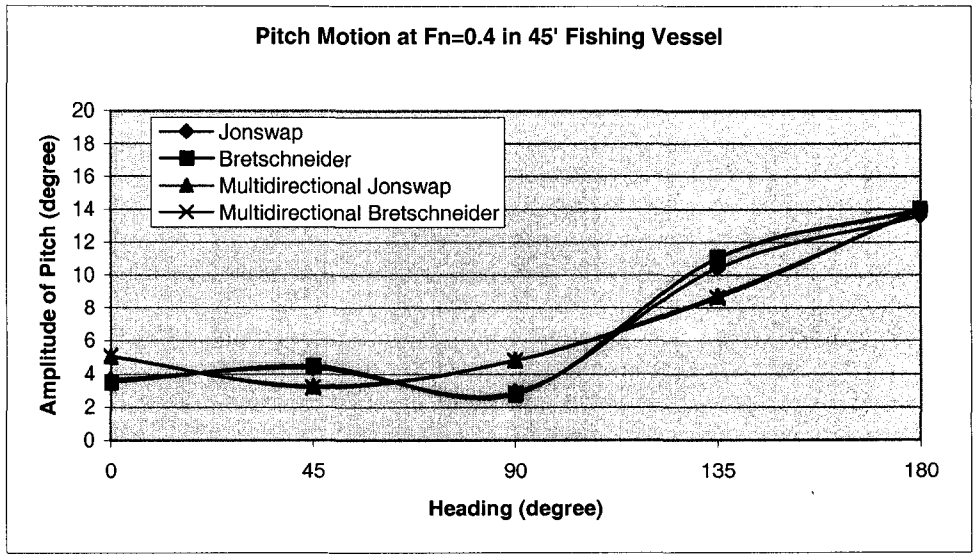

Figure 77.

The 65' Length Class.

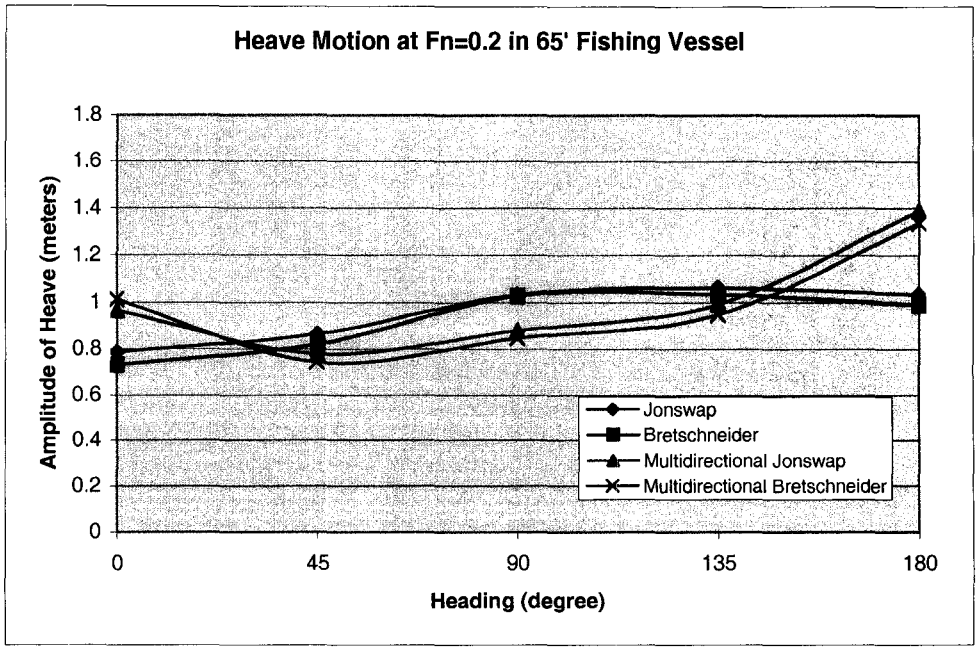

Figure 78.

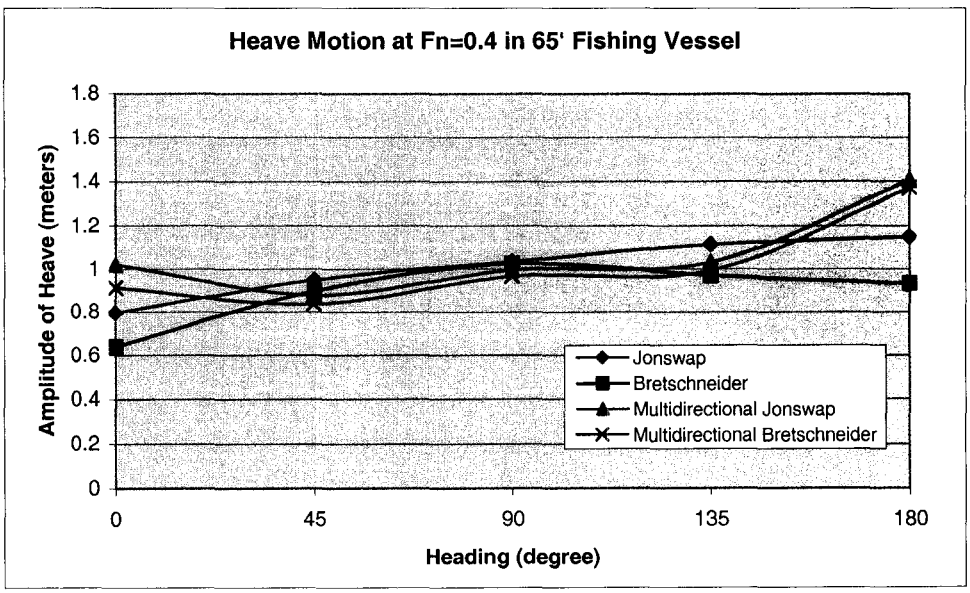

Figure 79.

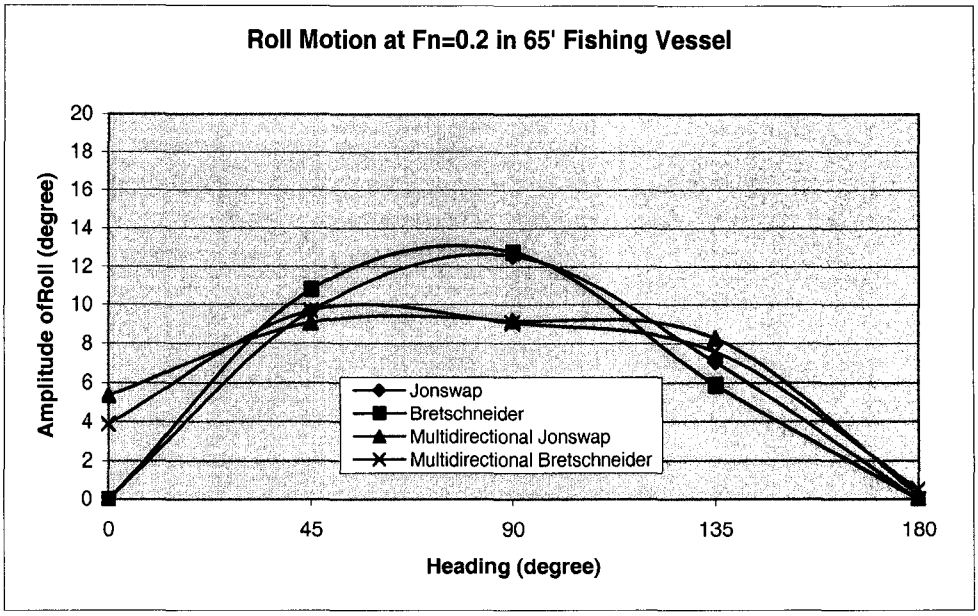

Figure 80.

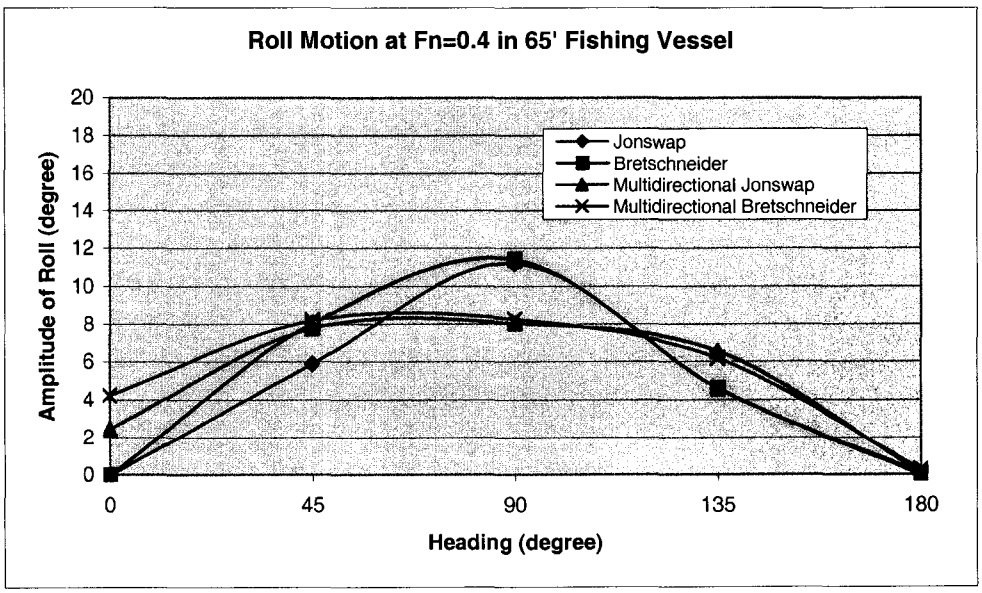

Figure 81.

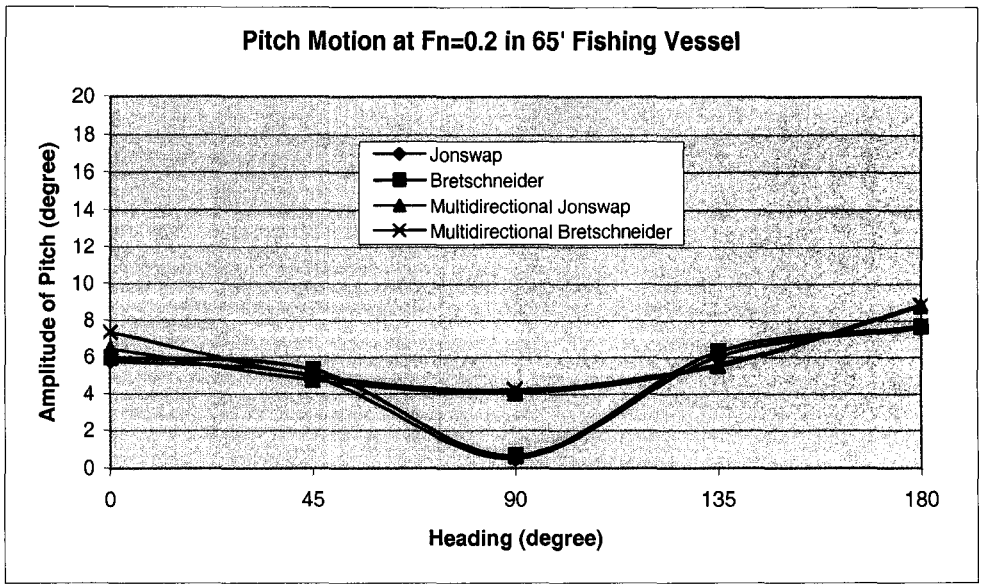

Figure 82.

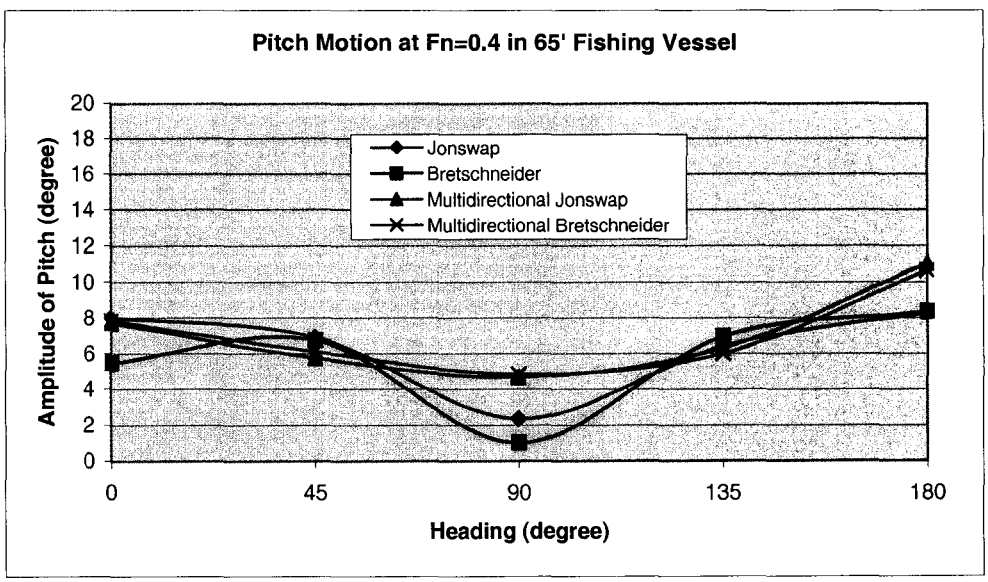

Figure 83.

The 75' Length Class.

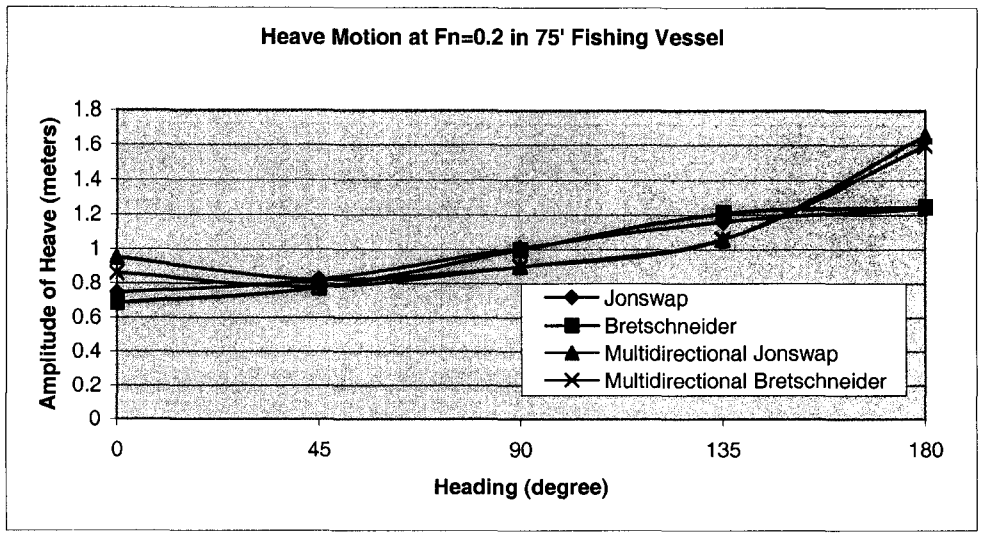

Figure 84.

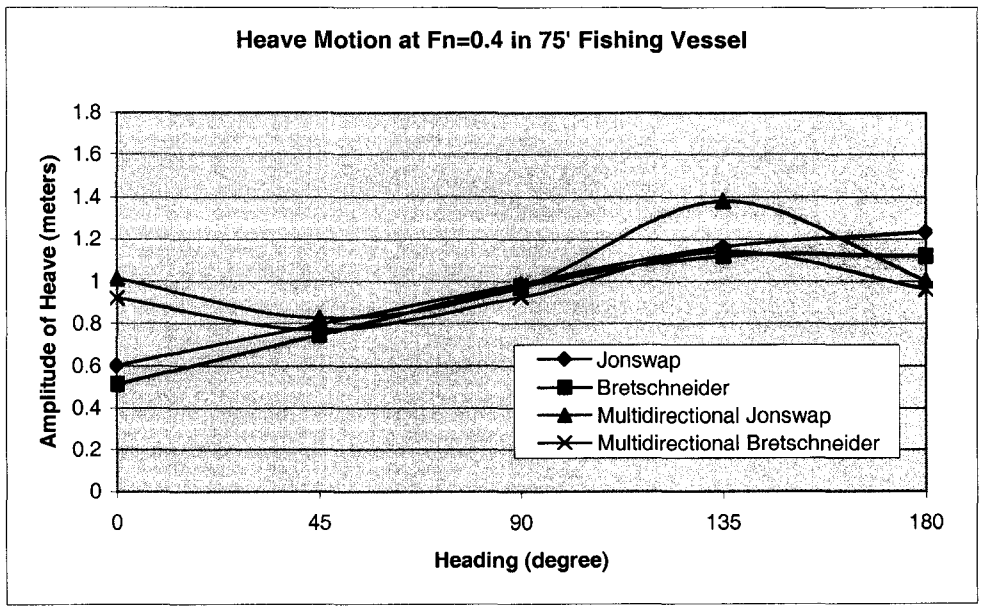

Figure 85.

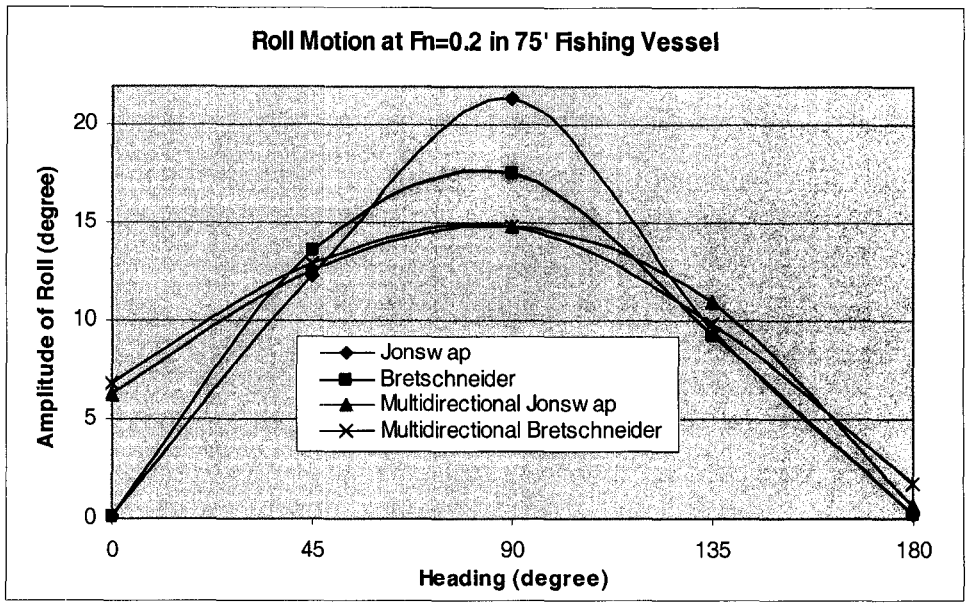

Figure 86.

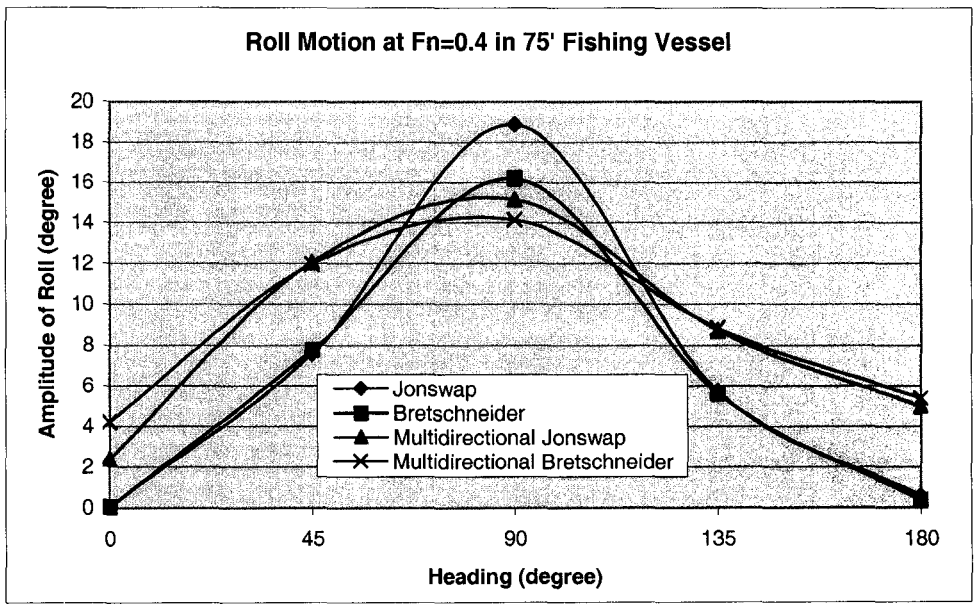

Figure 87.

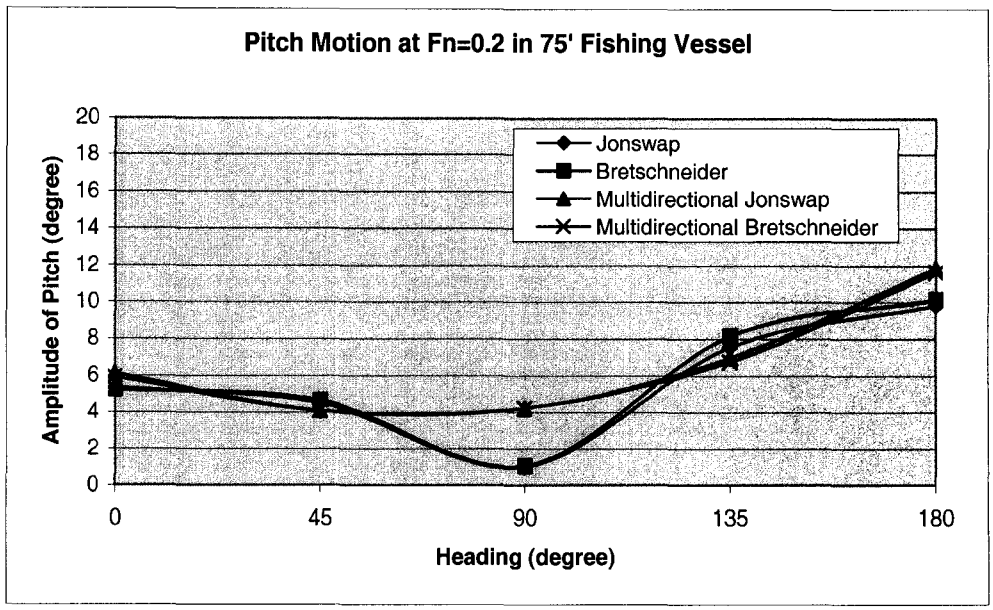

Figure 88.

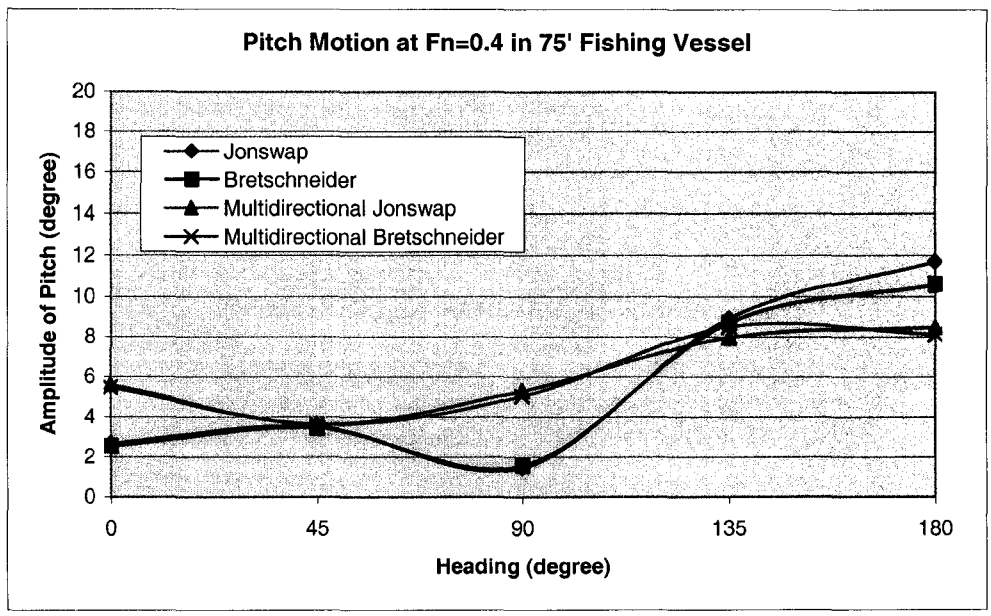

Figure 89.

Appendix B

MII for five points and five headings:

The numerical simulation gives the number of MII per minute at each point selected on the vessel. This information includes the response of the vessels determined by six headings in four wave conditions at low and high speed. No average is introduced in this evaluation and the complete set of graphs is presented in appendix A. The following set of graphs describe the MII on five points on the 35, 45, 65, and 75 feet fishing vessel in Uni-directional and Multi-directional spectrum at low and high speeds respectively.

MIIs of 35' in Uni-directional Waves:

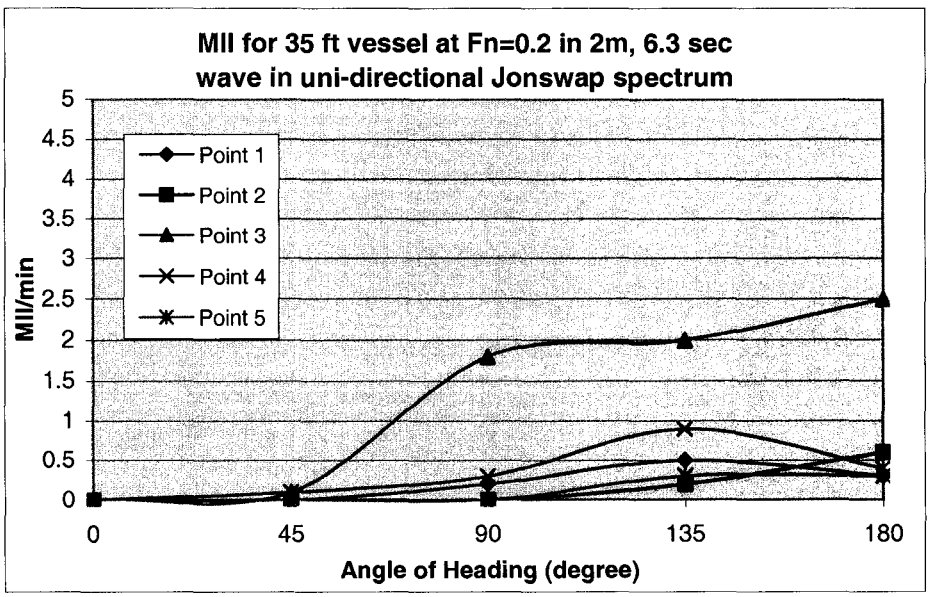

Figure 90.

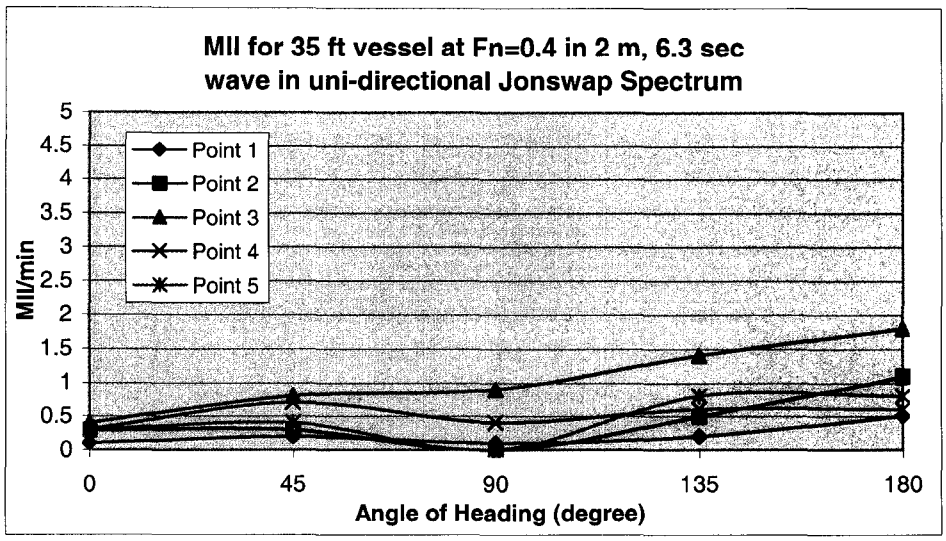

Figure 91.

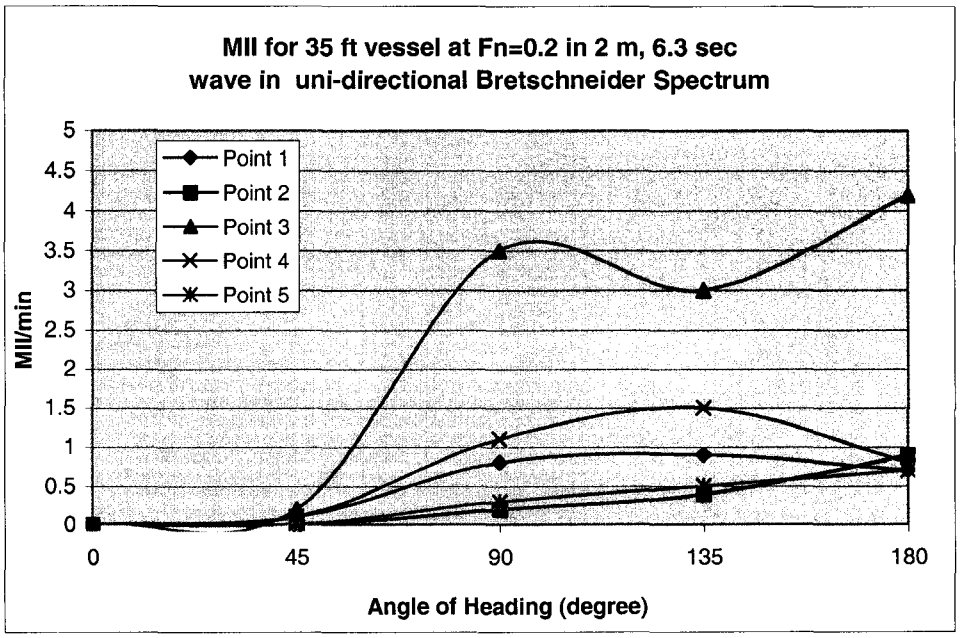

Figure 92.

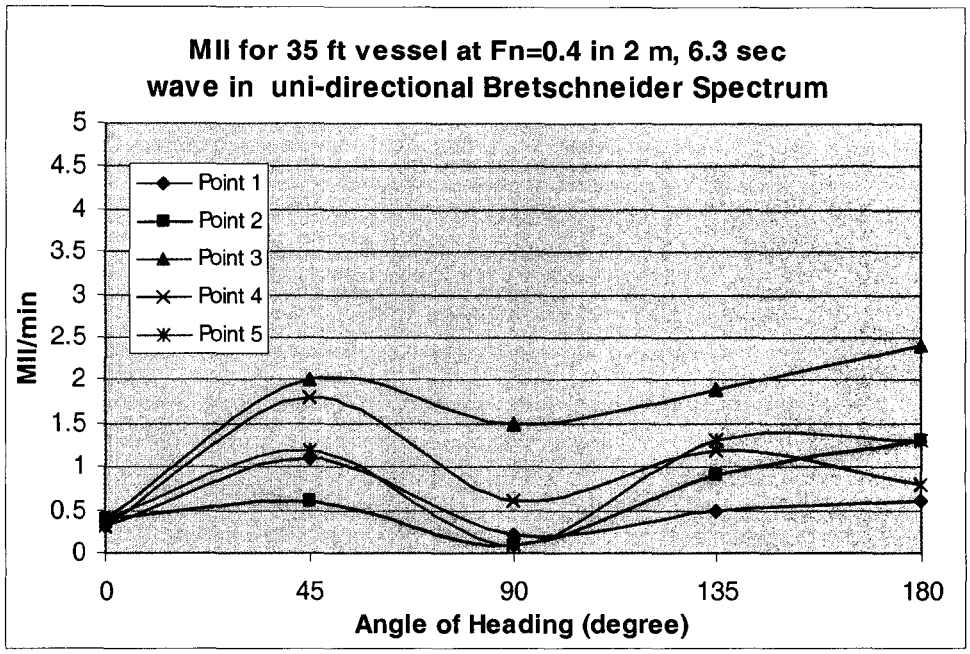

Figure 93.

MIIs of 35' in Multi-directional Waves:

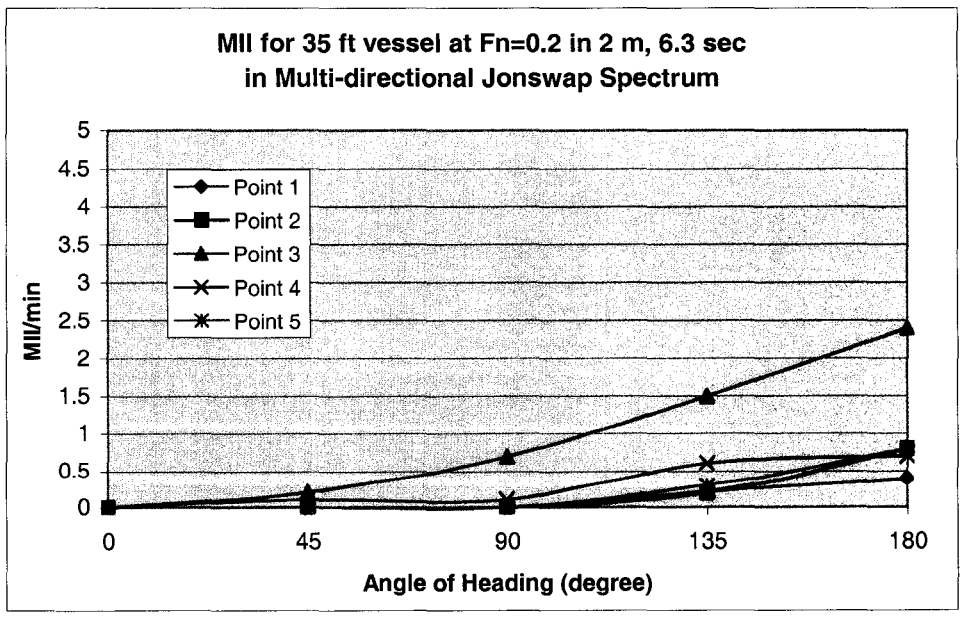

Figure 94.

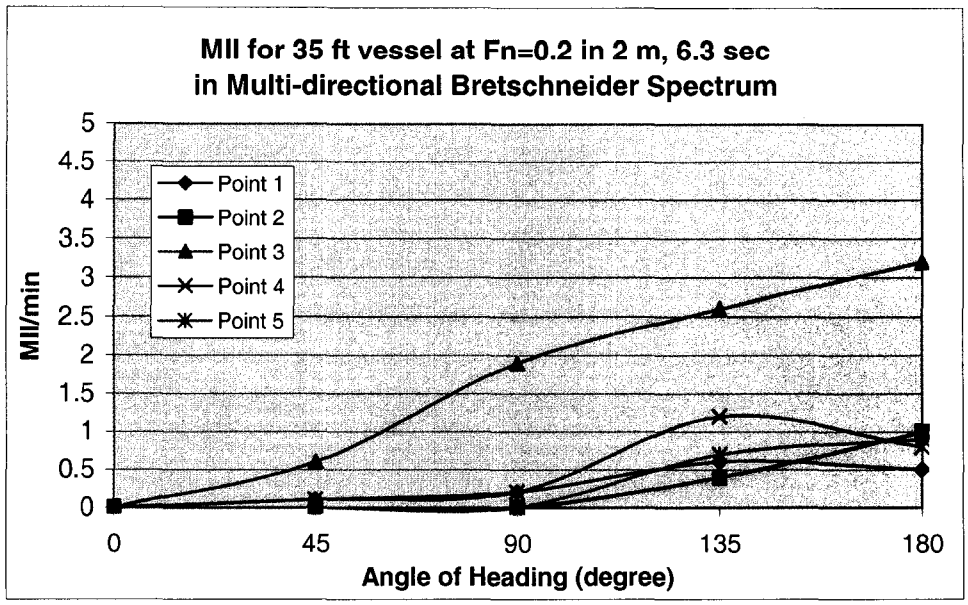

Figure 95.

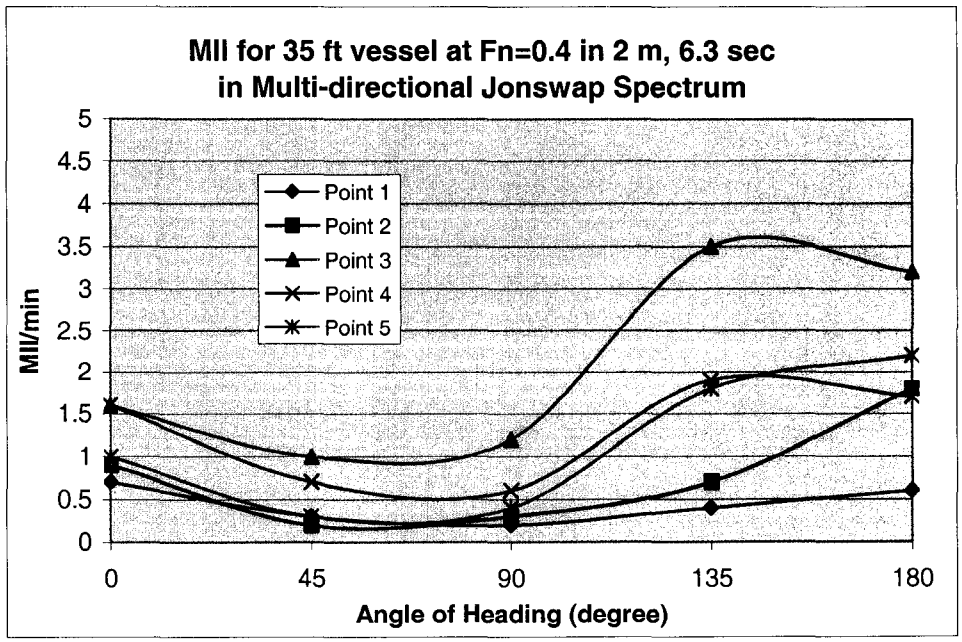

Figure 96.

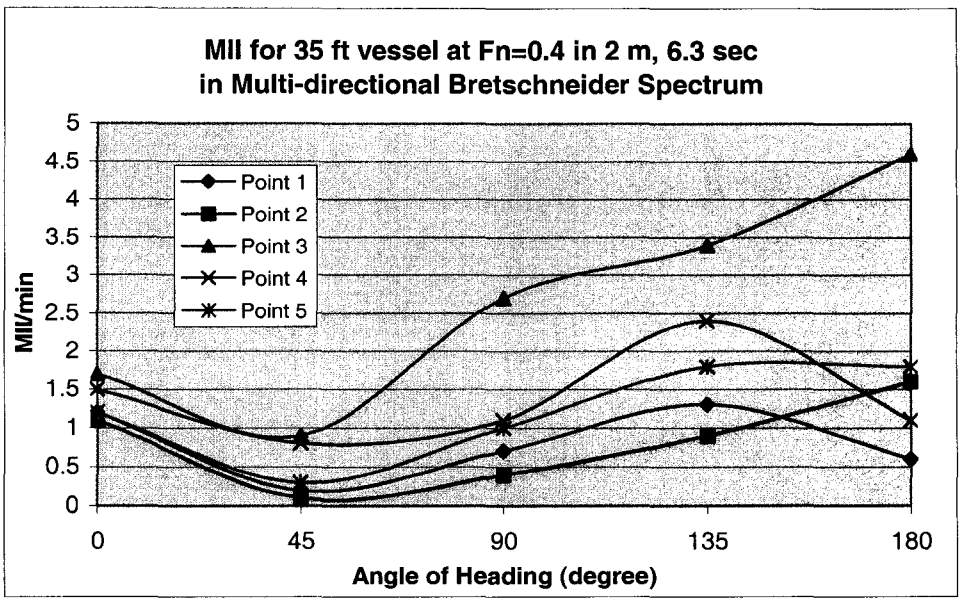

Figure 97.

MIIs of 45' in Uni-directional Waves:

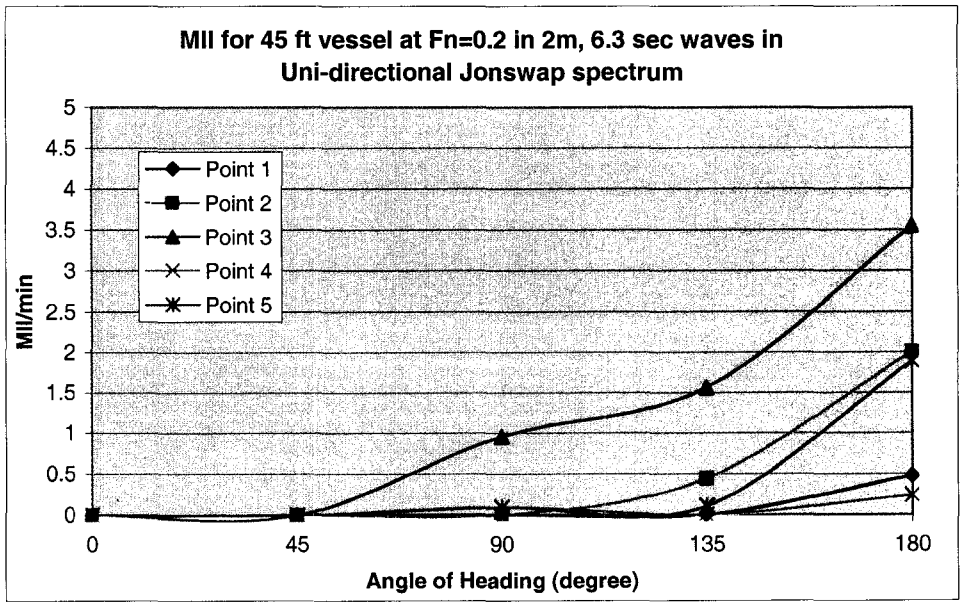

Figure 98.

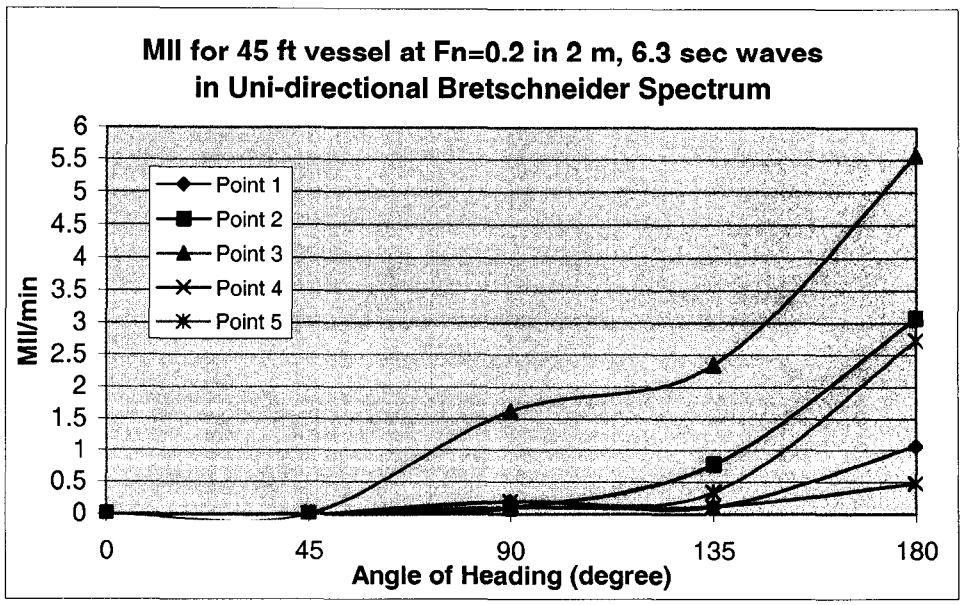

Figure 99.

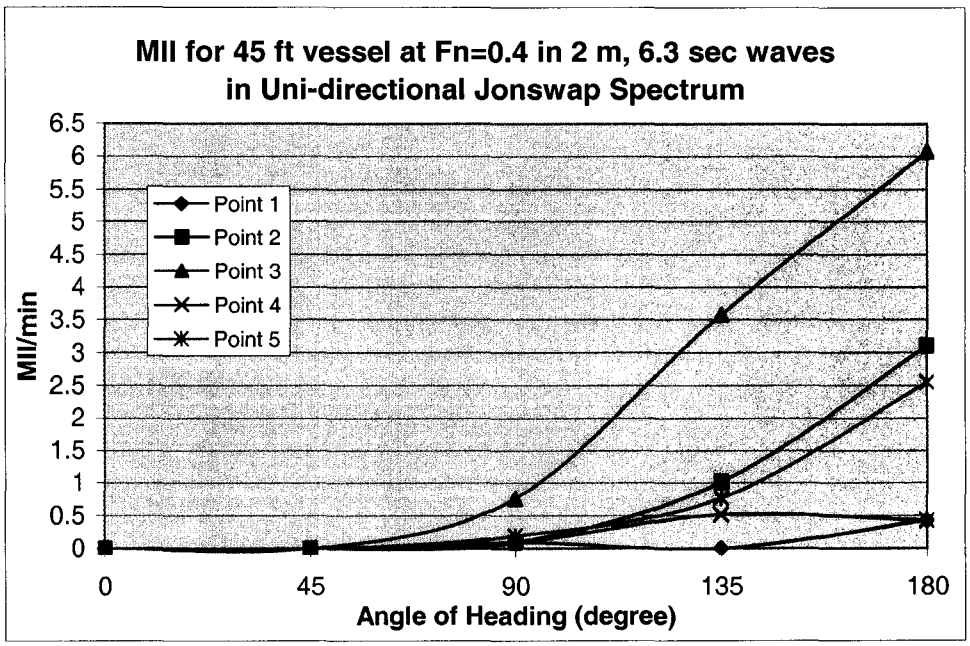

Figure 100.

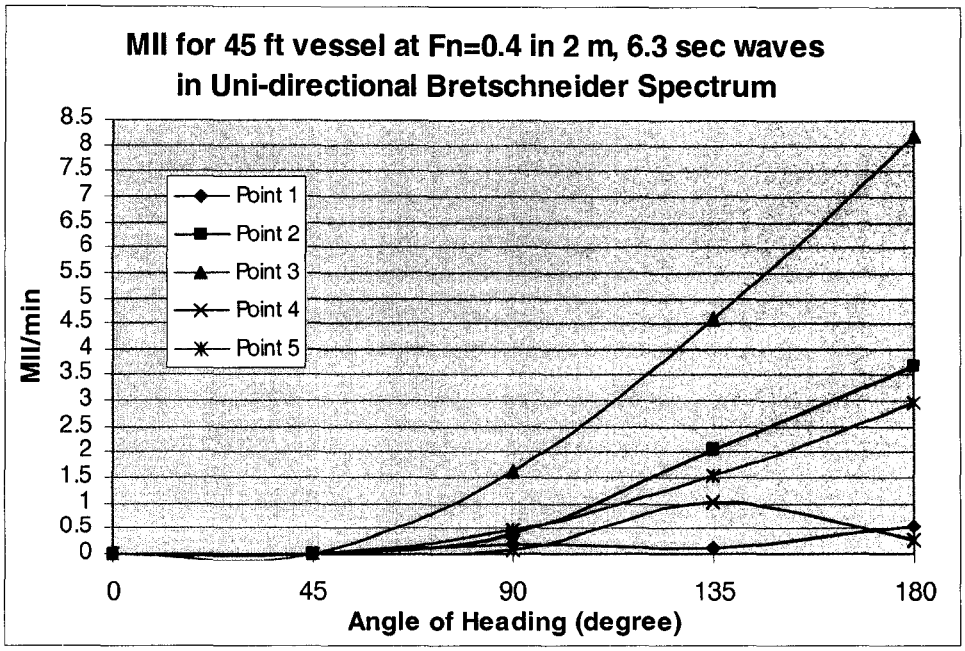

Figure 101.

MIIs of 45' in Multi-directional Waves:

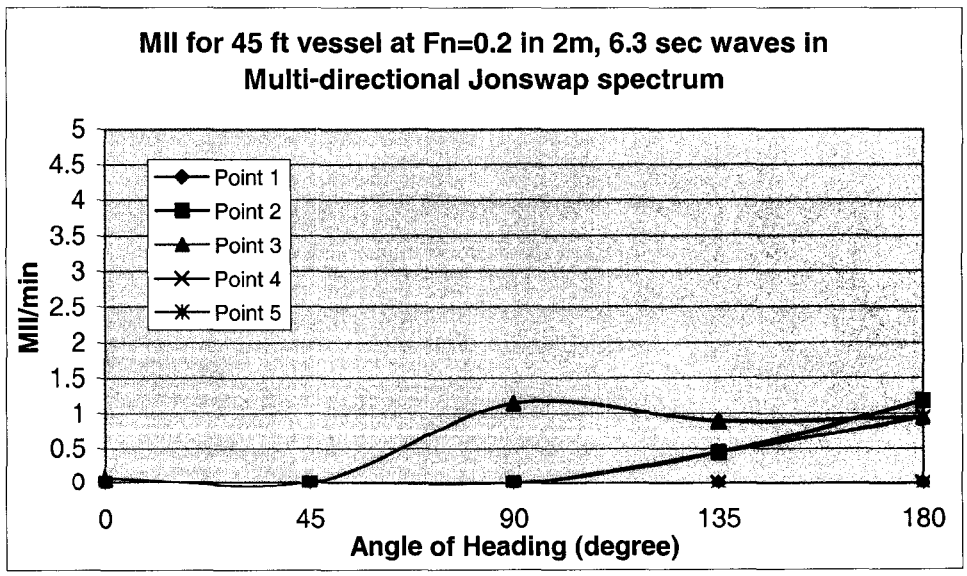

Figure 102.

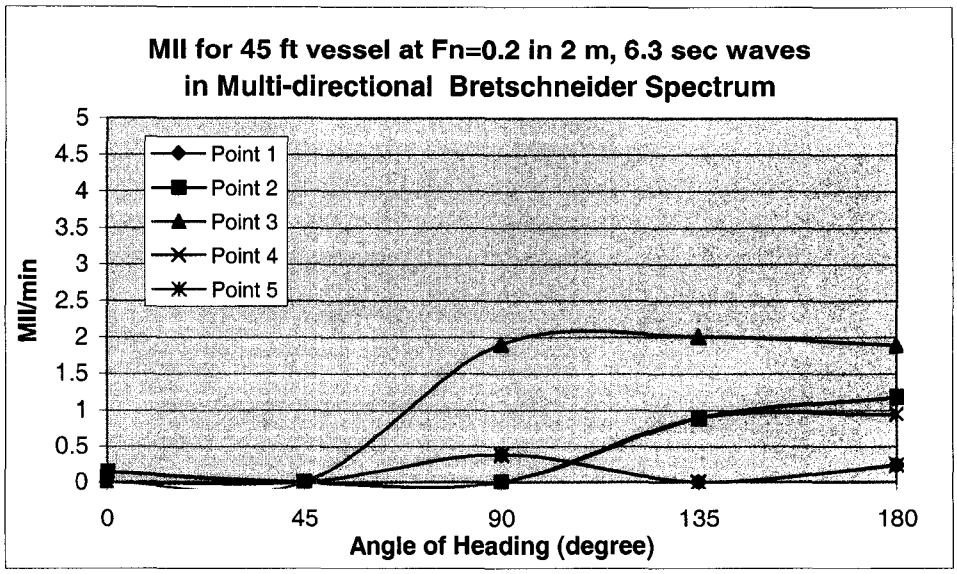

Figure 103.

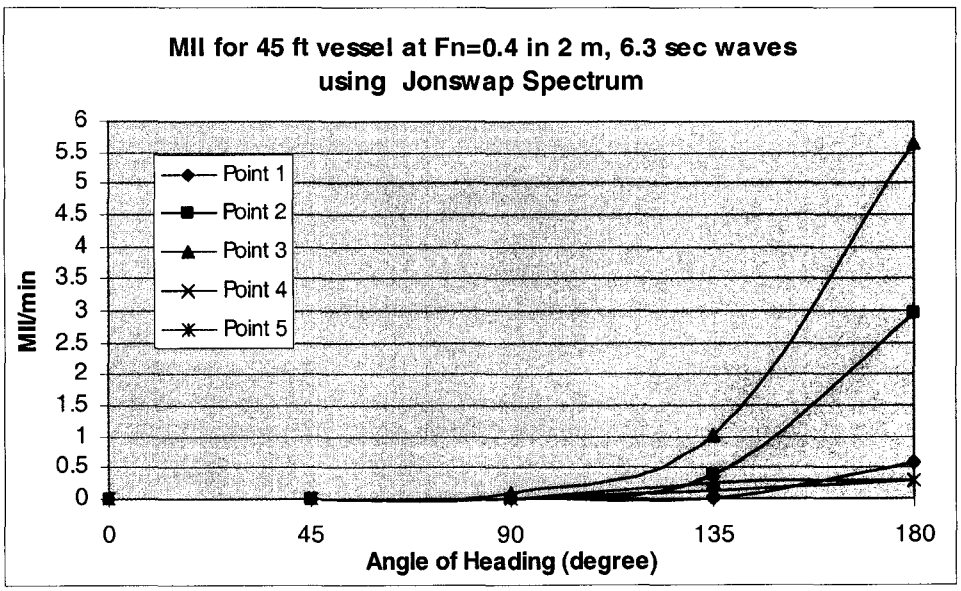

Figure 104.

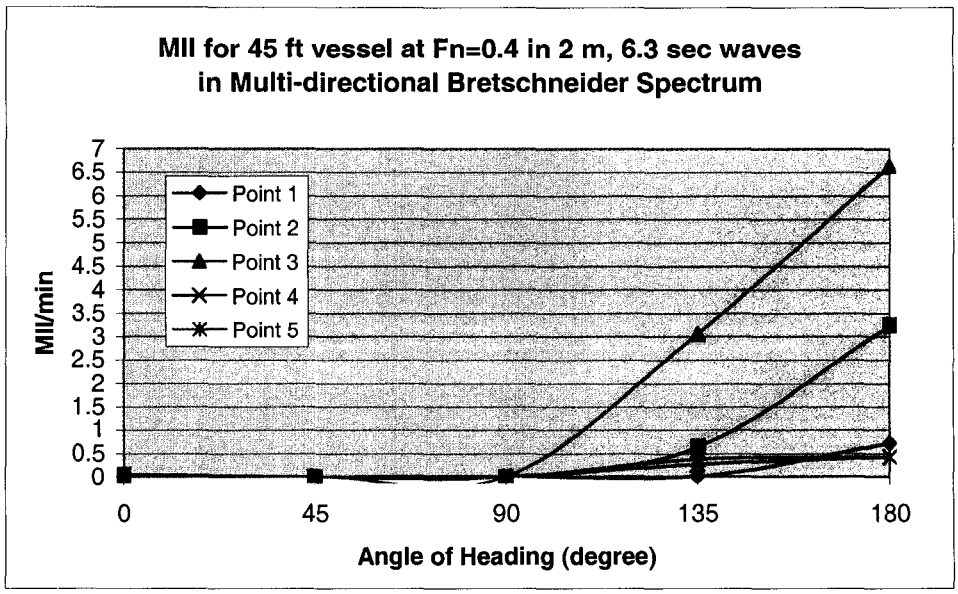

Figure 105.

MIIs of 65' in Uni-directional Waves:

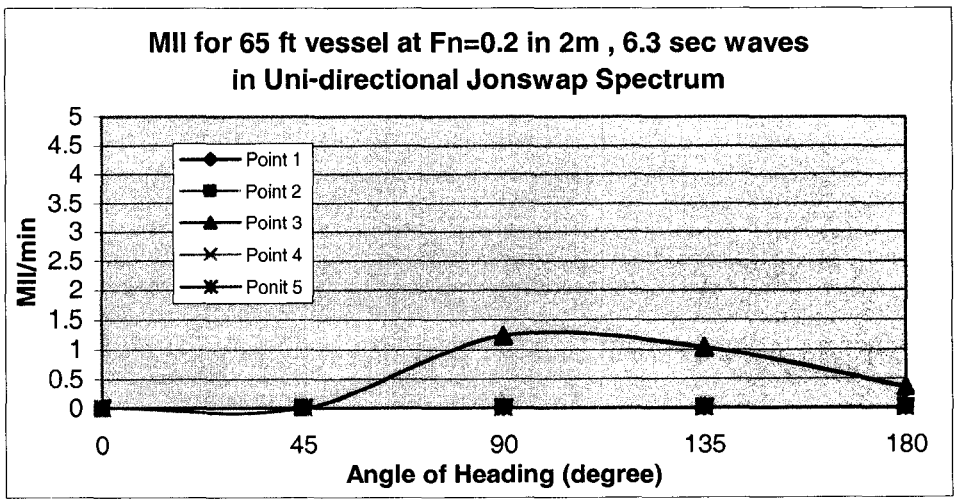

Figure 106.

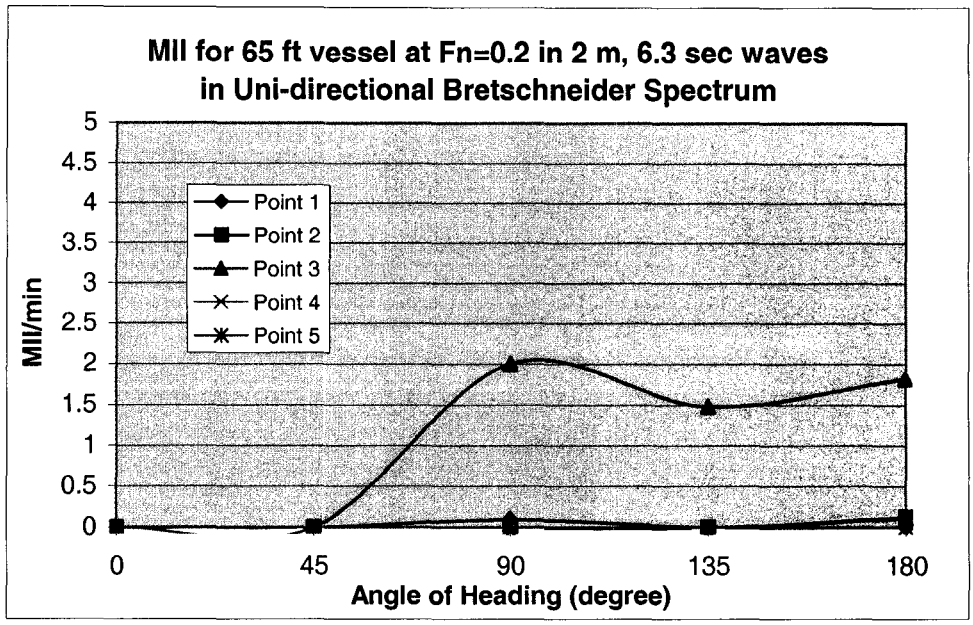

Figure 107.

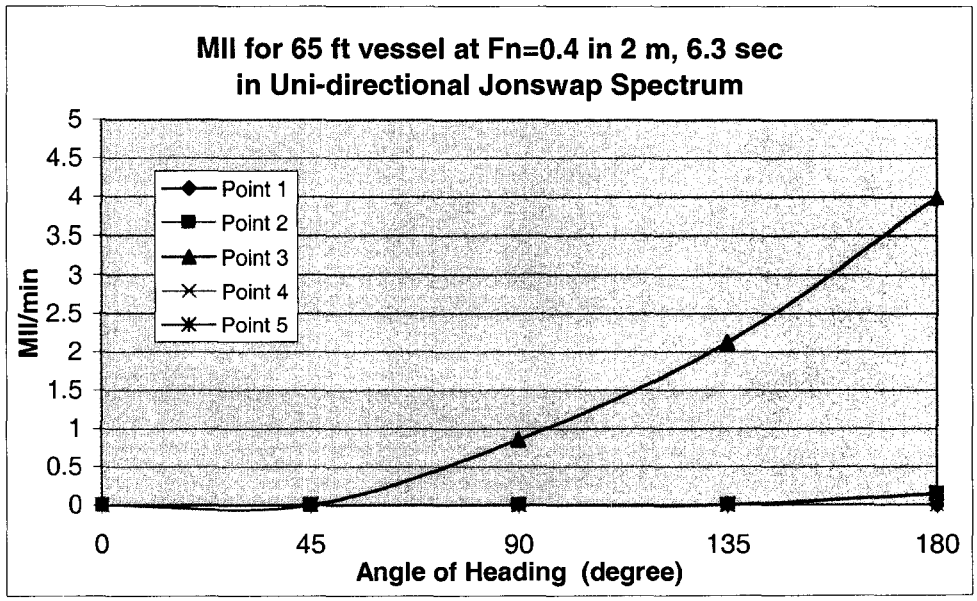

Figure 108.

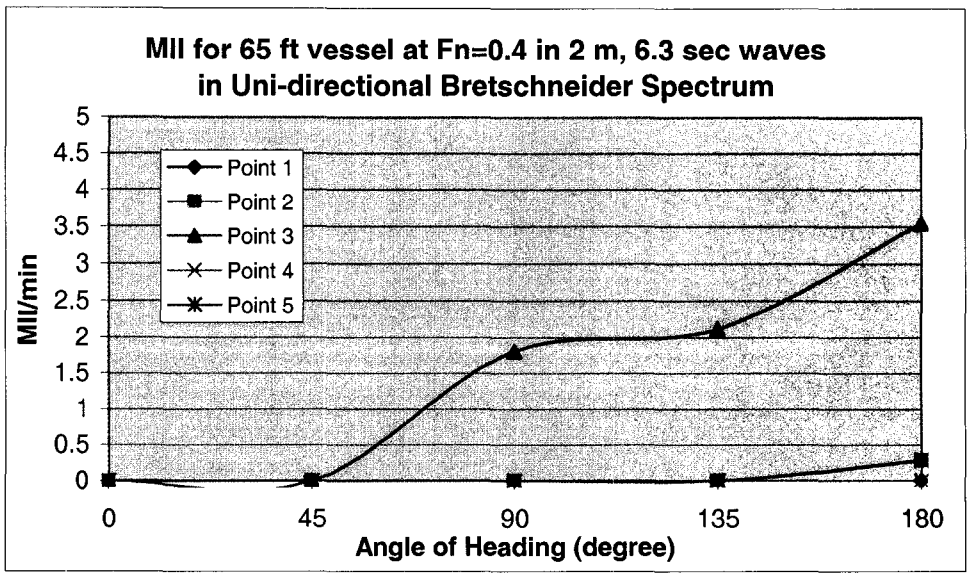

Figure 109.

MIIs of 65' in Multi-directional Waves:

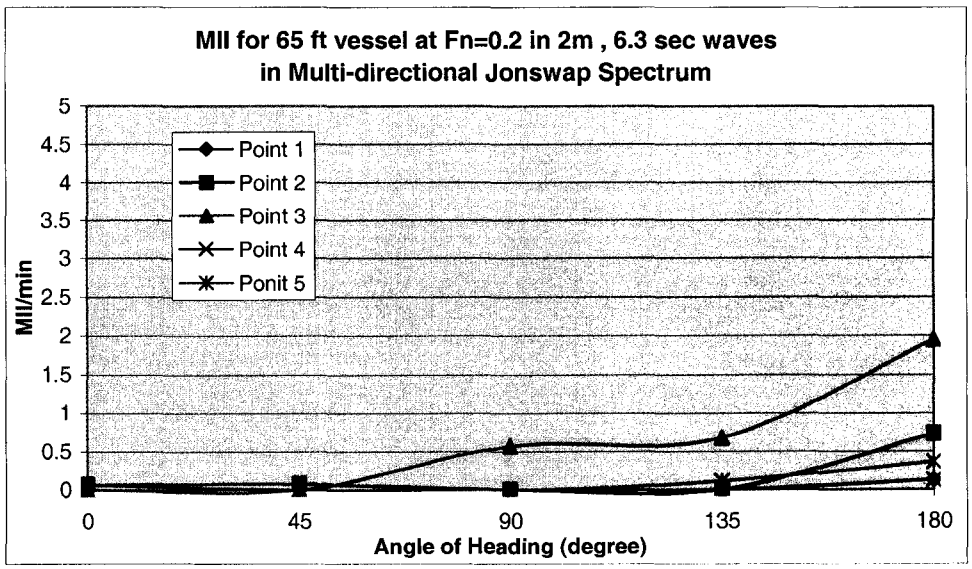

Figure 110.

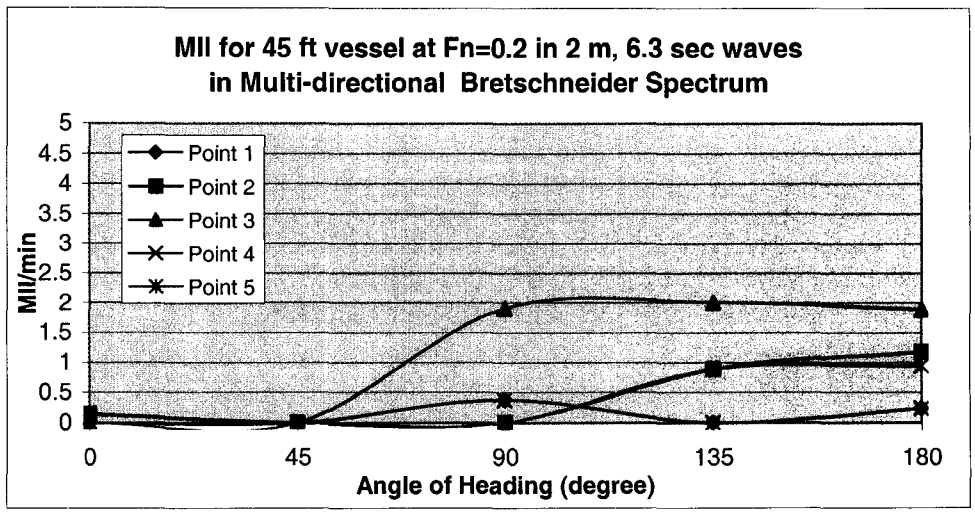

Figure 111.

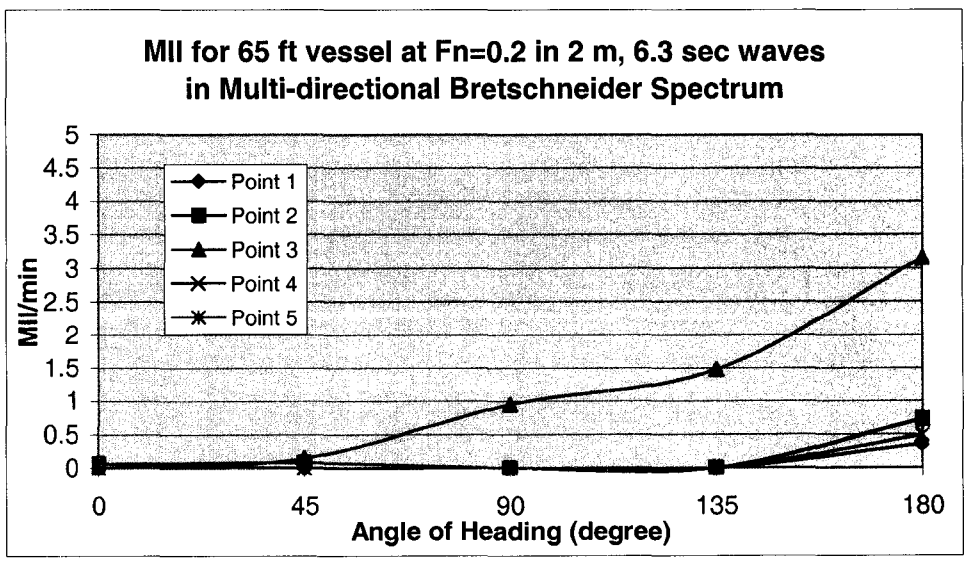

Figure 112.

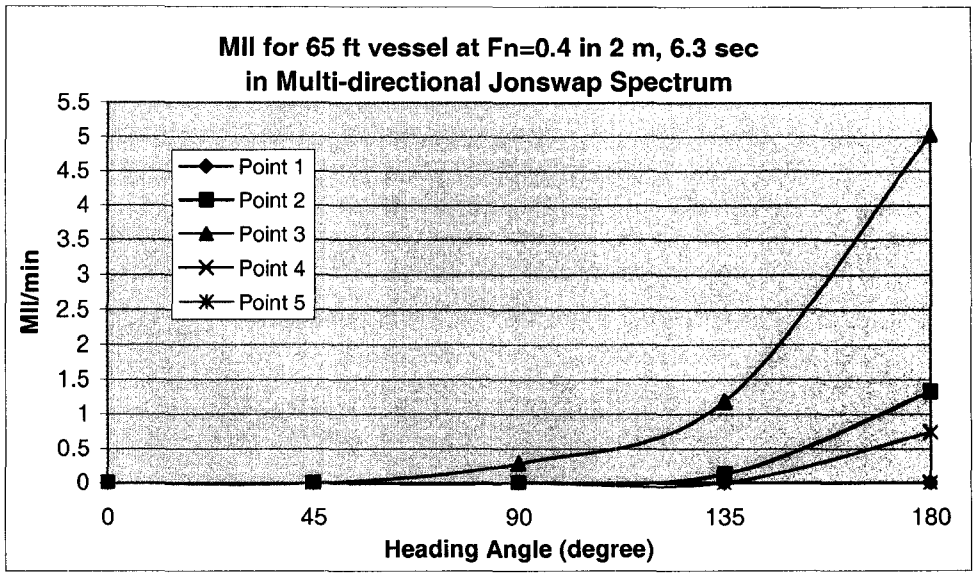

Figure 113.

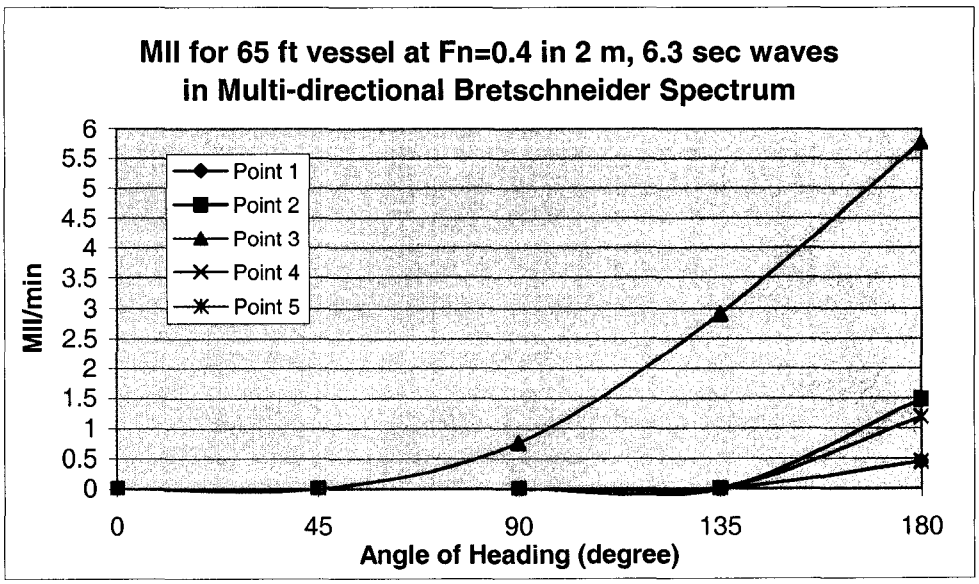

Figure 114.

MIIs of 75' in Uni-directional Waves:

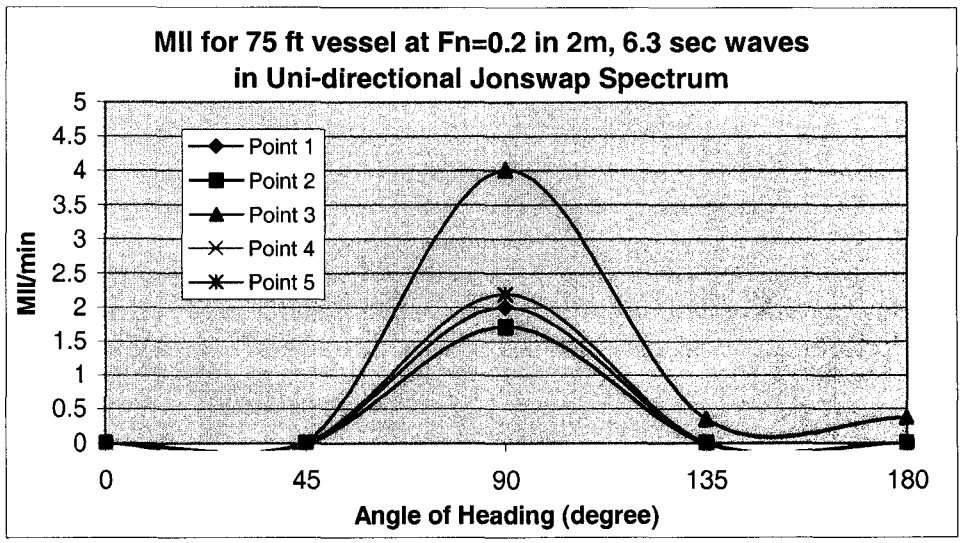

Figure 115.

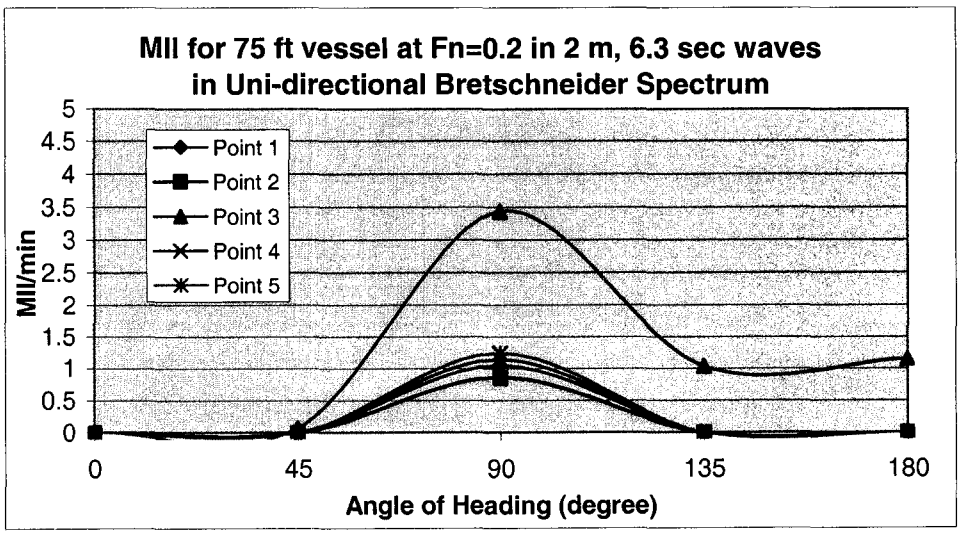

Figure 116.

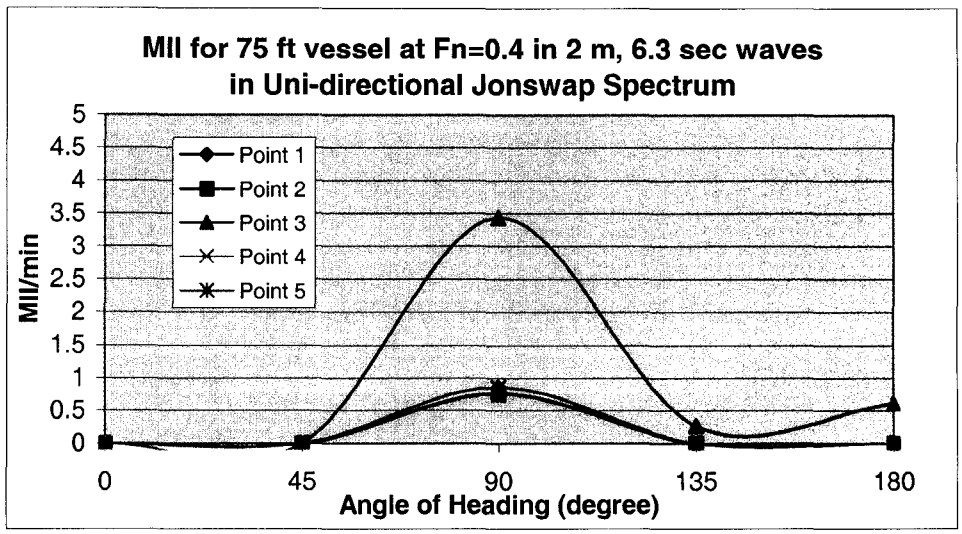

Figure 117.

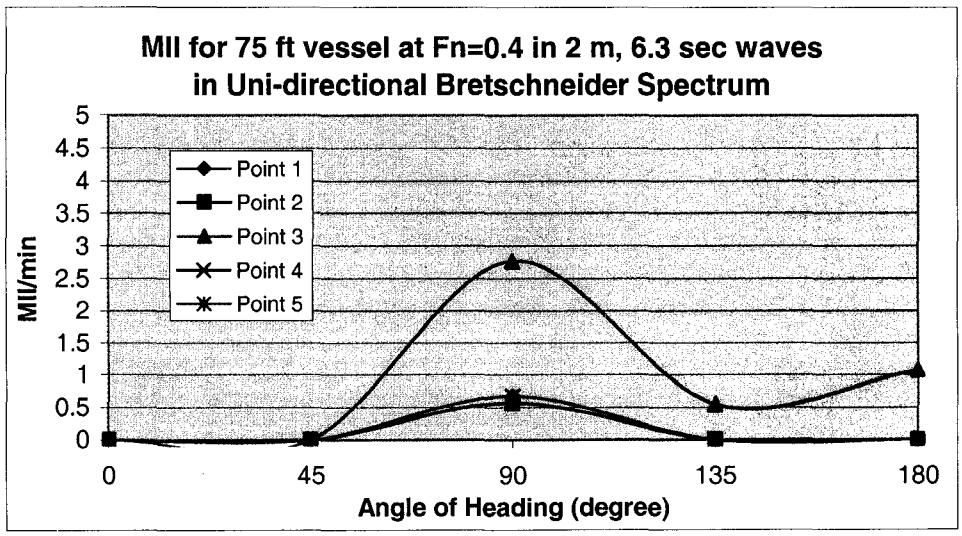

Figure 118.

MIIs of 75' in Multi-directional Waves:

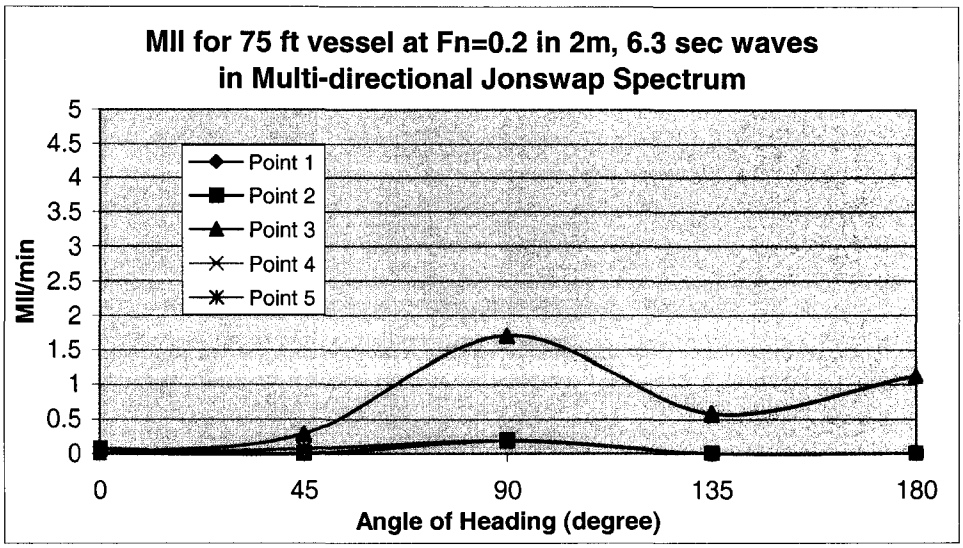

Figure 119.

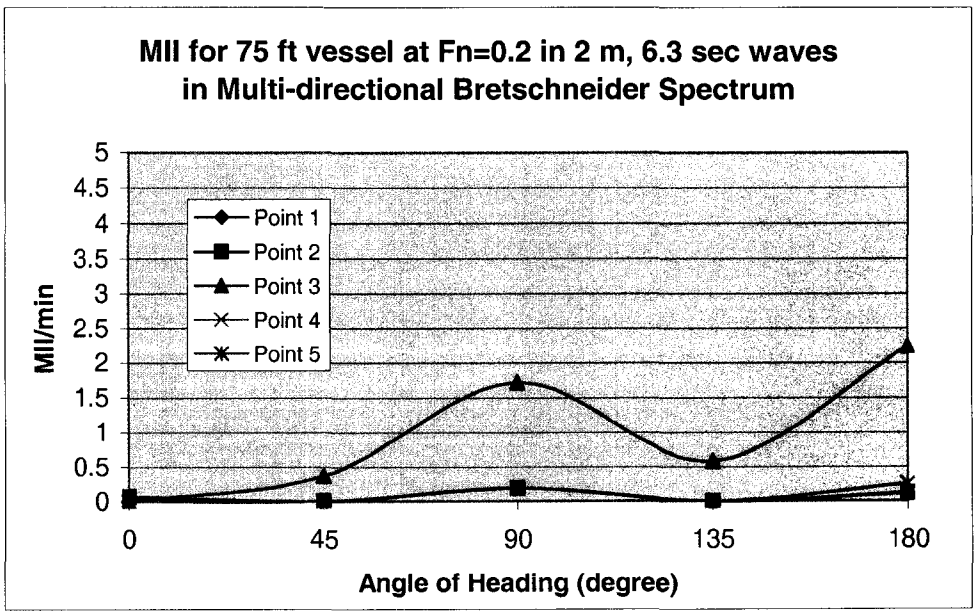

Figure 120.

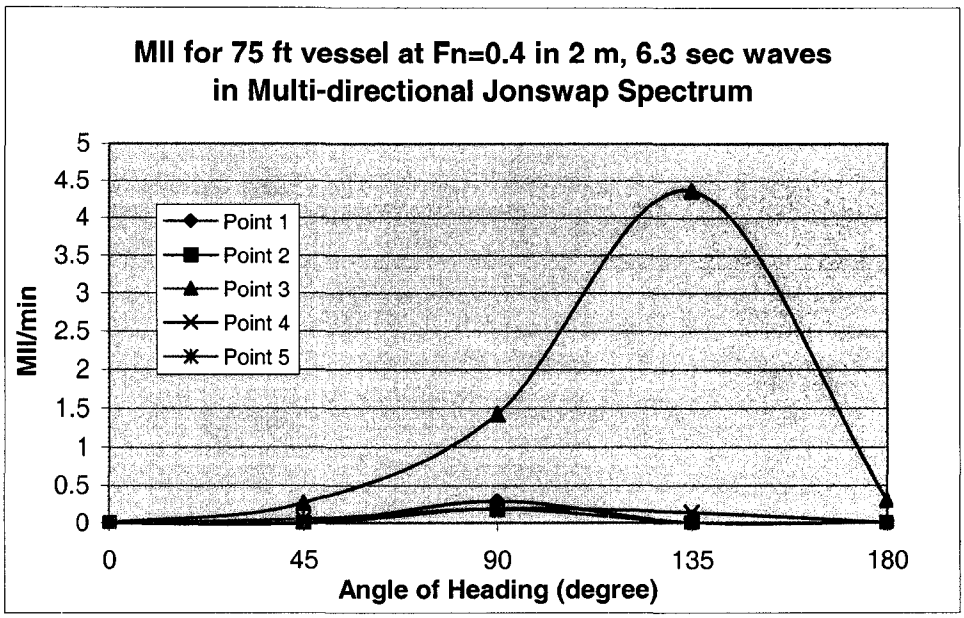

Figure 121.

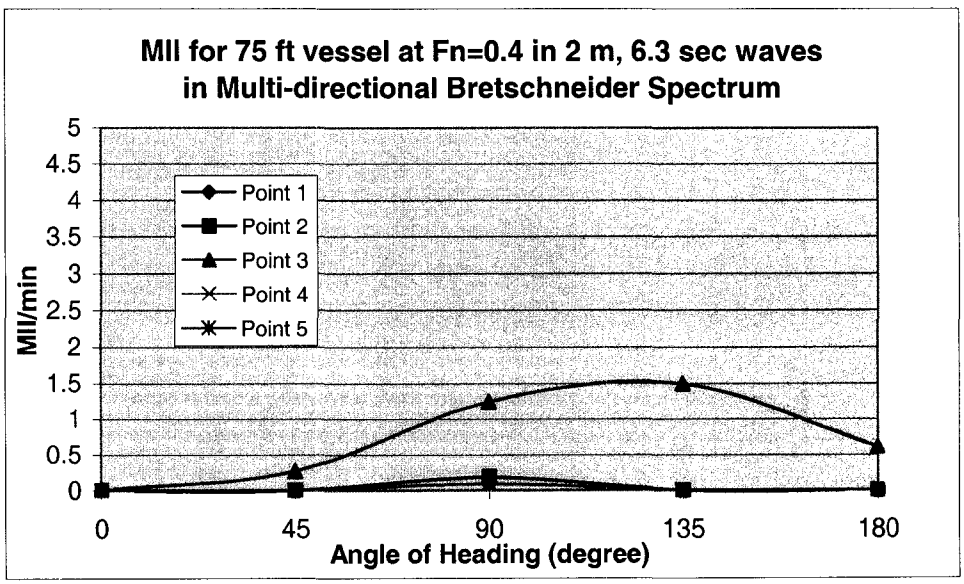

Figure 122.

Appendix C

Average Number of MIIs:

The average MII value over bow headings is estimated to determine the number of MII per minute for each length class in any wave direction.

At low speed, Fn=0.2:

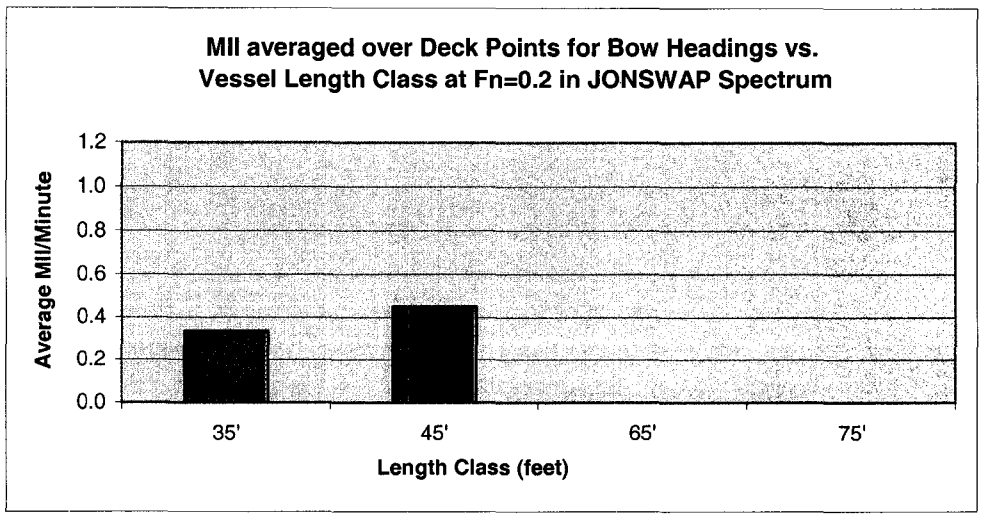

Figure 123.

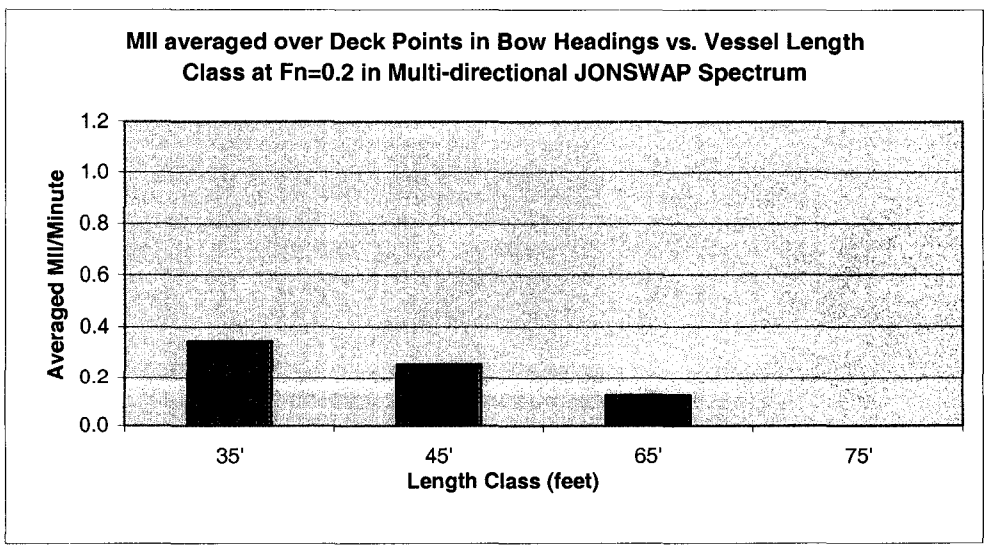

Figure 124.

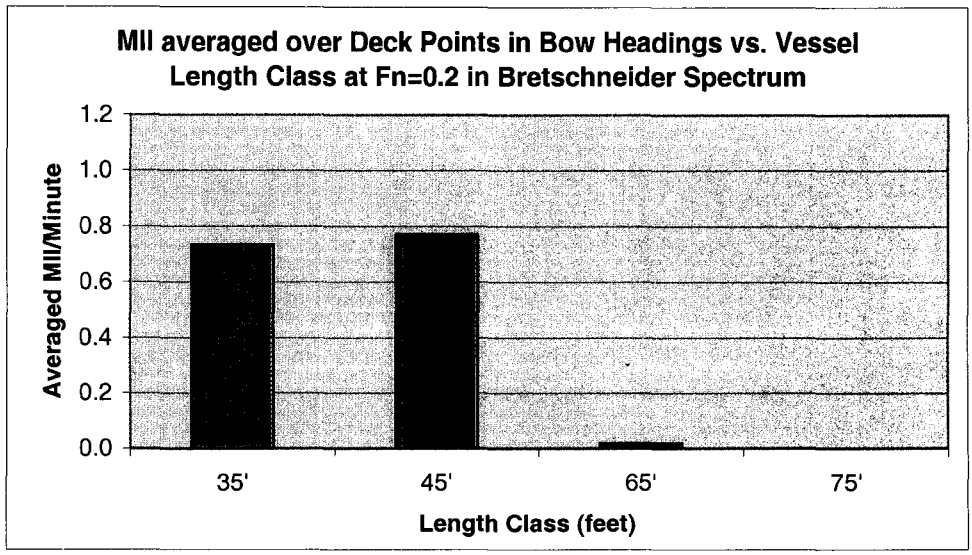

Figure 125.

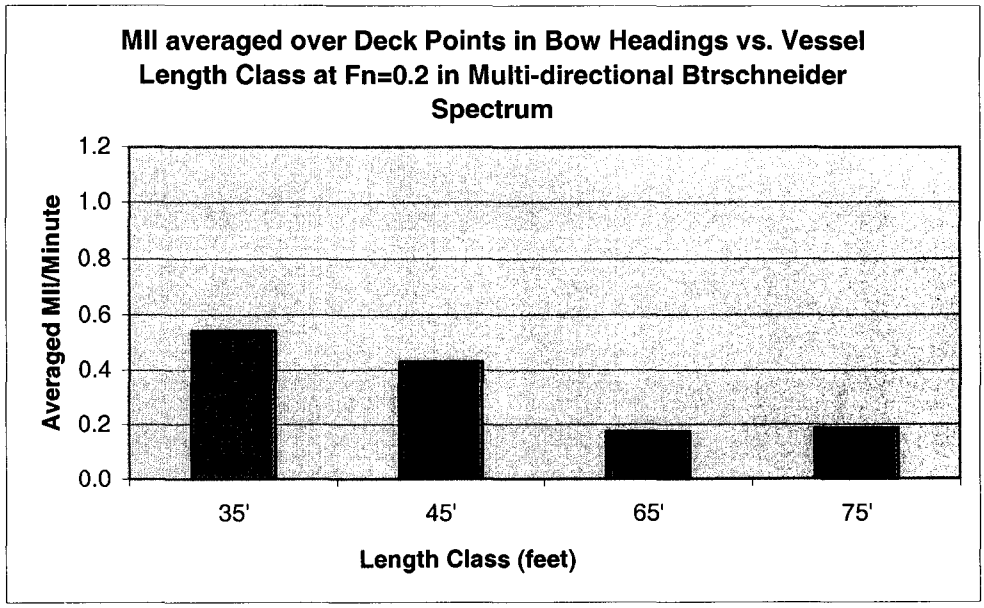

Figure 126.

At high speed, Fn=0.4:

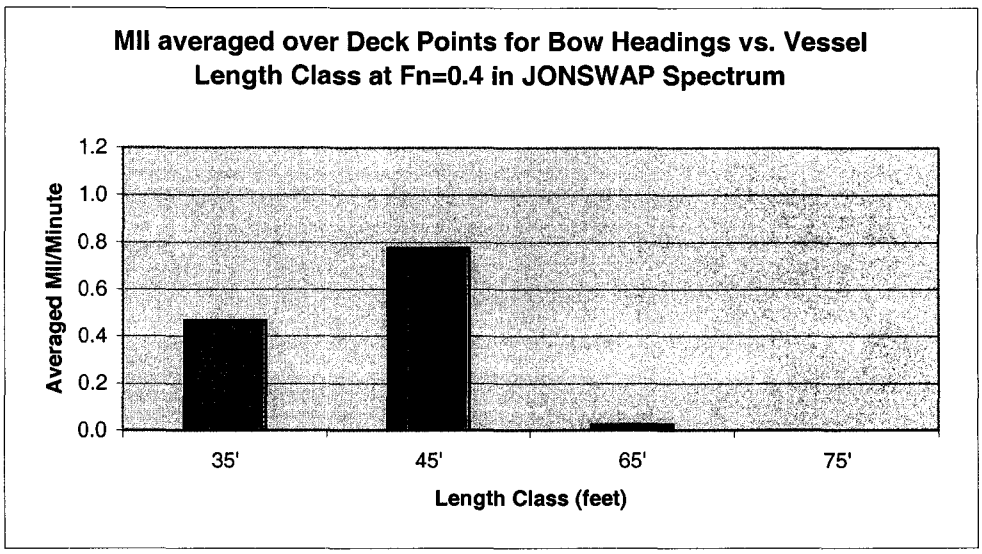

Figure 127.

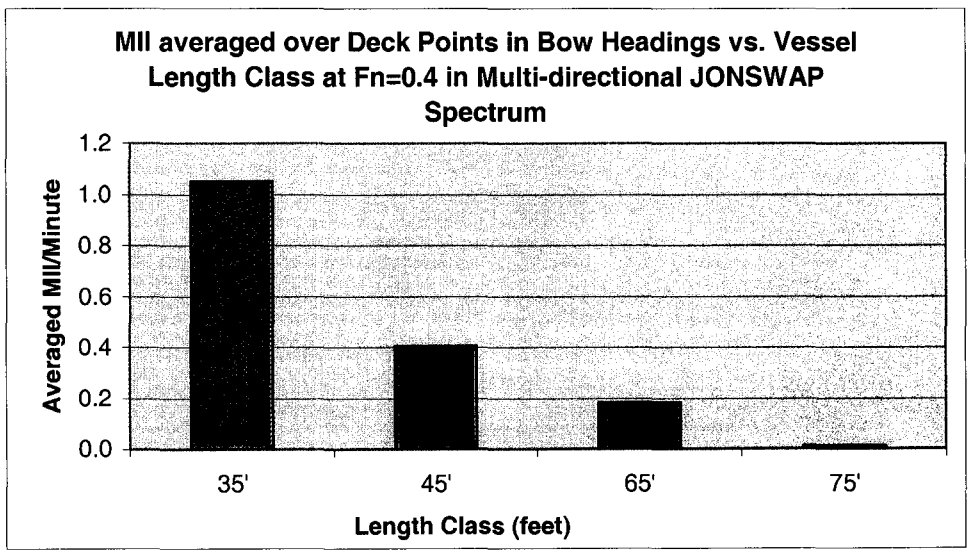

Figure 128.

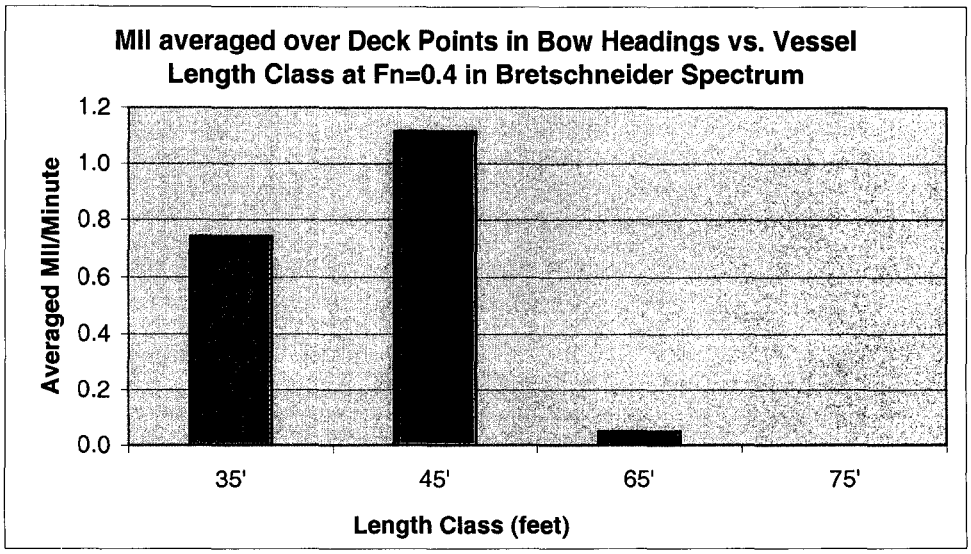

Figure 129.

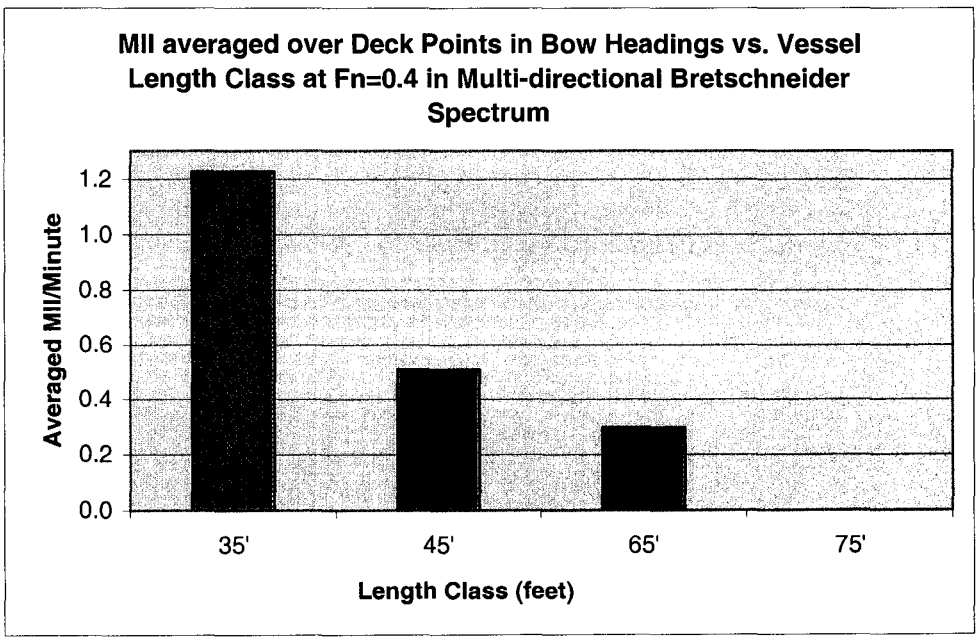

Figure 130.